Diss. ETH No. 19113

Improving climate model projections by model evaluation and regional aggregation

A dissertation submitted to the
ETH ZURICH

for the degree of
DOCTOR OF SCIENCE

presented by

Irina Mahlstein
Dipl. Sc. Nat. ETH Zurich
born on 4 July 1979
citizen of Schenkon (LU) and Luzern (LU)

accepted on the recommendation of

Prof. Dr. Reto Knutti, examiner
Dr. Christof Appenzeller, co-examiner
Dr. Susan Solomon, co-examiner

Zurich 2010

Für meine Eltern Heidi und Heinz Mahlstein.

Abstract

Climate change is and will be challenging societies and policy makers. Decisions for mitigation or adaptation are based on climate projections produced by climate models. However, due to structural and parametric differences between the models uncertainties are introduced into the projections. Efforts have been made to reduce these uncertainties, however it is not a trivial task to make climate projections more accurate. This thesis shows three different approaches how uncertainties can be reduced in the existing model data. The focus is set on regional projections and regional aggregation of climate change results.

In Chapter 2 the role of the ocean heat transport to the Arctic is analyzed in greater detail. Global warming caused by anthropogenic greenhouse gases impacts this region severely by changes in sea ice cover which have strong implications for the heat budget. Simulating future temperature increase in this region is difficult due to the complexity of this particular climate system. Atmosphere Ocean Global Circulation Models (AOGCM) show large uncertainties in their temperature projections for this region. In this study we show that the main differences in the pattern of the simulated surface temperatures of the AOGCMs are localized over the Barents Sea. This is a region where surface temperature depends on ocean currents, namely the North Atlantic Drift Stream bringing warm surface water to high latitudes. The strength of the northward ocean heat transport on the other hand impacts the sea ice cover in this region. Less sea ice leads to a stronger warming. Comparisons with observations reveal that those models which have a stronger northward ocean heat transport simulate the sea ice extent more accurately than those which have a weaker ocean heat transport. A major new finding of this thesis is that transporting less energy to the north induces more sea ice in the Arctic and consequently the future polar warming is less pronounced in these model projections.

In Chapter 3 a statistical approach is described which reduces uncertainties in regional projectionssignificantly . So far, regional climate change results have often been presented on simple rectangular areas defined in a rather ad hoc way instead of being based on climatic features. Cluster analysis algorithms offer the opportunity to define regions in which certain variables of interest, e.g. the current climate, or the projected changes, have similar values. Working with the k-means algorithm it is possible to define regions for which the number and the shape depend on the variable(s) of interest. For a regional classification focused on one variable (e.g. temperature or precipitation) the spatial spread of the projections can be reduced significantly without introducing too much uncertainty in the model disagreement compared to the old set of regions used in previous studies. One disadvantage of the k-means algorithm is that the number of clusters (regions) needs to be pre assigned. In order to determine the optimal number of regions the uncertainty of the projection in each region is mini-

mized. A key finding of this work is that the suggested number of regions required to best represent climate similarity is larger compared to the regions used in the past for all variables looked at. This leads to regions encompassing climatic features of a rather small scale. Cluster analysis also offers the possibility to combine different aspects of a climate such as temperature and precipitation, two characteristics which are important for impact studies because of their relevance in plant phenology and therefore in ecosystems.

The poles, namely the North Pole, show the greatest absolute warming, today and in future. But relative to their climate variability these changes are not very large. The regions where the smallest global warming is needed for a significant change in their temperature regime are the tropical regions. Due to their small decadal variability a smaller global warming is needed for the signal to emerge out of the noise than in other regions as is shown in Chapter 4. Hence, large parts of the Tropics need to address sooner to climate change than others. However, the countries being affected earlier by the warming climate are largely the ones which are not responsible for the warming observed because the countries in the Tropics emit the least amount of CO_2. Based on these findings the small scale detectability of precipitation is analyzed using the same methods in Chapter 5. Local detectability of precipitation is difficult, especially in already dry regions due to their large variability in precipitation. In Chapter 6 a climate index is built based on the results in Chapter 4 and 5. Futhermore, an indicator for vulnerability and adaptive capacity are included in the index. Most tropical countries are in an unfavorable condition compared to others.

Summerized the major conclusions from this thesis are: (1) the northward ocean heat transport influences sea ice cover in the Arctic and has therefore an influence on temperature projections in the Arctic, (2) cluster analysis provides a tool to define homogenous climate regions at a higher spatial resolution than in past works, and (3) significant local warming in low latitudes is unavoidable.

Zusammenfassung

Die Klimaänderung zwingt die Mitglieder unserer Gesellschaft und Entscheidungsträger zum handeln. Entscheidungen darüber, wie man den Kilmawandel abschwächen kann oder ob man sich daran anpassen soll, basieren auf Klimaprognosen welche von Klimamodellen berechnet werden. Allerdings führen die strukturellen und die parametrischen Unterschiede zwischen den Klimamodellen zu Unsicherheiten in den Prognosen. Frühere Studien haben sich bereits damit auseinandergesetzt, wie Unsicherheiten in Klimaprojektionen reduziert werden können. Diese Arbeit zeigt drei neue Möglichkeiten auf, wie Unsicherheiten in regionalen Klimaprognosen reduziert werden können.

In Kapitel 2 wird die Rolle des ozeanischen Wärmetransports in die Arktis detailliert untersucht. Die durch anthropogene Treibhausgase verursachte Erwärmung führt zu starken Veränderungen in dieser Region. Die Erwärmung verändert die Meereisbedeckung, was wiederum zu Veränderungen in der Energiebilanz führt. Die Klimamodelle weisen grosse Unsicherheiten in der Arktis auf, da die physikalischen Zusammenhänge in dieser Region sehr komplex sind. In dieser Studie wird gezeigt, dass sich die von den Klimamodelle berechneten Bodentemperaturen am stärksten in der Barentssee unterscheiden. Die Temperaturen in dieser Region werden stark durch den nordatlantischen Driftstrom beeinflusst, welcher warmes Oberflächenwasser in die hohen Breiten transportiert. Die Meereisbedeckung wird ebenfalls durch die Stärke des nordwärts gerichteten Wärmetransports beeinflusst. Wird weniger Energie in die hohen Breiten transportiert, kann das Meereis in der Arktis stärker wachsen und daher ist die polare Erwämung weniger stark ausgeprägt. Eine kleinere Meereisbedeckung führt über Rückkopplungsprozessen zu einer stärkeren Erwärmung. Jene Modelle, die einen stärkeren Wärmetransport aufweisen simulieren im Vergleich mit Beobachtungen die Meereisbedeckung besser als jene Modelle, die einen schwächeren Wärmetransport aufweisen.

Im dritten Kapitel dieser Arbeit wird eine statistische Methode beschrieben mit welcher Unsicherheiten in regionalen Klimaprognosen reduziert werden können. Bis jetzt wurden Klimaprognosen in rechteckigen Regionen aggregiert. Diese Regionen wurden allerdings eher ad hoc definiert und basieren weniger auf klimatischen Eigenschaften. Die Clusteranalyse ermöglicht es Regionen zu definieren in welchen bestimmte Variablen ähnliche Werte aufweisen. Der k-means Algorithmus bietet die Möglichkeit die Anzahl und die Form der Regionen so zu wählen, dass sie der Charakteristika der betrachteten Variable(n) am besten entsprechen. Im Vergleich zu den “alten” Regionen kann bei einer regionale Klassifizierung, die auf einer Variable basiert (z. B. Temperatur oder Niederschlag), die räumliche Unsicherheit signifikant reduziert werden ohne dabei die Unsicherheit, die von der Modelunstimmigkeit herrührt, stark zu erhöhen. Der k-mean Algorithmus besitzt allerdings den Nachteil, dass die Anzahl von Gruppen (hier Regionen) vordefiniert werden muss. Durch die Bestimmung der

optimalen Anzahl von Regionen kann die Unsicherheit in der Prognosen minimiert werden. Dies führt dazu, dass im Vergleich zu den “alten” Regionen mehr Regionen entstehen. In diesen kleineren Regionen werden nun klimatische Charakteristika abgebildet, wie es in den grossflächen “alten” Regionen nicht möglich gewesen ist. In der Clusteranalyse können aber auch mehrere Klimavariablen gleichzeitig betrachtet werden, zum Beispiel Temperatur und Niederschlag. Diese beiden Grössen sind für die Phänologie der Pflanzen und die Ökosysteme sehr wichtig und damit eignen sich diese Regionen für Studien über die Auswirkungen des Klimawandels.

Die Pole, insbesondere der Nordpol, zeigen die stärkste absolute Erwärmung, heute wie auch in der Zukunft. Relativ zur Klimavariabilität gesehen, ist diese Erwärmung allerdings weniger stark. Bereits eine schwache globale Erwärmung führt in den Tropen zu einer signifikanten Änderung ihres Temperaturregimes. Das Signal der Änderung taucht entsprechend früh aus dem natürliche Rauschen des Klimas auf, wie in Kapitel 4 gezeigt wird. Folglich muss sich ein grosser Teil der Länder in den Tropen früher mit den Auswirkungen des Klimawandels auseinandersetzen als andere. Sie gehören jedoch nicht zu den Ländern, die diesen Wandel zu verantworten haben, da sie am wenigsten CO_2 ausstossen. Basierend auf diesen Resultaten wurde im fünften Kapitel mit denselben Methoden die Nachweisbarkeit des Klimawandels in den modellierten Niederschlagsdaten untersucht. Regionale Nachweisbarkeit von Niederschlagsänderungen ist sehr schwierig, vor allem in Regionen, die bereits wenig Niederschlag erhalten. Im sechsten Kapitel wird ein Klimaindex eingeführt, welcher auf den Resultaten der beiden vorhergehenden Kapiteln basiert. Weiter wurde ein Indikator für die Schadenanfälligkeit und einer für die Anpassungsfähigkeit mit einbezogen. Im Vergleich mit den anderen Regionen befinden sich die meisten tropischen Länder in einer unvorteilhaften Ausgangslage.

Zusammenfassend können folgende Aussagen gemacht werden: (1) der ozeanische Wärmetransport beeinflusst die Meereisbedeckung in der Arktis und hat deshalb ebenfalls einen Einfluss auf die zukünftige arktische Erwärmung, (2) die Clusteranalyses bietet die Möglichkeit homogene Klimaregionen zu definieren, die zudem eine höhere räumliche Auflösung aufweisen als in älteren Studien und (3) eine signifkante Erwärmung in den tiefen Breiten lässt sich nicht mehr vermeiden.

Contents

Chapter 1

Introduction

...if the quantity of carbonic acid increases in geometric progression,
the augmentation of the temperature will increase nearly in arithmetic progression...
Svante August Arrhenius (1859 - 1927)

Svante Arrhenius formulated this first greenhouse law in a paper published in 1896. At least in a scientific article he was probably the first person to predict that emissions of carbon dioxide from the burning of fossil fuels would cause global warming. More than 100 years later there is general agreement that the Earth climate system has warmed over the past decades and that it is very likely that most of this warming is caused by anthropogenic greenhouse gases (IPCC, 2007). Climate change has attracted a growing interest in research but also in the public over the past years. Especially policy makers and economic experts have become interested in climate projections. However, large uncertainties still exist in forcasts of future changes and therefore, controversary surrounds discussions about matters of climate change. This thesis aims to contribute to understanding and reducing uncertainties in climate projections.

1.1 The relevant processes for climate change

The driver of climate change is a perturbation of the Earth's energy balance. The amount of energy transmitted, reflected or absorbed by the atmosphere can vary due to changes in the concentration of anthropogenic greenhouse gases, aerosols, volcanic eruptions and changes in the solar irradiance. This energy imbalance that is imposed on the climate system is termed radiative forcing (ΔF). Using a simple energy model the change in temperature (ΔT) can be described as follows:

$$\Delta Q = \Delta F - \lambda \Delta T, \tag{1.1}$$

where ΔQ is the increased heat flux and λ the climate feedback parameter. Oceans take up large parts of the increased heat which in turn increases the temperature of the oceans. Due to the changes in temperature the outgoing longwave radiation is changing, as well. This radiation flux is further influenced by climate feedbacks. For a constant forcing the climate system approaches a new equilibrium.

If ΔF is constant ΔQ will eventually be zero. A more detailed description can be found for example in Knutti and Hegerl (2008). The concept of climate change and its feedback is illustraded in Figure 1.1.

Changes in temperature will inevitably lead to changes in other climate parameters as well. If the surface temperature is increased, more water can be evaporated which leads to changes in the hydrological cycle. These changes influence the cloud processes which in turn is significant for albedo changes and precipitation. Hence, an imbalance in the energy balance triggers a chain reaction which involves every aspect of the climate system. But as the climate system changes, ecosystems are also exposed to changes. Species can react sensitively to changes in their environment. If the changes are irreversible some species are forced to migrate to other regions or they are threatened to become extinct.

1.2 Why should we care about climate change?

Climate change already has and will further affect many aspects of natural and human life. Increasing temperatures and changing precipitation patterns lead to severe impacts as for example:

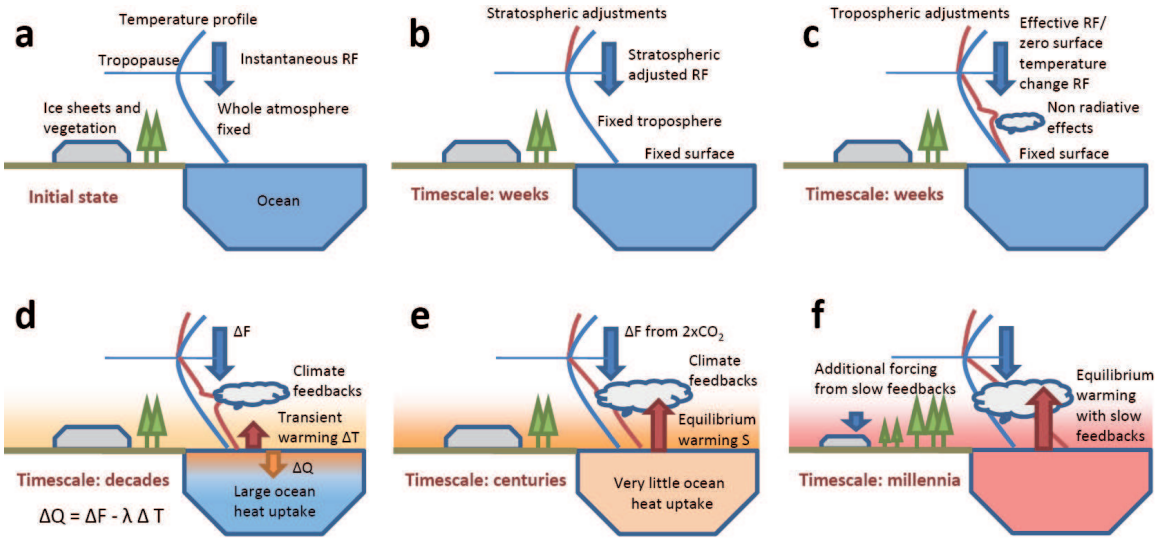

Figure 1.1: *The concept of radiative forcing, feedbacks and climate sensitivity. a) A change in a radiatively active agent causes an instantaneous radiative forcing (RF). b) The standard definition of RF includes the relatively fast stratospheric adjustments, with the troposphere kept fixed. c) Non-radiative effects in the troposphere (for example of CO_2 heating rates on clouds and aerosol semi-direct and indirect effects) occurring on similar timescales can be considered as fast feedbacks or as a forcing. d-f) During the transient climate change phase (d), the forcing is balanced by ocean heat uptake and increased long-wave radiation emitted from a warmer surface, with feedbacks determining the temperature response until equilibrium is reached with a constant forcing (e,f). The equilibrium depends on whether additional slow feedbacks (for example ice sheets or vegetation) with their own intrinsic timescale are kept fixed (e) or are allowed to change (f). Modified from Knutti and Hegerl (2008).*

- Melting of sea ice (Boé et al., 2009c)
- Sea level rise (Cazenave and Llovel, 2010)
- Decrease of fresh water availability (Heathwaite, 2010)
- Loss of biodiversity (Omann et al., 2009, John et al., 2009)
- Reduction in agricultural crop yields (Ainsworth and McGrath, 2010)
- Extreme climate conditions (Fischer et al., 2007)
- Ocean acidification (Byrne et al., 2010).

These examples represent only an illustrative subset of some of the most dangerous changes caused by increased anthropogenic greenhouse gas concentrations. Through couplings of the various elements of the Earth climate system changes in one compartment lead to changes in another which can then have a feedback on the first again, and of course this may lead to changes in a third. An illustration of these complex mechanisms is shown in Figure 1.2.

Due to the complex interactions, climate change influences a number of processes which are important for the economic sector. Reductions in agricultural crop yield is already mentioned above. But also

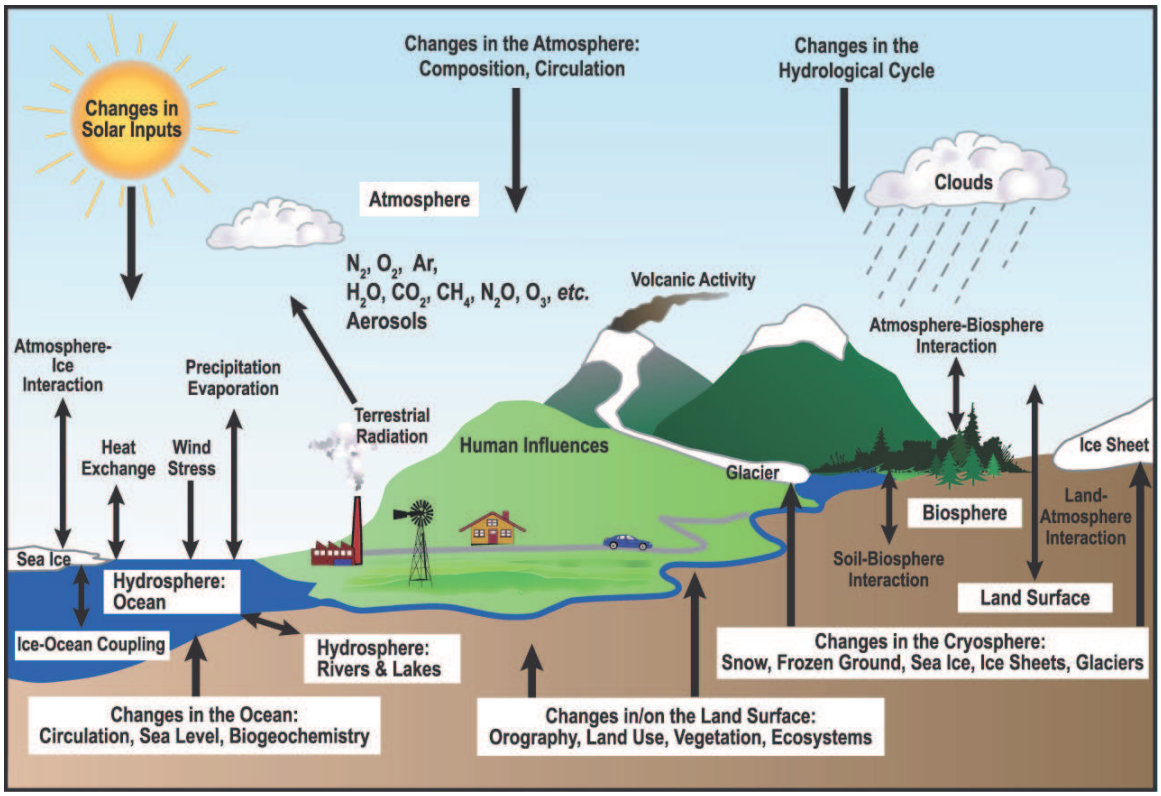

Figure 1.2: *Interactions between the different compartments of the Earth climate system. From IPCC (2007).*

economical sectors which deal with climate risks and climate hazards will be affected through an increase in climate extremes which cause large costs. The overall loss of monetary value caused by climate change is estimated by Stern (2007). Because the consequences of climate change reach different economical sectors and the daily life of people it is indispensable to determine projections of the expected changes in climate as accurate as possible. On the basis of these results policy makers can arrange the best opportunities for adaptation and mitigation.

Climate change projections are obtained by running numerical climate models. The required complexity of the global climate models (GCM) makes it expensive to run the GCMs. Therefore, only about twenty structurally different GCMs exist worldwide.

1.3 Atmosphere Ocean General Circulation Models and their uncertainties

A climate model is built on fundamental equations (e.g. equations of motion, conservation of energy, mass and angular momentum) which are discretized on a grid. These equations are solved numerically on a large computer. Although the first climate models were relatively simple it was the first time that basic climate processes could be simulated. Before that, all knowledge about climate was based on theory and observations only. The development of GCMs has taken large steps forward over the past decades. For the First Assessment Report (FAR) of the Intergovernmental Panel on Climate Change (IPCC) a swamp ocean was introduced to represent the interactions between ocean and atmosphere. From the Second Assessment Report (SAR) onwards in the context of IPCC Atmosphere Ocean General Circulation Models (AOGCM) were used to simulate future changes as illustrated in Figure 1.3. More physical processes and modules were added to the AOGCMs from one generation to the next generation of models (Fig. 1.3) in order to draw the modeling world closer to the real world. As the complexity of the models increased, the resolution of models increased as well, as shown in Figure 1.4.

Today AOGCMs simulate future climate projections on regional to continental scales, timescales of a few decades to centuries and for a number of different variables. They feature the required complexity and resolution to include the relevant dynamics of the large scale atmospheric and oceanic circulation. However, small scale processes can still not be resolved on the model grid and have to be parameterized. These parameterizations plus other structural differences such as the choice of grid or numerical methods between the different AGOCMs lead to a disagreement in the model projections.

The structural uncertainty however is not the only source of uncertainty in model projections. A large uncertainty stems from the future development of policy and economy. But the projections are simulated for a certain scenario and therefore this uncertainty is often avoided in climate models. Initial conditions are not important on longer time scales, therefore they do not contribute to the model disagreement. It is the parametric and the structural uncertainties which are responsible for the large spread in the forecasted climatic changes. Figure 1.5 shows the combination of the different uncertainties plus the total uncertainty and how they evolve with an increasing lead time.

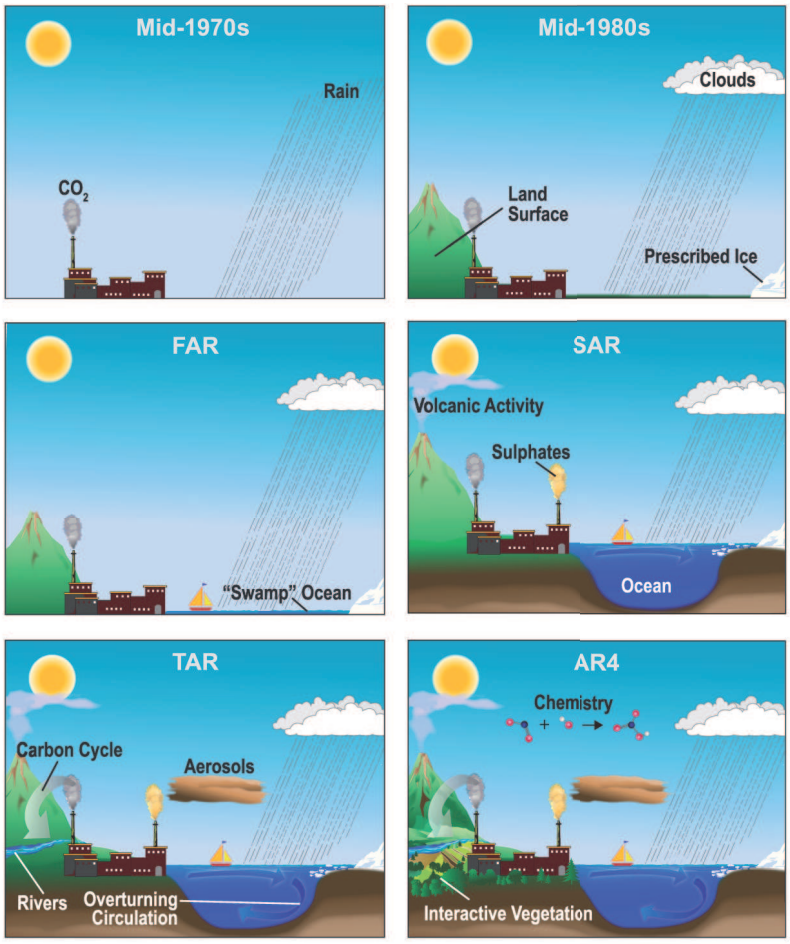

Figure 1.3: *Increasing complexity of the climate models used in the Mid-1970s, Mid-1980s, in the First Assessment Report (FAR), in the Second Assessment Report (SAR), in the Third Assessment Report (TAR) and the Fourth Assessment Report (AR4). From IPCC (2007).*

With the aid of perturbed physics ensemble using single parameter perturbations the parametric uncertainty has been studied with one base model (Murphy et al., 2004, Harris et al., 2006, Collins et al., 2006). On the basis of the Hadley Center model HadSM3 thousands of model versions were computed using multiple parameter perturbations (Piani et al., 2005, Stainforth et al., 2005, Knutti et al., 2006). But since these model versions are based on one single model the structural uncertainty is not represented in these studies. The different AOGCMs existing worldwide are relatively independently developed by the different institutions. Therefore, the structural uncertainty is partially sampled by the World Climate Research Programm's (WCRP's) Coupled Model Intercomparison Project phase 3 (CMIP3) multi-model dataset (Meehl et al., 2007a). This dataset includes about twenty AOGCMs simulating the climate from about 1850 to the present and for different emission scenarios (SRES) to at least the year 2100 (Meehl et al., 2005).

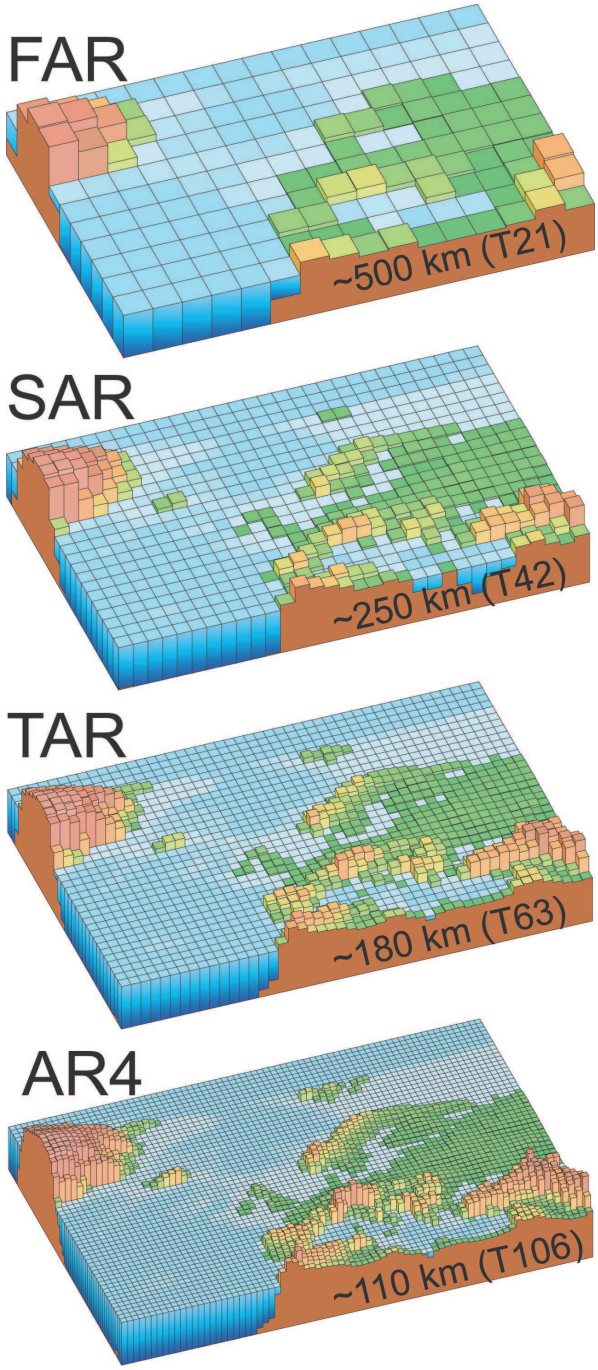

Figure 1.4: *Increasing resolution of the climate models used in the First Assessment Report (FAR), in the Second Assessment Report (SAR), in the Third Assessment Report (TAR) and the Fourth Assessment Report (AR4). From IPCC (2007).*

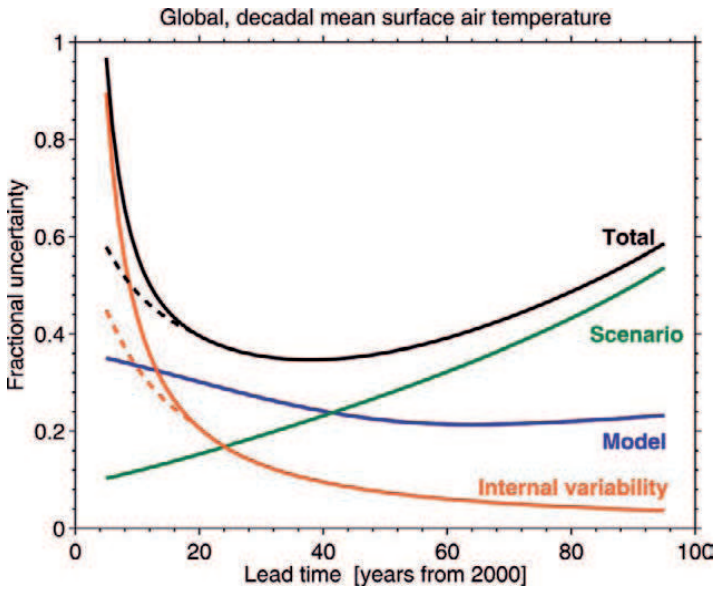

Figure 1.5: *The relative importance of each source of uncertainty in decadal mean surface air temperature predictions is shown by the fractional uncertainty (the 90% confidence level divided by the mean prediction), for the global mean, relative to the warming since the year 2000 (i.e., a lead of zero years). The dashed lines indicate reductions in internal variability, and hence total uncertainty, that may be possible through proper initialization of the predictions through assimilation of ocean observations (Smith et al., 2007). Modified from Hawkins and Sutton (2009)*

.

The existence of multiple climate models leads to disagreements in the global and regional climate change projections. One might ask the question why more than one climate model is needed. Instead of having a few models the existence of one good model would be enough. Why is the climate modeling community happy with having a number of models and going through the trouble to evaluate them? Because there is no unique model that fits best with observations, and there is no consensus on the metric to determine what 'best' means. Furthermore, if only one climate model existed it would be impossible to estimate the skill of the model. A good representation of the past does not necessarily imply that the future will also be accurately simulated. The information about the uncertainty of the future projections would be lost and the projection would be overconfident. Having an ensemble of climate models offers the possibility to generate probabilistic forecasts. This has been done by Räisänen and Palmer (2001) by giving the same weight to each model. However, it is questionable whether giving the same weight to each of the models is the best approach for generating multi-model mean results. Some of the models do not meet basic performance criteria for certain variables. Down-weighting or even excluding these models from analysis may improve the overall results. Similar ideas have been applied before (Giorgi and Mearns, 2003). Averaging all models with the same weight would only lead to a more accurate results if the models were randomly distributed around the true climate and independent of each other. But as Knutti et al. (2010) show the bias remaining after averaging 22 models is considerably larger than if the models were independent and hence the errors among the models are correlated.

Eliminating models from the analysis raises the question of a standard metric to evaluate model results. Often the skill of a model is determined by comparing the 20th century simulation with observational datasets and those models being closest to the observations achieve the best rating (Gleckler et al., 2008, Räisänen, 2007, Reichler and Kim, 2008). Although the models are getting better at reproducing the 20th century the spread in future projections is not decreasing significantly (Knutti et al., 2008) as depicted in Figure 1.6. As shown in Figure 1.3 climate models are getting more complex and they are better at reproducing the past compared to earlier analysis. However, it is still not clear how much of the convergence between models and observations is due to the increased complexity or due to model calibration. Datasets used for model evaluation are often the same as used for model development. Since climate models are producing projections on a long time scale, datasets to verify the projections do not yet exist.

As there are still numerous processes within the climate system and model behavior which are not well understood, not all uncertainties can be eliminated. But as for now we can only make best use of the data available today. The goal of many studies in this field is therefore to find ways to reduce the uncertainties in the existing climate simulation data. The 'physical approach' is one possibility to constrain climate models by detecting physical processes that can be observed today and show a strong relation to a changing future quantity. This method is explained in greater detail in Section 1.4.1. Another possibility to constrain climate model projections is by introducing complex methods such as neural networks (Knutti et al., 2003), Bayesian statistics (Tebaldi and Sanso, 2009, Tebaldi et al., 2004) or other statistical methods based on machine learning. A novel approach using machine learning is presented in Section 1.4.2.

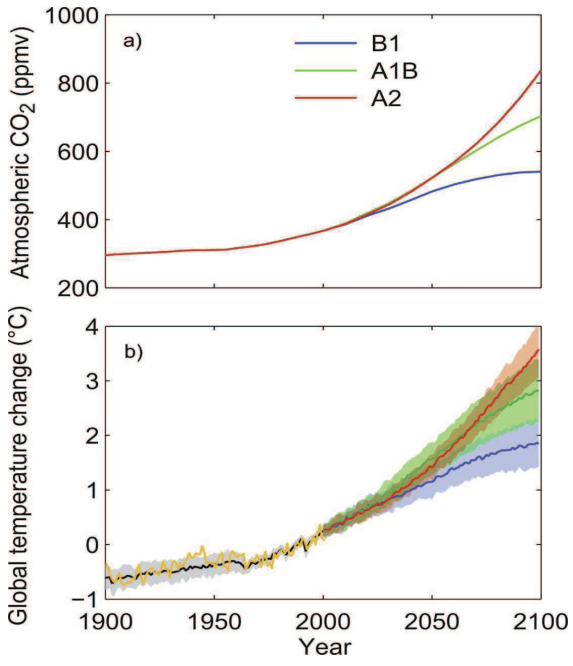

Figure 1.6: *(a) Atmospheric carbon dioxide concentration for the SRES scenario B1 (blue), A1B (green), and A2 (red) derived with the BernCC model (Joos et al., 2001) for the TAR. (b) Global-mean surface air temperature anomalies from the 1980-99 average SRES scenarios (B1), A1B (green), A2 (red), and for the historic twentieth-century simulation (black). Lines denote the ensemble mean and shaded bands denote one standard deviation of the multi-model response. Ensemble members were averaged first for each model, such that each model is given equal weight, although note that no all simulations are available for all models. The observed temperature for the twentieth century is given in orange for comparison (Jones and Moberg, 2003). Modified from Knutti et al. (2008).*

1.4 Reducing uncertainties in regional climate change projections

Producing accurate global climate projections itself is not a trivial task, as discussed above, and generating credible regional climate change projections is even more challenging (Hawkins and Sutton, 2009). To take appropriate adaption and mitigation measures accurate forecasts for individual regions are useful. Different regions will experience different changes in their climate. Some will suffer more from changes in the mean state, some more from interannual variability and some more from climate extremes. In some cases entire climate regimes may even disappear while new ones will form at other places (Williams et al., 2007). This thesis aims to introduce two examples showing how uncertainties of the climate mean state can be reduced in large-scale regional climate change projections. In the following two sections the underlying ideas of the methods developed are introduced.

1.4.1 Physical processes

On the basis of the publications by Hall and Qu (2006) and Knutti et al. (2006) an approach was developed to constrain AOGCM projections (see Chapter 2). The idea presented in Hall and Qu (2006) is that physical processes exist which are tightly correlated with global warming. In their study they show that a correlation of $r^2 = 0.92$ exists between the model simulated feedback strength in the seasonal cycle (which can be observed) and the climate warming as depicted in Figure 1.7. The model simulations of the feedback strength in the seasonal cycle can be improved using observations and as a result the spread of the feedback strength in climate change is reduced.

Thereafter two other studies based on the same idea demonstrated the robustness of this idea. Boé et al. (2009c) is a beautiful example how credible information can be extracted of an ensemble of 'wrong' models. Again by the use of observations and statistics Boé et al. (2009c) determine the time when the Arctic will be ice free in September, ending up with a much less uncertain estimate than by only averaging the spread of all models. Another study by the same authors explains that models with deeper baseline polar mixed layers are associated with larger deep ocean warming and smaller global surface warming (Boé et al., 2009b). The observational constraint suggests that many models may underestimate future surface warming in the Arctic(Boé et al., 2009b).

In Chapter 2 a similar approach is presented. The simulated northward ocean heat transport plays an important role in the sea ice extent and sea ice thickness simulated by the climate models. Models transporting more thermal energy to the Arctic produce less sea ice. Whether the ocean is covered by sea ice or not has a strong influence on the albedo feedback and ocean heat uptake. The models featuring a stronger northward ocean heat transport simulate a greater future warming, in the Arctic as well as globally.

1.4.2 Statistical Methods

Predefined regions as shown in Figure 1.8 are often used to aggregate model output over space. These regions, also called the 'IPCC regions' or 'Giorgi regions', were originally defined by Giorgi and Francisco (2000) and are rectangular. The Giorgi regions were used as basis for probabilistic studies (Giorgi and Mearns, 2002, Tebaldi et al., 2004, 2005, Tebaldi and Knutti, 2007) and in IPCC reports

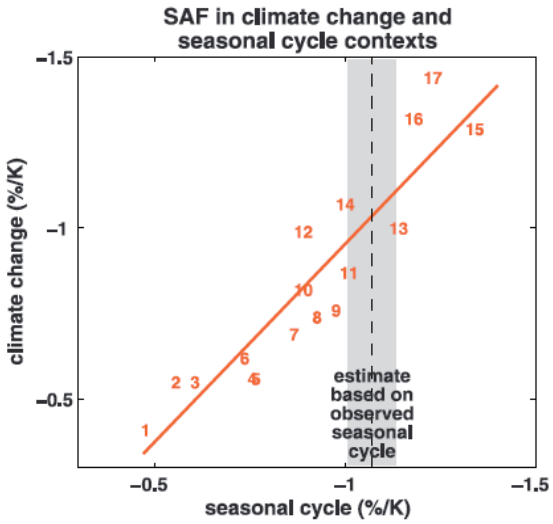

Figure 1.7: *Scatterplot of simulated springtime $\Delta\alpha_s/\Delta T_s$ values in climate change (ordinate) vs. simulated springtime $\Delta\alpha_s/\Delta T_s$ values in the seasonal cycle (abscissa). The numbers of the 17 AOGCMs are used as plotting symbols. Seasonal cycle $\Delta\alpha_s/\Delta T_s$ values, based on 20th century climatological means, are calculated by dividing the difference between April and May α_s as averaged over NH continents poleward of $30\,^{\circ}\mathrm{N}$ by the difference between April and May T_s averaged over the same area. Values of $\Delta\alpha_s$ were weighted by April incoming insolation prior to averaging. A least-squares fit regression line for the simulations is also shown. The two $\Delta\alpha_s/\Delta T_s$ parameters are highly correlated ($r^2 = 0.92$). The observed springtime $\Delta\alpha_s/\Delta T_s$ value based on ISCCP and the ERA40 reanalysis is plotted as a dashed vertical line. The grey bar gives an estimate of statistical error, calculated according to a standard formula for error in the estimate of the mean of a time series (in this case the observed time series of $\Delta\alpha_s/\Delta T_s$) given the time series length and variance. If this statistical error only is taken into account, the probability the actual observed value lies outside the grey bar is 5%. Modified from Hall and Qu (2006).*

(Giorgi et al., 2001, Christensen et al., 2007). The use of these regions has been questioned before because the regions are not only based on physical criteria but also on political issues.

Cluster analysis is a statistical method based on machine learning with the goal to partition groups of data in such way that two data points belonging to the same group (cluster) tend to be more similar than two data points belonging to two different groups. Making use of this technique the goal of Chapter 3 is to define climatological regions which are based on similar current mean state and similar changes in the future. The number of regions is determined in such a way that the overall uncertainty, stemming from the local climate pattern and model uncertainty, is minimized.

Various cluster analysis algorithms exist, each having advantages and disadvantages. The algorithm chosen for this study is the k-means algorithm (Jain et al., 1999). For a given set of datapoints $(x_1, x_2, ..., x_n)$ the first k centroids of the k clusters are chosen randomly. In an iterative process k-means minimizes the within-cluster sum of squares between datapoints and centroids:

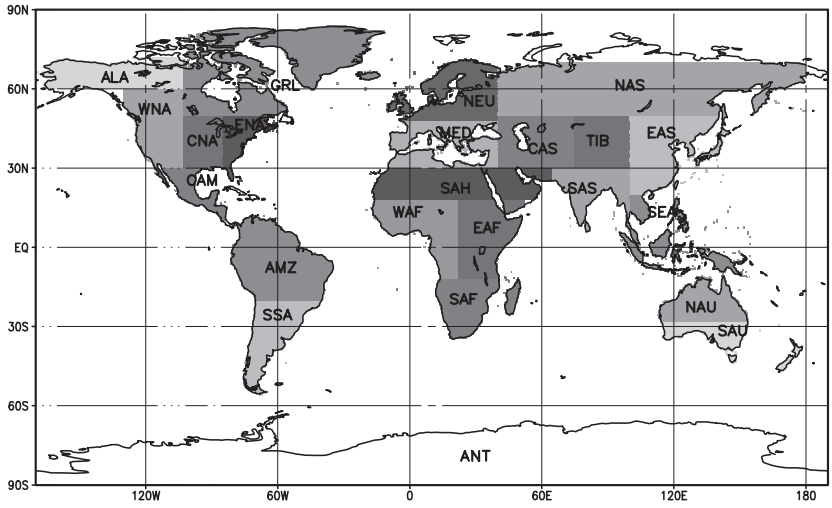

Figure 1.8: *The Giorgi regions, also termed the 'IPCC regions' introduced by Giorgi and Francisco (2000).*

$$J = \sum_{j=1}^{k} \sum_{i=1}^{n} \| \, x_i^j - c_j \, \|^2, \tag{1.2}$$

where k is the number of clusters, n the number of datapoints and c_j the centroid of cluster j. In the assignment step of the iterative procedure each datapoint is assigned to the cluster with the closest centroids:

$$S_i^t = \{x_i : \| \, x_i - {c_j}^t \, \| \;\; \leq \;\; \| \, x_i - {c_{j*}}^t \, \| \text{ for all } j* \; = 1, ..., k\}, \tag{1.3}$$

where t denotes the iterative step. In the update step simply the centroids of the newly assigned clusters are determined by taking the mean of the datapoints in one cluster:

$${c_j}^{t+1} = \frac{1}{\mid {S_j}^t \mid} \sum_{x_i \in {S_j}^t} x_i. \tag{1.4}$$

Once the assignments do not change any more the algorithm has converged.

The k-means algorithm is one of simplest unsupervised learning algorithms and has the advantage of being inexpensive and fast but with the disadvantage of being heuristic and therefore it does not necessarily converge to the global optimum. More details are discussed in Chapter 3.

1.5 Understanding why and where climate change is detected first

Reducing uncertainties in climate projections is only the first step to compute accurate climate change information. In a next step the informations needs to be aggregated meaningfully and appropriate quantities need to be chosen in order to be able to illustrate where the regions are where climate change can be detected best. There are very few studies which show where climate change is most

prominent. Giorgi (2006) define climate change hot-spots based on a regional climate change index which is based on regional mean precipitation change, mean surface air temperature change, and change in precipitation and temperature interannual variability. Altough he states that impacts are not taken into account, the use of the term climate change hot-spots can be misleading in this case because it implies that the impacts are most negative in these areas. The probability that it actually is the case is very high. However many uncertainties exist and it is the impact community's responsibility to give information on where and why climate change causes severe damage. Ecosystems can react differently to changes in temperature, precipitation, the diurnal cycle, changes in variability or mean state. Every species has its own preferences which makes it difficult to aggregate results worldwide. If regions are defined that are climate change hot-spots, impacts, vulnerability and adaptive capacity should also be taken into account.

Another example of a climate change index is presented by Baettig et al. (2007). They clearly state that the impacts are not included. The climate change index is built of extreme values. In both studies by Baettig et al. (2007) and Giorgi (2006) for a climate change index the uncertainties introduced by the climate models is not taken into account. It could be misleading to define a region as a climate hot-spot without considering the robustness of the results in this region.

The aim of Chapter 4 is to develop an understanding of the climate characteristics in terms of decadal variability, current signal, signal to noise ratio and model robustness of the land parts on Earth. The question how much global warming is needed before a signal of change can locally be detected is addressed. As the signal to noise ratio for temperature is largest in the Tropics the models included in this study were first tested in their ability to simulate tropical variability. Two statistical tests were applied as described below.

1. **Significance test described by Santer et al. (2008)**
   The test addresses the question whether the models can simulate the observed variability in the Tropics. The test statistic d is defined as follows:

$$d = (b_m - b_o)/\sqrt{s\{b_m\}^2 - s\{b_o\}^2}, \tag{1.5}$$

   where b_m is the trend of the model, b_o the trend of the observations.
   $s\{b_m\}^2$ and $s\{b_o\}^2$ are the standard errors of b_m respectively b_o. The standard errors are measures of inherent statistical uncertainty in fitting a trend to noisy data, which is in this case the variability. For model data $s\{b_m\}$ is given by:

$$s\{b_m\} = [s_e^2/\sum_{t=1}^{n_t}(t-\overline{t})^2]^{\frac{1}{2}}, \tag{1.6}$$

   where t is the time index, $\overline{t}$ is the average time index, n_t the number of time steps and s_e^2 is the variance of the regression residuals defined as:

$$s_e^2 = \frac{1}{n_t - 2}\sum_{t=1}^{n_t} e(t)^2, \tag{1.7}$$

where $e(t)^2$ are the regression residuals. The regression residuals is an atmospheric temperature series, $e(t)^2$ is not independent and has a lag-1 temporal autocorrelation. Therefore, the sample size is given by:

$$n_e = n_t \frac{1 - r_1}{1 + r_1}, \tag{1.8}$$

where r_1 is the lag-1 temporal autocorrelation coefficient.

Note that $s\{b_o\}$ is calculated similarly, but using observationsal data instead of model data.

2. **F-test**
   The F-test tests whether the variances of two time series belong to the same distribution or not. The null hypothesis is as follows:

$$H_0 : var_m = var_o, \tag{1.9}$$

where var_m is the variance of the model and var_o is the variance of the observations. The alternative hypothesis is:

$$H_A : var_m \neq var_o. \tag{1.10}$$

The test statistics is given by:

$$F = \frac{var_m}{var_o}. \tag{1.11}$$

It is plausible to assume that in regions with a high signal to noise ratio the signal of change emerges earlier out of the noise than in regions with a low signal to noise ratio. To estimate the time period when the signal emerges out of the noise a Kolmogorov-Smirnov test is applied on two different data samples from different time periods. This is a nonparametric test which determines whether the samples are drawn from the same distribution. Hence, the null hypothesis is:

$$H_0 : F_{t_b}(x) = F_{t_n}(x), \tag{1.12}$$

where $F_{t_b}(x)$ is the is the sample distribution of the baseline time period and $F_{t_n}(x)$ is the distribution of a time period n-years later than the baseline. The alternative hypothesis is consequently:

$$H_A : F_{t_b}(x) \neq F_{t_n}(x). \tag{1.13}$$

When $F_{t_b}(x) \neq F_{t_n}(x)$ the climate of the time period t_n has changed such that the distribution of the climate data is not the same. For more details see Chapter 4.

1.6 Detectability of precipitation change

The same analysis as presented in Chapter 4 for temperature can be done for precipitation. However, in case of precipitation on a small scale only a few regions show a clear signal emerging of the noise before 2100. Especially drying is difficult to detect. In already dry areas detection of a drying trend is very problematic due to the very high local variability in these areas. More details are shown in Chapter 5.

1.7 The ignorance of the climate system in regard to adaptive capacity

Some parts of the world warm more than others. Landmasses have warmed more than the oceans (Flato and Boer, 2001) due to differences in their physical characteristics. The poles are also warming stronger in absolute terms, especially in the Northern hemisphere (Flato and Boer, 2001). However, as is shown in Chapter 4 when working with the signal to noise ratio which is mainly used in detection studies, the signal of climate change is strongest and first visible in the Tropics, at least for temperature. In case of precipitation the results are rather patchy. Figure 1.9 illustrates that based on modeling studies Africa and southern Asia show the most prominent temperature signal.

Some of the poorest countries are located in these areas. This raises the question of the vulnerability of the affected regions and whether they have the capacity to adapt to the changes due to a different climate. Based on Figure 1.9 and the results presented in Chapter 4 and 5 a climate change index is built which incorporates information about climate change, vulnerability and adaptive capacity. In Chapter 6 the results of this climate change index are presented.

1.8 Aims and outline

The previous sections have shown that uncertainties in climate change projections still exist. This thesis explains some possible approaches for a reduction of uncertainties in regional climate change projections. Policy makers and end users ask for accurate climate change projections on a regional scale. The awareness of climate change has risen in the public and the desire for answers and strategies to avoid and/or adapt to coming changes is growing.

It is the main objective of this thesis to present more insights to the following themes:

- **Reducing uncertainty in areas showing a large model spread:** Certain physical processes strongly influence today's climate but also the future warming. These physical processes need to be determined and used in order to constrain AOGCMs. The representation of these processes in the models depend on model resolution and the implemented parameterizations. By pointing out deficiencies in the representations of the physical process, model results can be improved.
- **Evaluate the AGOCMs on their ability to simulate key processes:** Models which do not meet basic performance criteria may be excluded from the multi model ensemble. By doing so the model spread can be reduced significantly.
- **Reducing the uncertainty in aggregated climate change projections by choosing the optimal size of each region:** By varying the size of the regions the uncertainty of the projections due to model deficiencies and the local climate pattern can be reduced. Therefore, each climate parameter is analyzed individually.
- **Aggregating climate change results in meaningful climatic regions:** In order to aggregate the vast amount of model data into climate change results useable for end users a regional classification is needed. The regions should represent today's climate mean state as well as similar future changes in the climate parameter of interest.

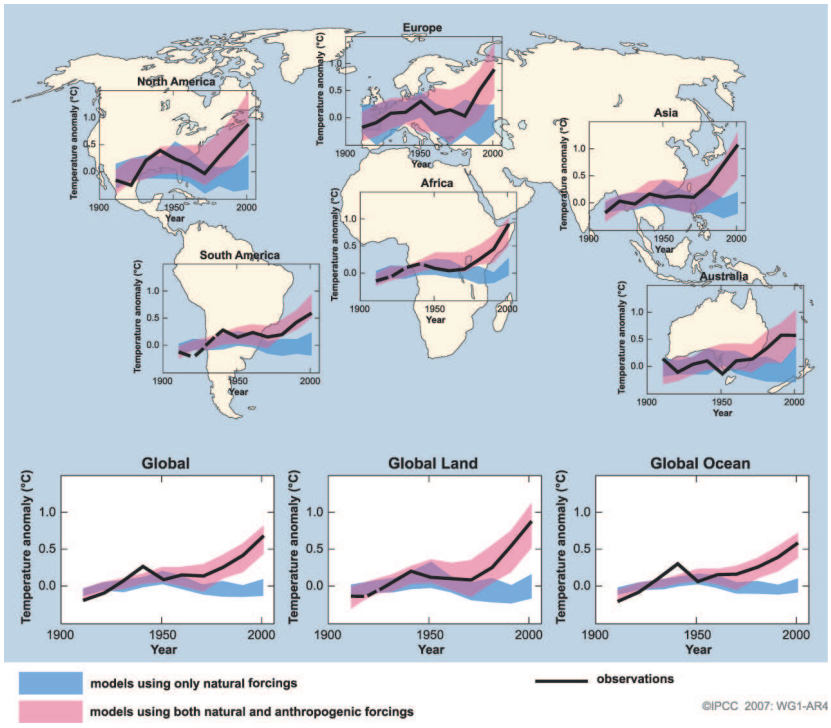

Figure 1.9: *Comparison of observed continental- and global-scale changes in surface temperature with results simulated by climate models using natural and anthropogenic forcing. Decadal averages of observations are shown for the period 1906 to 2005 (black line) plotted against the center of the decade and relative to the corresponding average for 1901-1950. Blue shaded bands show the 5-95% range for 19 simulations from five climate models using only the natural forcings due to solar activity and volcanoes. Red shaded bands show the 5-95% range for 58 simulations from 14 climate models using both natural and anthropogenic forcings. From IPCC (2007).*

- **How much global warming is locally needed to detect a significant change in temperature?** Based on the modelled signal to noise ratio I try to determine how much global warming is needed for a local significant change in temperature in summer season.
- **Detection of precipitation change:** When will changes in precipitation be detectable on a small scale?
- **Social aspects of climate change:** The questions whether some countries are in a difficult position with regard to climate change is addressed based on a climate change index.

When trying to answer all the above mentioned themes, particular emphasis is set on the goal to reduce uncertainty and produce results which are based on model data that is as robust as possible. This means that in some cases specific models were excluded from the analysis due to inabilities to represent climate characteristics which are important for the specific analysis. Consensus on metrics to weight models are not available which is reflected by the current IPCC Report where each model is given an equal weight. However, it is questionable wether all models should be included in studies even though some models do not meet the required quality (Knutti, 2010). In this doctoral thesis three

studies are presented where climate models are excluded in order to improve the results.
The overall aim of this thesis is to explore alternative ways on how to evaluate models, possibilities to reduce model uncertainties and to introduce methods which provide robust information on model performance. In order to improve model results information is aggregated and in some cases only a subset of models are used.

The thesis is structured in seven chapters. Three of these chapters are already published or are prepared for publication and are therefore presented as self-contained scientific publications. The detailed outline is as follows:

- **Chapter 2:** Ocean heat transport as a cause for model uncertainty in projected Arctic warming *(Mahlstein and Knutti 2010)*
- **Chapter 3:** Regional climate change patterns identified by cluster analysis *(Mahlstein and Knutti 2009)*
- **Chapter 4:** Substantial local warming unavoidable in low latitude countries *(Mahlstein et al. 2010)*
- **Chapter 5:** Small scale detectability of precipitation changes
- **Chapter 6:** The unfavorable situation of developing countries in climate change
- **Chapter 7:** Conclusion and outlook

Chapter 2

Ocean heat transport as a cause for model uncertainty in projected Arctic warming

Ocean heat transport as a cause for model uncertainty in projected Arctic warming

Irina Mahlstein and Reto Knutti

Institute for Atmospheric and Climate Science, ETH Zurich, Switzerland

(Accepted in Journal of Climate)

Abstract

The Arctic climate is governed by complex interactions and feedback mechanisms between the atmosphere, the ocean and solar radiation. One of its characteristic features, the Arctic sea ice, is very vulnerable to anthropogenically caused warming. Production and melting of sea ice is influenced by several physical processes. In this study we show that the northward ocean heat transport is an important factor in the simulation of the sea ice extent in the current general circulation models. Those models which transport more energy to the Arctic show a stronger future warming, in the Arctic as well as globally. Larger heat transport to the Arctic, in particular in the Barents Sea, reduces the sea ice cover in this area. More radiation is then absorbed during summer months and is radiated back to the atmosphere in winter months. This process leads to an increase in the surface temperature and therefore to a stronger polar amplification. The models which show a larger global warming agree better with the observed sea ice extent in the Arctic. In general, these models also have a higher spatial resolution.

These results suggest that higher resolution and greater complexity are beneficial in simulating the processes relevant in the Arctic, and that future warming in the high northern latitudes is likely to be near the upper range of model projections, consistant with recent evidence that many climate models underestimate Arctic sea ice decline.

2.1 Introduction

Anthropogenic greenhouse gases lead to a global warming of the climate system. The warming however is asymmetric, the high northern latitudes and landmasses show greater warming than the Southern Hemisphere and the oceans due to ocean heat uptake (e.g. Flato and Boer 2001). It is the Arctic where the greatest warming is expected by the end of this century (e.g. Holland and Bitz 2003). Due to differences in parameterizations and structural differences of the Atmosphere Ocean Global Circulation Models (AOGCM), projections of future warming show large uncertainties.

The Arctic region is characterized by a very large variability and complex physical processes which govern its climate. Climate change caused by anthropogenic greenhouse gases impacts this region severely by changes in sea ice cover which have strong implications for the energy budget. Additionally, positive feedback mechanisms are key factors driving the Arctic warming (e.g. Manabe and Stouffer 1980). Numerous physical processes account for the strength of the ice albedo feedback which is mainly responsible for the polar amplification (Deser et al., 2010). Polar warming is also strongly related to global warming as depicted in Figure 2.1 with a correlation of 0.87, i.e. a higher global temperature increase implies a higher warming in the Arctic. Understanding the complex Arctic climate system with all its feedbacks is therefore indispensable in order to reduce some of the uncertainties in global climate change projections. This process is hampered by the fact that observations in the Arctic are sparse and thus large uncertainties exist in observational datasets. Hence, temperature projections in the Arctic comprise a larger spread ($2.5 - 7.5$K, for scenario A1B, 2070-2099 relative to 1970-1999) of the AOGCM's than the global mean projections ($1.8 - 4$K), at least in absolute terms.

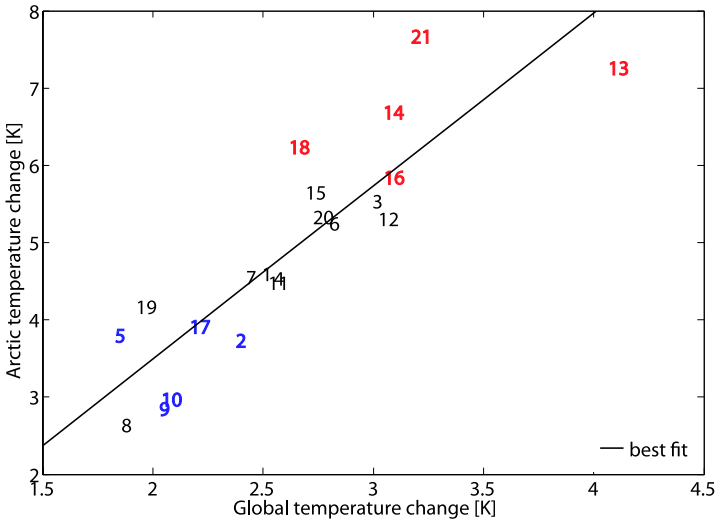

Figure 2.1: *Correlation (R=0.87) across the CMIP3 models between the Arctic warming and the global warming (2070-2099 relative to 1970-1999). Numbers correspond to the models introduced in Table 2.1. Red and blue labels mark the models that belong to the warm and cold composite, respectively, that is used in subsequent figures.*

As mentioned above, various physical processes influence future temperature projections but they are also important in simulating current climate and variability. Yet it has proven difficult to find metrics based on present day mean climatology that strongly relate to future projections (Murphy et al., 2004, Tebaldi and Knutti, 2007, Knutti et al., 2010, Knutti, 2010), and the community has struggled in many cases to define relevant metrics that would separate 'good' from 'bad' models, although there are some exceptions (Walsh et al., 2008, Wang and Overland, 2009, Zhang, 2010). Knutti et al. (2006) find a relation between the seasonal cycle in regional temperature and climate sensitivity. Hall (2004) show that the strength of the snow albedo feedback in spring is coupled to the strength of future temperature increase in each model. Physical processes such as the longwave feedback parameter of the models (Boé et al., 2009a) and the deep ocean heat uptake (Boé et al., 2009b) partly explain the large spread of future model projections in temperature. Simulating such processes properly and improving agreement with observations may be one possibility to reduce uncertainty in future projections. In this study we show that the main differences in the pattern of surface temperature in the Arctic are localized over the Barents Sea. This is a region where surface temperature depends on ocean currents, namely the North Atlantic Drift Stream bringing warm surface water to high latitudes. The strength of the northward ocean heat transport on the other hand impacts the sea ice cover in this region. Sea ice is a key player causing a large albedo feedback and together with the sea ice thickness feedback leads to a large Arctic warming. We show that process based model evaluation can provide interesting insight into climate feedbacks and at the same time help to reduce model uncertainties.

2.2 Data and Method

For the evaluation of the models different observational datasets are used. The bias of the surface temperature (TAS) is compared to the ERA40 dataset (Uppala et al., 2005). Though the newer product ERA-interim exists it is not used for the bias analysis because the dataset does not start before 1989 and therefore the time series is too short for a climatological analysis. Station data is very sparse in the Arctic and therefore ERA40 is considered to be the most reliable to calculate the bias (Bromwich et al., 2007). The investigated time period for TAS starts 1970 and ends with the year 1999. For sea ice the Met Office Hadley Center's sea ice and sea surface temperature (SST) data set (HadISST) (Rayner et al., 2003) is used for comparison with model data. In this study only the time period from 1980 to 2008 is considered.

The model data set consists of up to 23 of the global coupled atmosphere ocean general circulation models (AOGCMs) used for the Intergovernmental Panel on Climate Change (IPCC) Fourth Assessment Report (AR4) (IPCC, 2007) which are available from the World Climate Research Programme (WCRP) Coupled Model Intercomparison Project Phase 3 (CMIP3) (Meehl et al., 2007a). More information about the participating models is available on the Program for Climate Model Diagnosis and Intercomparison (PCMDI) website: $http://www-pcmdi.llnl.gov/ipcc/about\_ipcc.php$. All models providing the relevant data are included in the analysis except for the FGOALS-g1.0 model. This model shows sea ice extent much larger than observed (Arzel et al., 2006). Since this study is focusing on the Arctic region this model is excluded. The models used in this study are listed in Table 2.1. For all models and all variables one ensemble member (run1) of the A1B scenario is used for the

analysis. Not all modeling groups provide the ocean heat transport in the data archive. Therefore, for seven models the ocean heat transport is approximated by an energy balance as in Figure 8.6 of the IPCC (2007).

All model data is regridded to a common T42 grid using a bilinear interpolation to be able to compare model results. Only for the northward ocean heat transport the data is used on the original grid to minimize issues with conservation of energy.

The projected warming is the difference between the mean TAS of the period 2070 to 2099 and the period 1970 to 1999. For the evaluation of the models using observations the time period 1970 to 1999 is used. Only for sea ice the time period 1980 to 2008 is used when observations are included because the observational data is more reliable due to use of satellite techniques after 1980. The Arctic region in this study is defined as the area north of $60°$N. Time averages are for the above mentioned time periods and spatial averages cover the region $60°$N to $90°$N throughout the paper.

2.3 Results and discussion

2.3.1 Surface temperature

In order to find a physical explanation for the large spread in global and the even larger spread in the Arctic warming two different composites are built: One consisting of the five models with the largest warming in the Arctic (marked in red in Fig. 2.1), the other consisting of the five models with the smallest Arctic warming (marked in blue in Fig. 2.1) excluding model number eight (see Table 2.2 for details of the two groups). This model is excluded of the composite due to its special behavior of its ocean heat transport and its warming (see Section 32.3.3).

Though selecting the members for the composites has a subjective component, sensitivity tests with more 'cold' or 'warm' models in the respective composites show that the results do not depend on details of selecting the composites.

For these two composites the mean surface temperature (TAS) over the period 1970-1999 in April and September in the Arctic is calculated and the bias against the ERA40 observational dataset is determined for each composite. Figure 2.2 shows that in general, the warm composite reveals too warm temperatures compared to ERA40, whereas the cold composite has a bias towards too low temperatures, i.e. models with a warm (cold) current state show more (less) warming. It must be noted however, that the ERA40 reanalysis shows a cold bias over the Arctic ocean (Bromwich et al., 2007). This implies that the warm composite features a reduced warm bias, on the other hand the bias of the cold composite may be even larger. The main differences are over the ocean and most apparent over the Barents Sea as is also stated by Chapman and Walsh (2007). Especially in September the differences between the two composites are particularly pronounced. The sea ice extent reaches its minimum at this time of the year and the ocean is capable of absorbing most energy at this time while energy is radiated back to the atmosphere during winter which enhances the large Arctic warming. Thus, differences in TAS in this region may strongly affect future warming in the polar region. Reasons for the large bias of both composites may be complex feedback mechanism including sea ice

Table 2.1: *CMIP3 models and data availability.*

Number	Model	Sea ice	Ocean heat transport	Calculated ocean heat transport
1	BCCR-BCM2.0	x		x
2	CCCma CGCM3.1	x		x
3	CCCma CGCM3.1 T63	x		x
4	CNRM-CM3	x	x	
5	CSIRO Mk3.0	x	x	
6	GFDL CM2.0	x		x
7	GFDL CM2.1	x		
8	GISS-AOM	x	x	
9	GISS-EH			
10	GISS-ER	x	x	
11	INMCM3.0	x	x	
12	IPSL CM4	x		x
13	MIROC3.2(hires)	x	x	
14	MIROC3.2(medres)	x	x	
15	MIUB-ECHO-G	x	x	
16	ECHAM5	x		x
17	MRI CGCM2.3.2a	x	x	
18	CCSM3.0	x	x	
19	PCM1			
20	UKMO HadCM3	x	x	
21	UKMO HadGEM1	x		x
22	CSIRO Mk3.5	x	x	

Table 2.2: *CMIP3 models of the two composites in alphabetical order.*

Warm models	Cold models
MIROC3.2(hires)	CCCma CGCM3.1
MIROC3.2(medres)	GISS-EH
ECHAM5	GISS-ER
CCSM3.0	CSIRO Mk3.0
UKMO HadGEM1	MRI CGCM2.3.2a

cover and the associated ice albedo feedback as well as the ocean heat transport. The details of this assumption will be discussed in the following sections.

2.3.2 Sea ice

Because large parts of the Arctic ocean are covered with ice throughout the whole year or part of it and because the main differences are found over the ocean the mean sea ice concentration is shown in Figure 2.3 for the same two composites to investigate whether the differences arise from sea ice cover. The GISS-EH model is missing in the cold composite in case of sea ice because the data is not available. Note that since the HadISST observational dataset is used, the time period from 1980 to 2008 is examined. Figure 2.3 shows two interesting features. First, the composite using the warm models simulate the sea ice cover in April and September more accurately than the four cold models. Note that the conclusions are not dependent on the specific month in the year looked at. Second, the cold composite not surprisingly has a greater sea ice extent than the warm composite. Similar to Figure 2.2, the main differences between the two composites are over the Barents Sea. This suggests that the models simulating a smaller sea ice for today's climate conditions show a larger decrease of sea ice and therefore less remains in a future climate. The findings in Boé et al. (2009c) support this hypothesis. The five coldest models belong to the group of models showing the largest remaining area of September sea ice at the end of this century (Boé et al., 2009c). On the other hand, three models of the warm composite belong to the four models with the smallest area of September sea ice at the end of this century. One model of our warm composite is not used in the study by Boé et al. (2009c) and one model is in the lower half with less September sea ice left of the sample used by Boé et al. (2009c). A reason for this difference could be that this model has a larger sea ice extent in the preindustrial conditions.

When correlating the mean temperature bias of September in the Artic region with the mean sea ice extent in September both for 1980-2008 it becomes evident that models with a larger bias towards warm temperature have smaller sea ice extent and vice versa with a correlation of -0.84 as shown in Figure 2.4. The reason why the models in the warm composite feature a relatively large warm bias but still simulate the sea ice extent very accurate may be due to the cold bias in the ERA40 product over the Arctic ocean.

The sea ice thickness in April and September clearly shows that the cold composite has thicker sea ice than the warm composite as depicted in Figure 2.5. The warm composite probably captures the sea ice thickness more realistically than the cold composite (personal communication M. Holland). Interestingly, according to the study by Holland et al. (2010) the largest scatter of sea ice thickness across the CMIP3 models is found in the Barents Sea. The ice thickness is an important factor for the melt in spring and summer since thinner ice is more vulnerable to melting during warm periods (Holland and Bitz, 2003). Generally speaking, both characteristics of Arctic sea ice, extent and thickness, are important for the processes governing the Arctic warming. In spring and summer the ice cover decreases due to the sea ice albedo feedback and the ocean absorbs shortwave radiation which is stored as thermal energy. In fall and winter on the other hand, thinning and decreasing sea ice reduces the isolation of the ocean. Therefore, more energy is transferred from the ocean to the atmosphere and

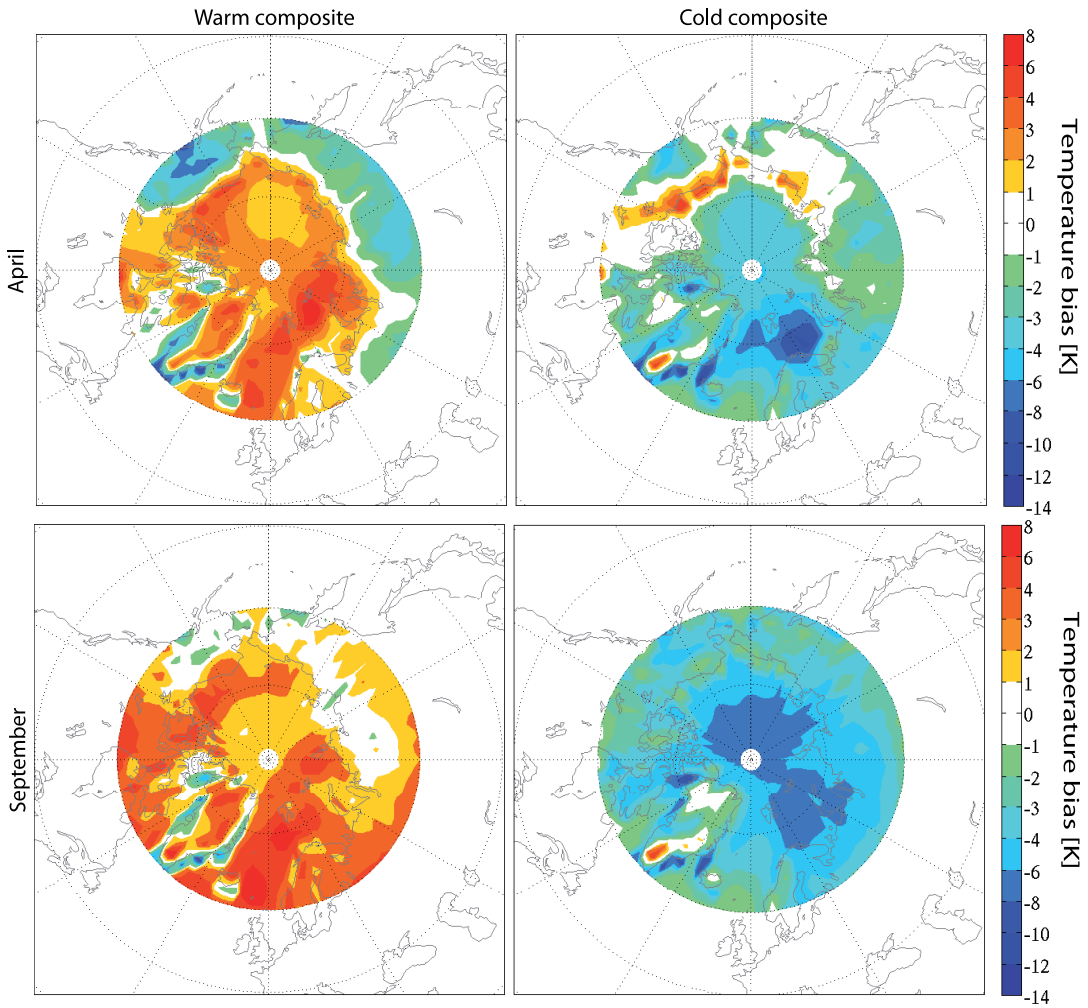

Figure 2.2: *Bias [K] of the surface temperature (1970-1999) for the warm composite (left) and cold composite (right). The top panel shows the bias in April and the bottom panel shows the bias in September.*

hence leads to an increase in surface temperature (Robock, 1985, Hall, 2004). Holland et al. (2010) support this thesis by stating that models with thicker sea ice in the annual mean simulate less net longwave heat loss at the surface during winter months.

2.3.3 The role of the northward ocean heat transport

The ocean is an important factor in the climate system. In the Arctic and especially over the Barents Sea, where the surface temperature is influenced by the North Atlantic Drift Stream which brings warm ocean water to the Arctic region, the northward ocean heat transport influences the Arctic TAS. Koenigk et al. (2009) state that differences in sea ice concentration strongly affect the ocean heat release to the atmosphere. Consequently, local and potentially large-scale climate conditions are influenced by different sea ice conditions in the Barents Sea. Jungclaus et al. (2006) conducted a modeling study showing that an enhanced northward ocean heat transport can cause a reduction in

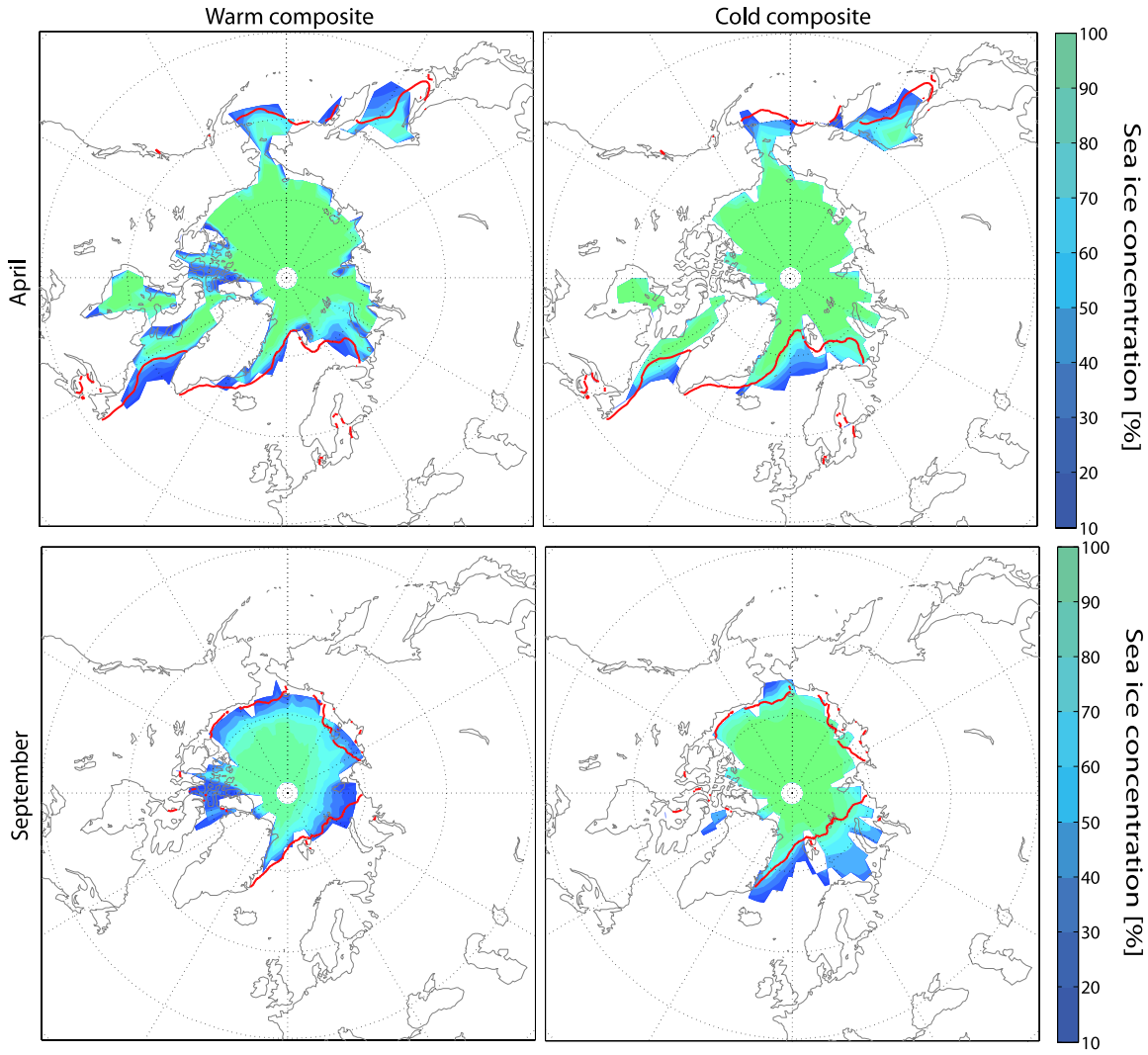

Figure 2.3: *SSea ice concentration [%] in April (top) and September (bottom) for 1980-2008, for the warm composite (left) and the cold composite (right). Only sea ice concentrations larger than 15% are shown. The red line shows the 15% line of the observations (HadISST). Also for the observations only sea ice concentrations larger than 15% are used.*

sea ice. This relation is observed across the CMIP3 models. The models simulating a stronger mean northward ocean heat transport, defined as the poleward flux at $60°$N, show a smaller sea ice extent in September and vise versa, shown in Figure 2.6. The correlation between the two quantities across the CMIP3 models is -0.72. When only the sea ice extent in the Barents Sea is used the correlation is -0.76. Since sea ice extent is also correlated with the TAS bias (Fig. 2.4), the ocean heat transport is also related to the TAS bias. Hence, those models which are already too warm for today's climate will probably warm more than average in a future climate. Figure 2.7 shows this dependency by correlating the future warming of each model with its current northward ocean heat transport. Including all the models results in a correlation of 0.48. But excluding the outlier (model 8, the same model that was excluded in Fig. 2.1) increases the correlation to 0.68. Furthermore, the correlation between

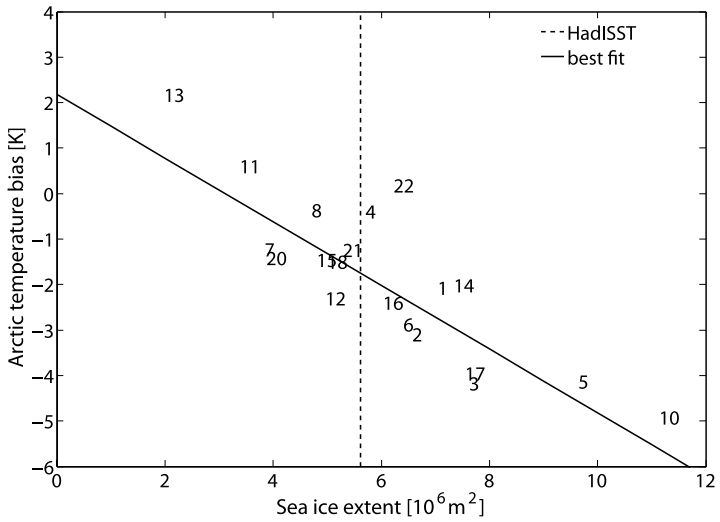

Figure 2.4: *Correlation (R=-0.84) across the CMIP3 models between the mean September surface temperature bias (using ERA40 as a reference) in the Arctic for 1980-2008 and the mean September sea ice extent for the same time period.*

the ocean heat transport of each model with its temperature bias is 0.44. And since the TAS bias is strongly related to the sea ice extent, the northward ocean heat transport influences sea ice extent in each model. It might be surprising that the northward ocean heat transport is responsible for the large spread of the models in their future warming projections since the northward ocean heat transport contributes only a small amount to the total energy budget of the Arctic (Serreze et al., 2007). But it has a strong influence on the sea ice extent by influencing the sea ice cover in the Barents Sea, where the main differences in sea ice cover are found (Fig. 2.2), which in turn affects the energy budget at the surface. Our results are supported by Holland and Bitz (2003) who find a significant correlation between polar amplification and control climate ocean heat transport. The correlation of the sea ice extent of each model with its northward ocean heat transport in their study is -0.67. It is likely that increased ocean heat transport results in a thinner sea ice cover (Holland and Bitz, 2003). The correlation between the northward ocean heat transport and the sea ice thickness in the Barents sea in this study is -0.61. By influencing the sea ice extent and thickness, the northward ocean heat transport has a crucial influence on how much energy can be absorbed and stored in the ocean, and more importantly how much of this energy is radiated back during winter. Boé et al. (2009a) find the capacity of the models to emit the stored energy in the oceans as one of the main reasons for the intermodel spread in the projections.

Meehl et al. (2000) compare two coupled climate models with different future warming and concentrate on regional processes, one of them being the sea ice mechanism. They state that ocean dynamics and heat transport significantly contribute to the model's response to sea ice developments. Additionally, they studied the changes in the ocean heat transport in a future climate and conclude that the changes in the ocean heat transport more than offset the influence on the decrease of sea ice area caused by changes in absorbed solar energy. Hence, a stronger ocean heat transport leads to a greater

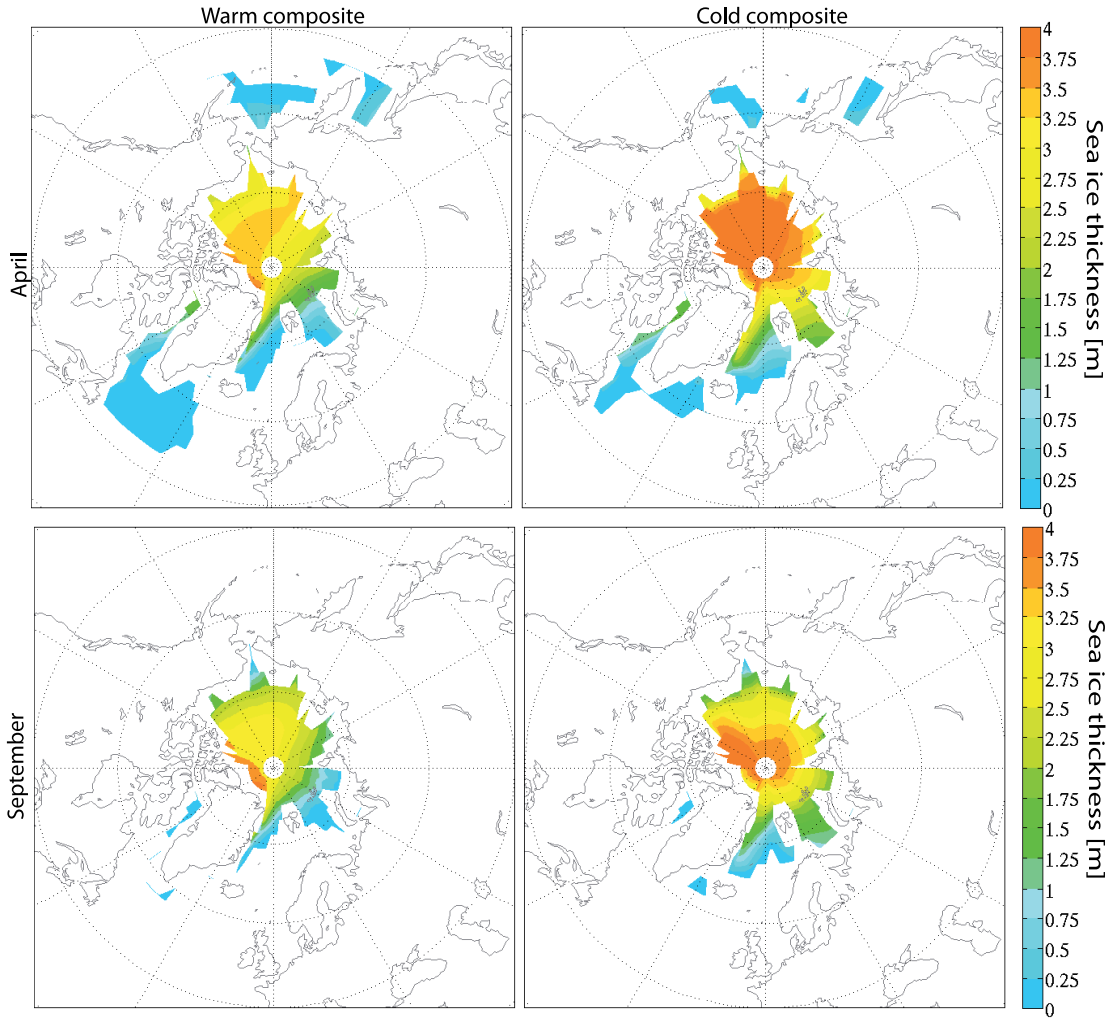

Figure 2.5: *Sea ice thickness [m] in April (top) and September (bottom) for 1980-2008, for the warm composite (left) and for the cold composite (right). Note that also the sea ice with a concentration smaller than 15% is shown here.*

decrease in sea ice and therefore to a greater warming than changes in the solar radiation budget. According to Meehl et al. (2000) changes in clouds characteristics are probably not the main reason for the large spread of the models in case of Arctic warming.

Comparing the amount of heat transported by the ocean in the models and the estimates by Trenberth and Caron (2001) (Fig. 2.7) reveal that all but one model overestimate the northward ocean heat transport. The same findings are reported in Figure 8.6 of the IPCC (2007) which shows the annual mean and zonally averaged ocean heat transport. However, observations of this parameter are difficult to obtain and large uncertainties exist. Bacon (1997) estimates the Atlantic ocean heat transport to be 0.35 PW (compare Fig. 2.7), much larger than that by Trenberth and Caron (2001) which is an estimate of the global transport. It must be noted though that almost all of the northward ocean heat at $60°$N is transported to the pole by the Atlantic. Ganachaud and Wunsch (2000) estimate the transport

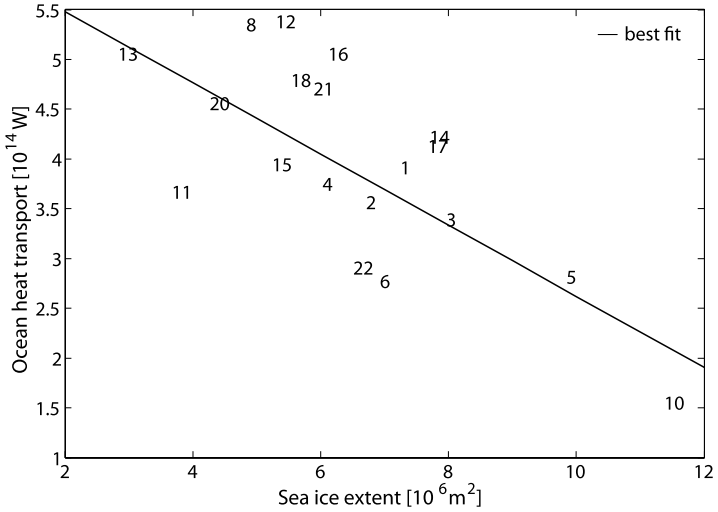

Figure 2.6: *Correlation (R=-0.72) across the CMIP3 models between the northward ocean heat transport and the sea ice extent averaged over the period 1970-1999.*

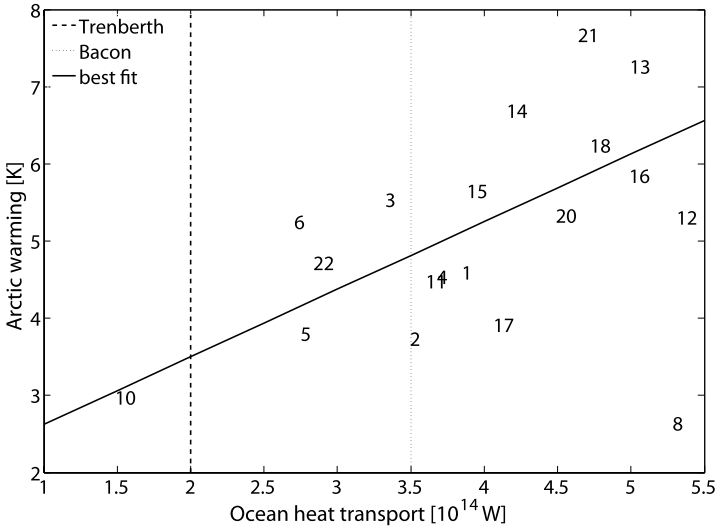

Figure 2.7: *Correlation (R=0.68 excluding model 8) across the CMIP3 models between future Arctic warming and the mean northward ocean heat transport (1970-1999). The dashed line is an estimate of the observed northward ocean heat transport by Trenberth and Caron (2001) and the dotted line is an estimate of Bacon (1997) at* $60°N$*. The best fit excludes model 8.*

across $50°$N to be 0.6 PW. Note that the decrease of the transport between $60°$N and $50°$N is only around a tenth of a PW (Trenberth and Caron, 2001). Monitoring ocean heat transport remains a challenging task, but more accurate estimates might help to constrain the AOGCMs in the future.

2.4 Conclusions

The large Arctic warming due to anthropogenic greenhouse gases and positive feedback mechanisms which cause a decrease in sea ice have been discussed before (Serreze and Francis, 2006, Winton, 2006, Wang and Overland, 2009, Holland et al., 2006, Stroeve et al., 2007, Zhang and Walsh, 2006) but the key factors for the spread of the CMIP3 model's future projectons, especially of sea ice and temperature, are still only partly known. In this study we show that large differences between the models in their simulated spatial patterns of current temperature (TAS) exist. Building two composites with the five models showing the highest and with the five models showing the lowest future temperature rise in the Arctic reveals new insights into model processes. Compared to observations the main differences can geographically be localized over the Barents Sea. This region, being influenced by ocean currents and their associated northward heat transport, shows the largest differences in sea ice cover as well as for TAS. The area covered by sea ice however is a major driver of the feedback mechanism in the Arctic. Furthermore, it has previously been shown that the capability of the models to radiate energy back from the oceans to the atmosphere contributes largely to the model spread of their future projections (Boé et al., 2009a). If the ocean is less covered with sea ice it can absorb more solar radiation and energy is radiated back more effectively since the sea ice has the function of an insulator. Thus, the ocean heat transport plays a key role in the Arctic climate system even if its energy flux to the Arctic is relatively small. The significant role this physical process plays in the whole climate system suggests that improving the simulation of ocean heat transport across the CMIP3 models would lead to more accurate future projections and smaller uncertainties across models. Although interannual variability of sea ice volume in the Barents Sea depends on local winds, the oceanic heat transport is important on longer time scales (Koenigk et al., 2009).

Improving model simulations of ocean heat transport implies studying the North Atlantic meridional overturning circulation (MOC) which affects sea ice in the Barents Sea through enhanced ocean heat transport in time periods with above normal MOC (Jungclaus et al., 2006). Sea ice extent and temperatures in the Barents Sea are also related to the North Atlantic Oscillation (NAO) since positive NAO-phases cause enhanced atmospheric and oceanic heat transport. As the ocean heat transport is a result of many complex physical processes and given that measuring ocean heat transport is difficult, expensive and requires long term monitoring to reduce the effect of decadal variability in the ocean, it may be very challenging to improve its simulation in a climate model due to several limitations such as model resolution, process understanding and data limitations.

Model evaluation is not a trivial task and different approaches exist. Gleckler et al. (2008) and Reichler and Kim (2008) define an overall metric of skill by evaluating a number of variables globally. However a ranking based only upon a single overall metric including many different variables may not be useful, as a single best model for all climate variables and regions is unlikely to exist. It is also unclear how rankings based on the present day mean climate relate to future projections (Knutti et al.,

2010, Tebaldi and Knutti, 2007). This is reflected in the current IPCC Report where all models are given equal weight and no performance metric is applied. However, a model ranking can be useful in case of an evaluation based on specific physical processes if they are shown to be relevant for a specific prediction. Some models do not meet basic performance criteria for a specific physical process (Eyring et al., 2007, van Oldenborgh et al., 2005) and therefore it is reasonable to exclude these models from the analysis (Knutti, 2010). In this study a successful approach of model evaluation is presented based on a few key processes that can be demonstrated to control the climate of a region.

In summary we show that the northward ocean heat transport contributes largely to the uncertainty in future Arctic climate projections based on correlations across the CMIP3 models. There is always a possibility that correlations occur by chance, or that they reflect that all models make similar simple assumptions. But we have demonstrated that the correlations across multiple variables provide a consistent picture and can be understood in terms of physical processes. Furthermore, the climate of the Arctic is determined by multiple components and processes that are represented quite differently in the various models. We are therefore confident that the correlations are indicating real differences in the physics of the models.

Comparing the CMIP3 Arctic temperature simulations with observations suggests that the expected Arctic warming is rather at the upper end of the simulated range because mean simulated temperatures of 1981-2000 are generally 1-2K too low compared to corresponding observations (Chapman and Walsh, 2007). The Barents Sea is an exception with a cold bias of 6-8K (Chapman and Walsh, 2007). Increasing model resolution on average indeed leads to more accurate results in case of Arctic climate simulations. The median of the cold composite of the amount of grid cells covering the area $60°$N- $90°$N is 768 compared to 4608 of the warm composite. We showed that the warm composite models simulate the current Arctic climate more accurately than the cold composite. Note that the resolution of a model may only be part of the story, as resolution is often also correlated with the overall complexity of a model. The number of people working on it, the experience in building a model, the amount of computational power and the amount of money spent on model development are also important factors for a model are expected to be correlated with resolution. Excluding the low resolution models in this specific case reduces the spread in future projections. This implies that the true future polar warming is likely to be at the upper end of the simulated range by the CMIP3 models. The lower end of the polar warming projections is then moved up from about 2.5K to about 4K. This means that a temperature increase of about 4-8K is expected by the end of this century in a SRES A1B scenario.

Acknowledgments

We thank Jan Sedlacek, Susan Solomon and Christof Appenzeller for fruitful discussions. We also acknowledge the modeling groups, the Program for Climate Model Diagnosis and Intercomparison (PCMDI) and the WCRPs Working Group on Coupled Modeling (WGCM) for their roles in making available the WCRP CMIP3 multi-model dataset. Support of this dataset is provided by the Office of Science, US Department of Energy.

Chapter 3

Regional climate change patterns identified by cluster analysis

Regional climate change patterns identified by cluster analysis

Irina Mahlstein and Reto Knutti

Institute for Atmospheric and Climate Science, ETH Zurich, Switzerland

(Published in Climate Dynamics, 2009, doi: 10.1007/s00382-009-0654-0)

Abstract

Climate change caused by anthropogenic greenhouse emissions leads to impacts on a global and a regional scale. A quantitative picture of the projected changes on a regional scale can help to decide on appropriate mitigation and adaptation measures. In the past, regional climate change results have often been presented on rectangular areas. But climate is not bound to a rectangular shape and each climate variable shows a distinct pattern of change. Therefore, the regions over which the simulated climate change results are aggregated should be based on the variable(s) of interest, on current mean climate as well as on the projected future changes. A cluster analysis algorithm is used here to define regions encompassing a similar mean climate and similar projected changes. The number and the size of the regions depend on the variable(s) of interest, the local climate pattern and on the uncertainty introduced by model disagreement. The new regions defined by the cluster analysis algorithm include information about regional climatic features which can be of a rather small scale. Comparing the regions used so far for large scale regional climate change studies and the new regions it can be shown that the spacial uncertainty of the projected changes of different climate variables is reduced significantly, i.e. both the mean climate and the expected changes are more consistent within one region and therefore more representative for local impacts.

3.1 Introduction

As a result of human induced changes in the atmospheric composition of trace gases, future climate is expected to change in different aspects, such as its mean state, interannual variability, and its extremes. Due to different feedbacks, climate will also change differently in the various regions in the world. Furthermore, the individual climate variables governing a climate regime show very distinctive patterns of change. Ideally, climate models should provide information on very small spatial scales, in particular for planning adaptation measures. Yet limitations in terms of processes and resolution prevent the interpretation of model results on single grid points. In order to simplify the communication of the results and to increase the robustness of the results, climate change patterns are therefore often aggregated over space. Regional climate change results have often been presented based on simple rectangular areas (Giorgi and Mearns, 2003, Tebaldi et al., 2004, 2005, Giorgi and Bi, 2005, Christensen et al., 2007) originally defined by Giorgi and Francisco (2000). The choice of these regions was rather pragmatic, based on a qualitatitive understanding of current climate zones and an expert assessment of the performance of climate models a decade ago. Here, a quantitive method is presented that attempts to address several shortcomings of the regions used so far. First, as computational capacity increases and models improve, the increasing complexity and resolution should provide information on smaller regional scales. Second, to facilitate communication of climate change results, regions should be based on similar expected future changes and not only on similar present day mean values. Third, climate is not bound to a rectangular shape. The shape of the region will rather depend on the variable of interest and the climate regime. Furthermore, local topography variations can influence climate. Especially precipitation patterns can vary strongly due to regional differences in topography. These small scale variations should be taken into account when looking at climate changes and defining regions for aggregating climate change results.

Cluster analysis methods can be used to define regions where the climate change signal is similar in all grid cells encompassed by the region. The hypothesis is that, based on the variable(s) of interest, there is an optimal number of regions where models can provide robust information. Model agreement generally improves on larger scales (Räisänen, 2007). Therefore, if a region is too small, the models may disagree in their signal. If the region is too large, the changes will be blurred and information is lost because different climate regimes are averaged together, e.g. averaging positive and negative precipitation changes will result in little net change. In addition, if the regions are very large, the information is no longer useful for local impacts, as the regional average is unlikely to be representative for local changes.

An algorithm is presented here which can contribute to answering the question of how and on what spatial scale regional climate change from global climate models should be communicated. There is of course no perfect definition of such regions. Different questions require different answers which one single set of regions will not be able to provide. People interested in future temperature change will not make best use to work with regions based on precipitation since changes in these two variables differ. Therefore, the goal is to present one possible procedure to define regions which can be used to find answers to the question asked, i.e. to group climate data in such a way that regions encompass similar characteristics. The characteristics looked at depend on the question of interest.

3.2 Data and Method

3.2.1 Data

This study uses up to 23 of the global coupled atmosphere ocean general circulation models (AOGCMs) (see Table 3.1) used for the Intergovernmental Panel on Climate Change (IPCC) Fourth Assessment Report (AR4) (IPCC, 2007) which are available from the World Climate Research Programme (WCRP) Coupled Model Intercomparison Project Phase 3 (CMIP3) (Meehl et al., 2007a). Detailed information of the participating models is available on the Program for Climate Model Diagnosis and Intercomparison (PCMDI) website: $http://www-pcmdi.llnl.gov/ipcc/about\_ipcc.php$.

All model data is regridded to a common T42 grid using a bilinear interpolation. One ensemble member of each model of the surface air temperature (TAS) and precipitation (PR) fields from the simulation of the 20th century (20C3M) and the scenario A1B (SRES-A1B) simulations are used to construct an equally weighted multimodel mean (M).
For the analysis, two 30-year monthly mean climatologies for the multimodel mean during the periods 1970-1999 and 2070-2099 were calculated. The simulated change in climate is simply the difference between these two time periods.

3.2.2 Method

a. Determination of the best cluster solution

The goal of a cluster analysis (CA) is to partition observations into groups (clusters) such that the pairwise dissimilarities between those observations assigned to the same cluster tend to be smaller than those in different clusters. Many different algorithms to obtain a classification exist in the literature (Jain et al., 1999). The one used for this analysis is the conventional k-means algorithm. It has the advantage of being simple and inexpensive. But on the other hand, the number of clusters needs to be preassigned before running the algorithm. Furthermore, when applying k-means on datasets with a large sample size and a relatively smooth character (i.e. lack of obvious groups) multiple solutions may exist which can not be improved any further by rearranging single objects of the different clusters. Although these solutions can be far away from the best solution (called the global optimum) the algorithm is trapped in a local optimum. Checking all possible combinations of the objects is computational infeasible due to the large sample size. Therefore, there is no way to determine whether a specific optimum is the global optimum (Philipp et al., 2007). One common way to apply k-means is to create seed partitions as first guesses, hence there is an arbitrary step in this procedure which leads to different realizations of solutions for the k-means algorithm applied on the same dataset. By running the algorithm multiple times the probability of converging to a local optimum of very low quality can be reduced. Other studies applied a similar technique in order to select the best cluster solution. Bonfils et al. (2004) repeated the clustering procedure several times with different drawings of initial centers. The best solution defined by the most distinct cluster was kept. Brewer et al. (2007a) ran the clustering procedure several times as well and checked visually that the clusters remained stable. Brewer et al. (2007b) decided to run the k-means algorithm 1000 times and the standard deviation of the value attributed to the centroid was calculated after they already obtained a solution. A low value

	Temperature data	Precipitation data
BCCR-BCM2.0 run1	x	x
CCCMA-CGCM3.1 run1	x	x
CCCMA-CGCM3.1-T63 run1	x	x
CNRM-CM3 run1	x	x
CSIRO-MK3.0 run1	x	x
CSIRO-MK3.5 run1		x
GFDL-CM2.0 run1	x	x
GFDL-CM2.1 run1	x	x
GISS-AOM run1	x	x
GISS-EH run1	x	x
GISS-ER run1	x	
FGOALS-g1.0 run1	x	x
INGV-ECHAM4 run1		x
INM-CM3.0 run1	x	x
IPSL-CM4 run1	x	x
MIROC3.2(hires) run1	x	x
MIROC3.2(medres) run1	x	x
ECHO-g run1	x	x
ECHAM5/MPI-OM run1	x	x
MRI-CGCM2.3.2 run1	x	x
NCAR-CCSM3 run1	x	x
NCAR-PCM run1	x	x
UKMO-HadCM3 run1	x	x
UKMO-HadGEM1 run1	x	x

Table 3.1: *Climate models and their runs used in this study.*

indicates that the centroids do not vary significantly and the found solution therefore is stable.

In this study the best solution is selected by comparing the within cluster sum of deviations (WWS) (Philipp et al., 2007):

$$WWS = \sum_{j=1}^{k} \sum_{i \in C_j} D(X_i, \overline{X}_j)^2, \tag{3.1}$$

where k is the number of clusters C, i is the object number, $\overline{X}$ is the centroid of the cluster, and D is the Euclidean distance between the objects and its cluster centroids:

$$D(X_i, \overline{X}_j) = \left(\sum_{l=1}^{m} (X_{il} - \overline{X}_{jl})^2 \right)^{\frac{1}{2}}, \tag{3.2}$$

where m is the number of parameters describing the object. Thus, WSS needs to be minimized in order for the solution to be as close as possible to the global optimum.

One way of testing the convergence of the algorithm is to compare the few best solutions out of a large sample of solutions. If these are very similar, the resulting regions are robust and it is unlikely that a much better solution exists. This is tested here by calculating a correlation that measures the similarity of the ten best solutions (lowest WWS value) at each grid cell. For a given grid cell and for each of the ten best solutions, the cluster where the grid cell belongs to is determined, and all the grid cells belonging to the same cluster are labelled with one, whereas all other grid cells are set to zero. The correlation between two such maps indicates whether the regions (to which the particular grid cell is assigned to in the two solutions) are similar in shape and size. The average of all 100 pairwise correlations is determined at each grid point in that way. Figure 3.1a shows the correlation indices at each grid point. For comparison, Figure 3.1b shows the best solution determined by the lowest WWS value. It shows a CA solution for 22 regions based on the multimodel mean M of the mean 30-year annual cycle of temperature data (details see Section 3.3). The high correlation leads to the conclusion that the solutions are of high quality since the different solutions do not differ greatly from each other. The largest differences are found at the edges of the clusters (compare with the regional classification shown in Fig. 3.1b), which is not surprising. The data used for the CA are relatively smooth fields, especially in case of temperature data. Precipitation data may be less smooth, but it is still rather difficult to define groups of data which are separated by a sharp border. Thus it is difficult for the algorithm to distinguish clearly between groups of data. In the following analysis, out of 60 realizations the best in terms of lowest WSS is chosen in order to guarantee a solution of high quality.

b. Defining the number of clusters

Several methods have been proposed to determine an appropriate number of clusters for a dataset. Kaufmann and Rousseeuw (1990) define a silhouette index which gives an idea of how well-separated the resulting clusters are. High values indicate that the objects are very distant from neighboring clusters. Wilks (1998) introduces a method based on the distances of the centroids. Furthermore, a stability index was tested which calculates the number of clusters leading to the most stable solution of all given clustering problems with a given data set. However, for the question addressed here, none of these methods were able to give a clear indication of how many clusters would be appropriate. Therefore, from a purely statistical side there seems to be no reliable procedure to determine the number

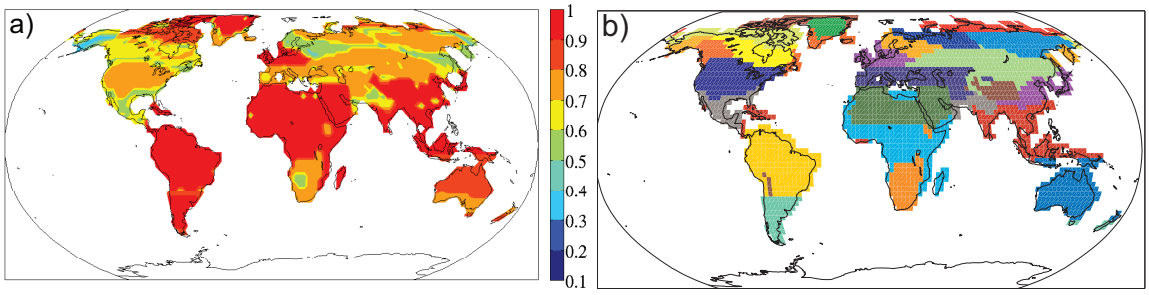

Figure 3.1: *Correlation of ten best k-means CA solutions for 22 clusters based on surface annual temperature data (a) and the best CA solution selected by the lowest WWS value (b). In panel b grid points marked in the same color belong to the same region.*

of clusters. This finding agrees with the conclusion of Philipp et al. (2007). Defining an appropriate number of clusters seems to require specific solutions which depend on the problem looked at. Bonfils et al. (2004), Brewer et al. (2007a,b) for example developed a method which involves the inter-group and the intra-group variance to find the optimum number of clusters.

For this study one possibility to estimate the number of clusters is by trying to find a solution that minimizes the total uncertainty in local climate change given the information about the regional changes. From an impact perspective there are two contributions to the climate change uncertainty at a single grid point: First, models disagree about the changes in the region. This can be quantified by the spread of the different CMIP3 models relative to the change in each region, averaged over all regions:

$$UM(k) = \frac{1}{k}\sum_{c=1}^{k}\left(\frac{\sigma(\overline{\triangle V_{M(c)}})}{\frac{1}{m}\sum_{i=1}^{m}(\overline{\triangle V_{M(c)}})_i}\right), \tag{3.3}$$

where $UM(k)$ is the model uncertainty for k clusters, $\sigma(\overline{\triangle V_{M(c)}})$ is the standard deviation across models of the mean expected change of parameter V in cluster c, m is the number of models used in the analysis and $\frac{1}{i}\sum_{i=1}^{m}(\overline{\triangle V_{M(c)}})_i$ denotes the mean of the expected change of parameter V in cluster c across models.

Second, an uncertainty is introduced by the difference between the local climate signal (e.g. expected temperature rise in one single grid cell) which does not necessarily correspond to the mean expected climate in a region (e.g. mean expected temperature rise over all grid cell within one cluster). This uncertainty can be defined as the spread of the change at different grid points within one region:

$$UC(k) = \frac{1}{k}\sum_{c=1}^{k}\left(\frac{\sigma(\triangle V_{G(c)})}{\frac{1}{g}\sum_{i=1}^{g}(\overline{\triangle V_{G(c)}})_i}\right), \tag{3.4}$$

where $UC(k)$ is the uncertainty of the climatic pattern within one cluster for k clusters, $\sigma(\triangle V_{G(c)})$ is the standard deviation of the expected change of parameter V across all the grid cells belonging to cluster c, g is the number of gridcells within cluster c and $\frac{1}{g}\sum_{i=1}^{g}(\overline{\triangle V_{G(k)}})_g$ is the mean expected change of parameter V in cluster c.

If the world is divided into many but very small regions, the models will often disagree on the projected changes. On the other hand, if a small number of large regions is chosen, the models will agree better but the changes aggregated over large regions may not be useful from an impacts point of view. The aim is therefore to minimize both types of uncertainties discussed above. Hence, adding up these two relative uncertainties and finding a minimum in this function (U_{tot}) is one way of defining an optimal number of clusters in terms of uncertainty. In order to reduce the noise in these functions the average of the best five solutions defined by the lowest WWS is taken.
This method was applied on univariate datasets. In most studies performed before, as well as in the IPCC reports the changes in climate are communicated for only one variable at a time, such as temperature or precipitation. Therefore, the CA is executed for one variable only. More information

can be found by performing a CA for precipitation and temperature combined. These results compare very well with the Köppen-Geiger climate classification (see Section 3.3.3).

3.3 Results

The best information about the expected changes can be provided by carrying out a CA for the different variables individually. Changes in precipitation are substantially different in where they are most pronounced as well as the direction of change and differ compared to patterns of temperature change. Therefore, the shape and the number of regions depend on the variable of interest.

3.3.1 Comparison to the old set of regions

In order to decide whether the new regions contain more information in terms of spatial and model spread of each variable, the same number of regions (22) as in the old set used by previous studies (Tebaldi et al., 2004, Giorgi and Bi, 2005, Christensen et al., 2007, Furrer et al., 2007a) is generated. The regions are based on the monthly means of the current 30-year climatology (1970-1999) of the multimodel mean M of the variable of interest (temperature and precipitation in this case), the projected monthly mean changes, altitude, latitude and the labels of the continent are included for each grid cell over land areas only. The reason for working with land areas only is simply that these areas are mainly the ones leading to impacts concerning society. Since Europe and Asia are not seperated by an ocean, these two continents denote one single continent termed Eurasia. The purpose of labeling the continents is to reduce the tendency of grouping grid cells in the same cluster which do not belong to the same continent. By doing so we introduce categorical values in addition to the smooth character of the other parameters. This leads to difficulties in the standardization procedure. This is circumvented by adding each continent individually to the dataset, i.e. for each continent a binary vector (of length n where n is the number of land grid points) is defined where elements are set to one for grid points belonging to that particular continent and zero elsewhere, rather than using a single vector where a different number is given to each continent. Furthermore, Antarctica was excluded in this study because both spatial and model variations are large and because in terms of impact studies it is of interest to make accurate projections in those regions which have direct influence on society. Thus, a CA for 22 regions needs to be computed not taking into account Antarctica. Hence, the regions defined here are based on climatic feature as well as on geographical and political considerations.

The choices made here on which parameters are included in the CA are partly subjective. Including continental labels simplifies communication because regions tend to be restricted to one continent only. The regions defined here are based on current climate as well as on the projected changes. An alternative approach would be to consider the changes only. However, from an impacts perspective it is of interest to look at existing climatic regimes as well as the expected changes (e.g. Tebaldi and Lobell, 2008), as a drying of 10 % for example will have more serious consequences in an area that is already dry and water limited compared to a wet area.

In Figure 3.2a and b the CA solutions based on temperature and precipitation data are shown. Compared to the regions proposed by Giorgi and Francisco (2000)(Fig. 3.2c), both the regions based on

temperature as well as on precipitation include climatic characteristics (e.g. the influence of mountains) as well as features which are of a smaller scale than found in the old regions. These findings are consistent with the fact that the model resolution has improved over the past decades, although it is not clear what size and shape the regions derived with the same algorithm applied on the output of older models would have looked like. But since the spatial scale is smaller, the uncertainty stemming from large regions which blur different climate zones should be reduced.

Table 3.2 lists an area weighted mean spread over all regions and all months for the old set of regions and the regions defined by CA. This spatial spread is defined as the difference between the 90th and 10th quantile of all values (grid cells) within one region. It is calculated in each region and for each month for the 1970-2000 climatology and the projected changes. These values are then averaged over all months and over all regions, weighting by the size of the region. This provides an aggregated measure of how similar the present day climate and the projected changes are within one region, with smaller values indicating a more homogeneous pattern within each region, i.e. a better cluster solution. Thus, Table 3.2 provides information about the homogenity of the climate within one region. This number should not be confused with UC, which is introduced to determine the number of clusters.

As Table 3.2 indicates, the spatial spread in the current temperature within the regions is reduced by more than three Kelvin, or almost 25 percent compared to the old regions. For the expected warming the spatial spread is reduced by 0.4 Kelvin, more than 26 percent. For precipitation the improvement for current precipitation rates is $1.2\,\mathrm{mm\,d^{-1}}$, for the expected change in precipitation the spread is similar in both cases. The spatial spread is therefore much smaller in the new regions, i.e. the regions capture the present day climate regimes and the expected changes better.

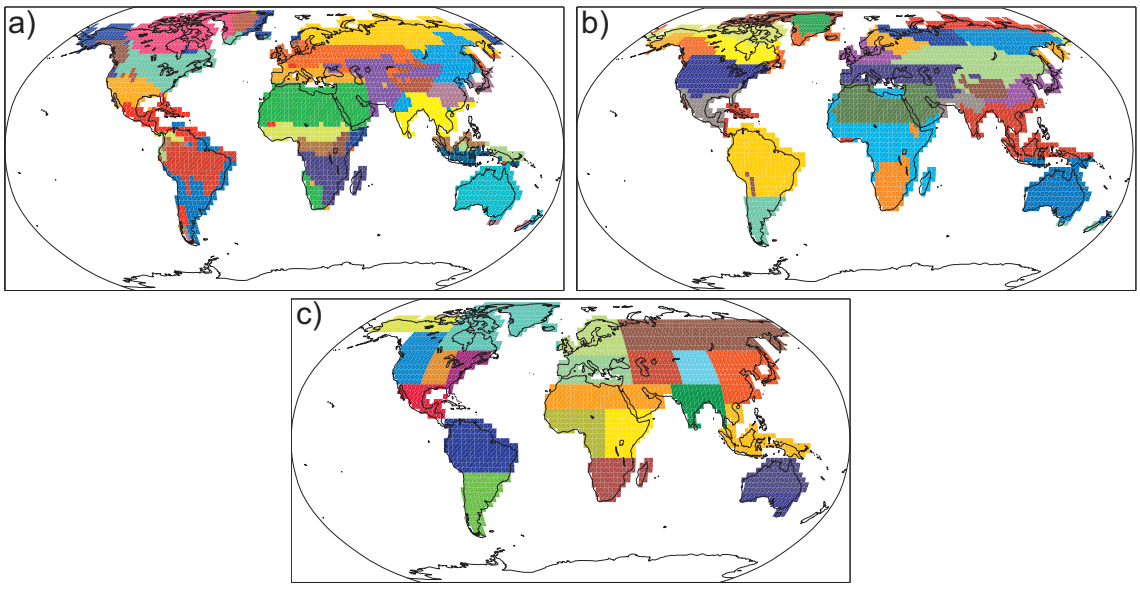

Figure 3.2: *Best solution of 22 regions generated using CA based on a) precipitation data, b) temperature data using the multimodel mean of the annual cycle and mean projected changes. For comparison the old set of regions is shown in c).*

On the other hand, there is a danger that the models agree less in the regions defined by CA since the models tend to agree less on smaller scales (Räisänen, 2001). Indeed, analysing the model spread in an analogous way to above over the old set of regions and the ones defined by CA (see Table 3.3), the weighted mean over all regions and months indicates a slight decrease in model agreement, except for the projected changes in precipitation, which shows a slight improvement. The differences, however, are negligible small. These numbers should not be mistaken with UM, which was introduced to find the optimal number of clusters.

Overall, the reduction in the spatial spread is much larger than the increased model spread and should thereafter lead to more consistent signals within regions.

3.3.2 The effect of resolution on the number of regions

As mentioned before, increasing complexity and resolution of models should provide information on smaller regional scales. Therefore, one may argue that the number of regions should increase for better models. From a modeling perspective, one criteria could be to minimize the total uncertainty (see section 3.2.2), i.e. minimizing the sum of the uncertainty in the spatial spread as well as in the model spread.

a. Temperature

Figure 3.3a shows the total (U_{tot}), spatial (UC) and model uncertainties (UM). As expected, the spatial uncertainty UC approaches zero as the number of clusters increases. This is expected since the fewer grid cells belong to one cluster, the smaller is the spread of the temperature pattern within this cluster. On the other hand, for the model spread the more clusters there are, the larger is the model spread UM. Adding up UM and UC leads to the function U_{tot} in which we seek a minimum in order to minimize the total uncertainty. Indeed, there is a minimum for about eight clusters but theses small variations are unlikely to be robust. For a large number of clusters the function converges to 0.35 (see Fig 3.3a). The results suggest that a range of values for the number of regions is possible without changing the uncertainty significantly. Having a large number of regions leads to the difficulty of how to communicate the findings in for example 50 different regions. By choosing a rather small number of regions we might loose information about regional climates. The number of regions is partly subjective but the conclusions will not strongly depend on the choices made. Figure 3.3b suggests a number of 35 to about 50 regions, because for more than 50 regions U_{tot} stays more or

	$T_{current}[K]$	$\triangle T[K]$	$P_{current}[mm\,d^{-1}]$	$\triangle P[mm\,d^{-1}]$
Old regions	12.9	1.5	3.4	0.49
Clustered regions	9.7	1.1	2.2	0.36
Difference	-3.2 (-24.8%)	-0.4 (-26.7%)	-1.2 (-35.3%)	-0.13 (-26.5%)

Table 3.2: *Spatial spread and improvement in the spatial spread of current mean temperature ($T_{current}$), of the expected changes of temperature ($\triangle T$), of current precipitation ($P_{current}$) and of the expected changes in precipitation ($\triangle P$) in the two sets of regions.*

	$T_{current}[K]$	$\triangle T[K]$	$P_{current}[mm\,d^{-1}]$	$\triangle P[mm\,d^{-1}]$
Old regions	5.7	4.3	1.2	0.50
Clustered regions	5.8	4.4	1.2	0.48
Difference	0.1 (1.8%)	0.1 (2.3%)	0.0 (0%)	-0.02 (-4%)

Table 3.3: *Model spread and changes in the model spread of current mean temperature ($T_{current}$), of the expected changes of temperature ($\triangle T$), of todays precipitation ($P_{current}$) and of the expected changes in precipitation ($\triangle P$) in the two sets of regions.*

less constant, i.e. the gain of information is small for more than 50 regions and the changes in U_{tot} are rather large for less than 35 regions. But as mentioned before, due to communication issues and based on subjective considerations we argue that an upper limit of 35 clusters and a lower limit of 20 clusters is desirable. According to theses limits and the function of uncertainty 35 regions would be optimal.

In Figure 3.3c and d the correlation index for different numbers of clusters is shown. This correlation index is derived by taking the mean of the correlations indices across all grid cells as shown in Section 3.2.2. For two clusters, the correlation index is very high as there are only few different plausible possibilities in clustering. The same is true for a high number of clusters. There is a minimum for about 80 clusters, apparently the solutions are most unstable for this number of clusters. Correlations are above 0.7 in all cases.

Taking into account the two contrary effects of either prefering a large number of clusters to minimize uncertainty, or rather fewer to guarantee stable cluster solutions, we conclude that the number of clusters for temperature should be between 30 and 35. The quantitative conclusions drawn here do not depend on the number of clusters, except for extreme choices. For illustration Figure 3.4a shows the CA solution for 33 regions.

By introducing more but smaller regions the question whether the model disagreement is too large needs to be addressed. Looking at the distribution of all possible simulated changes (i.e. every single grid cell of a cluster in every model) and by doing the same for the old set of regions we can compare whether the increase in the number of regions leads to a loss of information due to model disagreement. Note that this assumes that each model is an equally plausible representation of the real world, and that the models are approximately covering the range of uncertainty. These assumptions are strictly not correct but hard to overcome (Tebaldi and Knutti, 2007). For illustration the different distributions for South America are shown in Figure 3.5. Comparing Figure 3.5a and b it becomes obvious that there are different effects in different regions. The northernmost region has about the same distribution in both cases, the new regions provide no improvement in this case. The southern region has a distribution which is narrower in the case of the CA solution, the new regions show the advantage of having less uncertainty concerning the expected warming. But on the other hand the mountain region only found in the CA solution shows a rather broad distribution, but still being of the same range or even less compared to the two regions in Figure 3.5b.

b. Precipitation

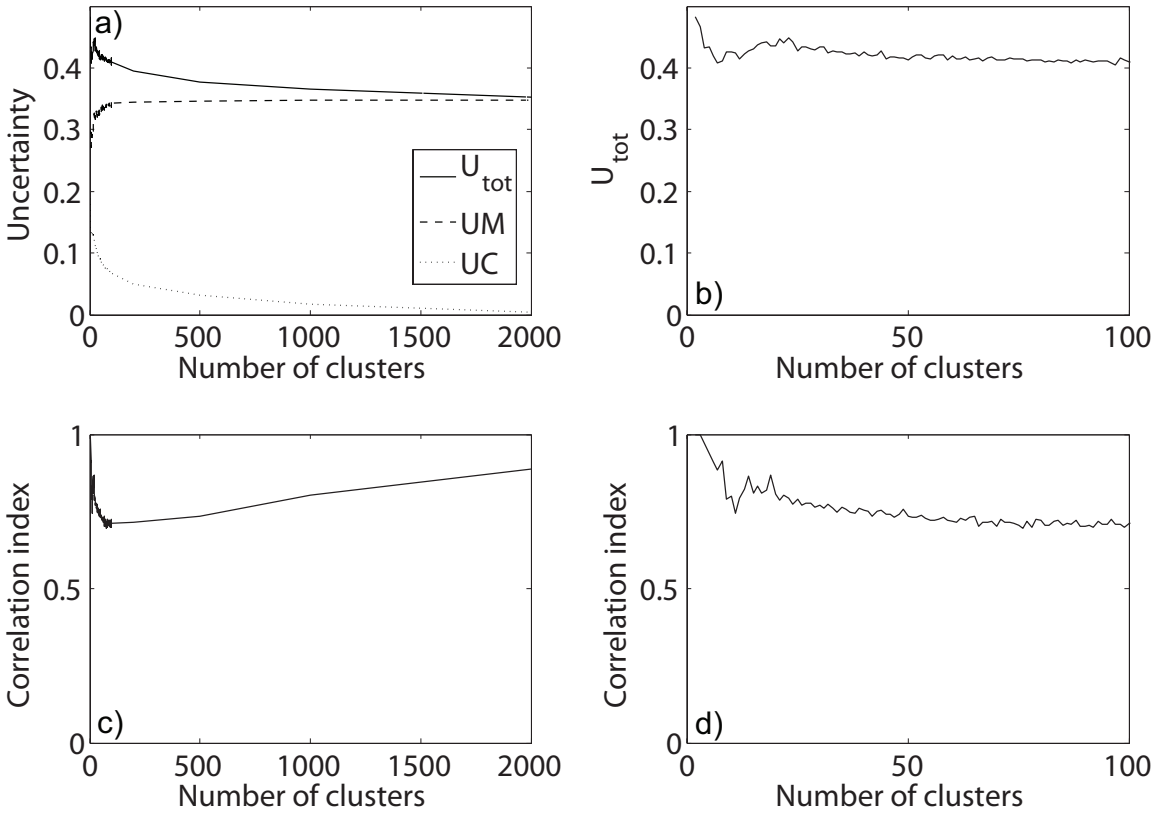

Figure 3.3: *a) Total relative error (U_{tot}), model uncertainty (UM) and the uncertainty of the climatic pattern (UC) for the CA solutions for different numbers of regions of the annual cycle of temperature, b) detailed view of U_{tot}, c) correlation for different number of clusters for the annual cycle of temperature and d) its detailed view.*

The case for precipitation it is not as clear as for temperature. As illustrated in Figure 3.6 the uncertainties are much larger for precipitation. Note that due to very small mean precipitation changes in some areas, the denominator of equation 3.3 and 3.4 leads to high uncertainties. Therefore, these two terms are limited here to a maximum value of 100%. We find a minimum in U_{tot} for about 200 clusters. But as mentioned above, due to communication problems the same lower and upper limit of 20 and 35 regions can be used for precipitation. The two curves of the uncertainty and correlation suggest that in case of precipitation it is desirable to have a rather low number of clusters. We believe that restricting the number of clusters to 20 to 25 makes best use of the information available. Both, Figures 3.6b and d suggest a low number of clusters since the uncertainty increases with an increasing number of clusters and the correlation decreases with increasing number of clusters. For more than 25 regions the function U_{tot} reaches its maximal value and the decline thereafter is rather slow. Furthermore, in case of precipitation it is rather difficult to find a clear signal of change. As shown in Zhang et al. (2007) a signal in twentieth-century precipitation trends is found only by averaging the data in latitudinal bands. Thus, using small regions the signal of climate change may be lessend. Therefore, it is more suitable to work with larger and hence fewer regions in case of precipitation to improve the

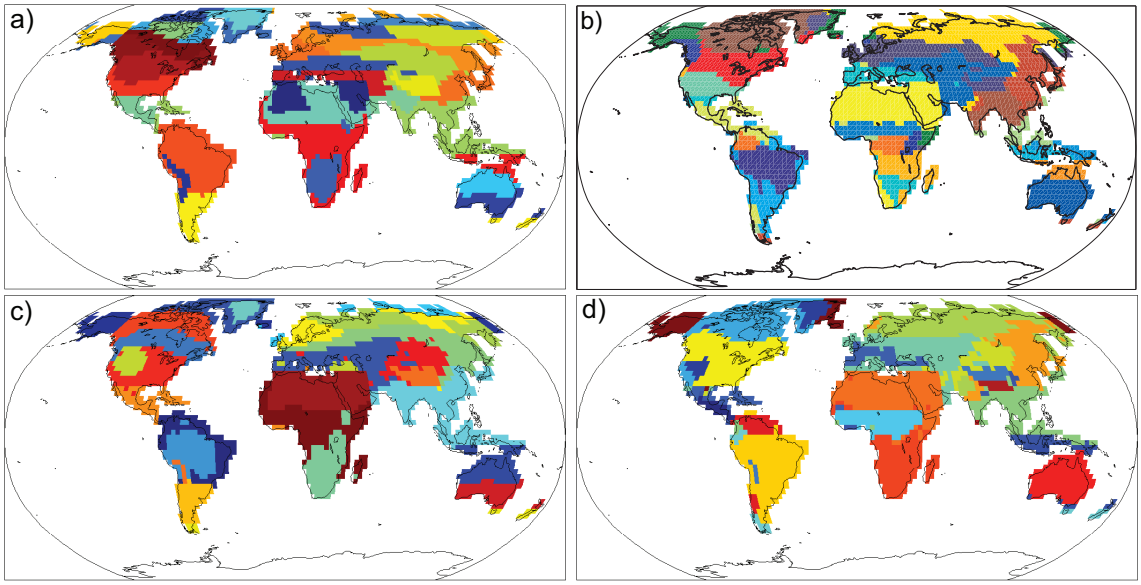

Figure 3.4: *CA solution for a) temperature based on the current mean and the projected changes in the annual cycle (33 regions), b) precipitation based on the current mean and the projected changes in the annual cycle (24 regions), c) current mean and projected changes of JJA temperatures (26 regions), and d) current mean and projected changes of JJA precipitation (22 regions).*

signal to noise ratio. In Figure 3.4b the 24 regions for precipitation is shown.

Again the question needs to be addressed whether introducing a higher number of regions leads to a decrease in model agreement which offsets the increased spatial detail. As for temperature data, the distribution of the projected changes in precipitation is derived by looking at the distribution of all the grid cells in one cluster for all models. In the case of precipitation the results are shown for North America. Note that due to the rather complicated regional mask, some regions shown in Figure 3.7 are not limited to North America, i.e. there are grid points on other continents belonging to the same region. For the analysis all grid cells belonging to the same region are taken into account, not only the ones shown in the frames. Figure 3.7 highlights two results. First, the spread (width of box plots) is slightly reduced by defining the regions using CA. Note again that in Figure 3.7 the spatial spread plus the spread of the models are included. Furthermore, by defining the regions using CA the signal for changes in precipitation can be enhanced. There are two cases in the CA-derived solution (the two northern most regions) for which both the 10 and 90 % quantiles are positive. For the old set of regions this is only true for one region.

c. Monthly versus annual data input

For some studies it is not desirable to look at regions based on the whole annual cycle but based on a specific season. Figure 3.4c and d show the CA solution for temperature or precipitation based on monthly means of the current climate and projected changes in June, July and August (JJA). The two solutions derived by using the annual cycle or only JJA show great similarities, but still there are some

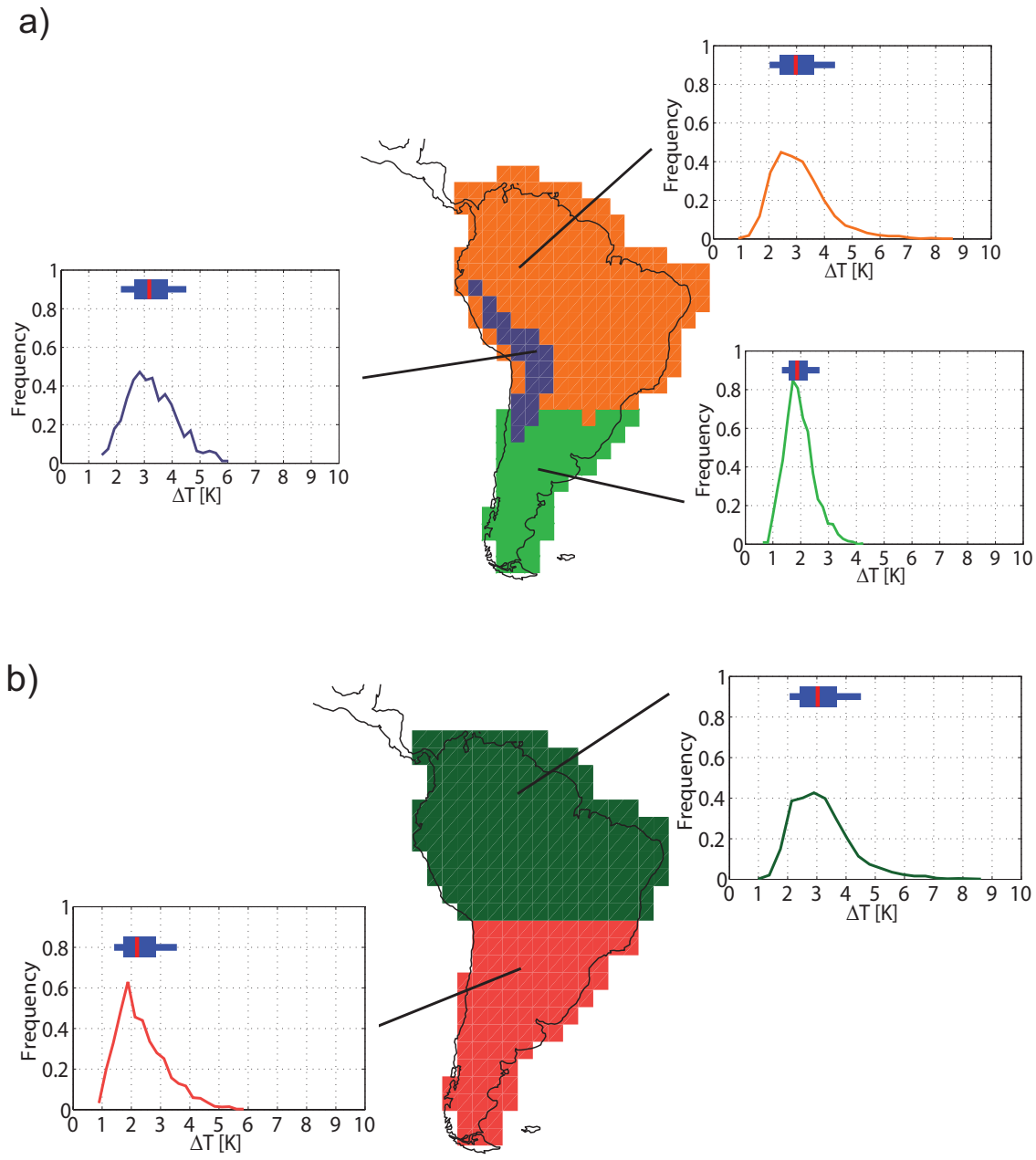

Figure 3.5: *a) CA solutions for 33 regions based on the annual cycle of temperature (shown here is only South America). b) shows for the same area the old set of regions. For each region the distribution of the expected warming for each grid cell in the region and across all the models is shown. The boxplot indicates the median (red), the 25 and 75 percent quantile (box) and the 10 and 90 percent quantile (blue line).*

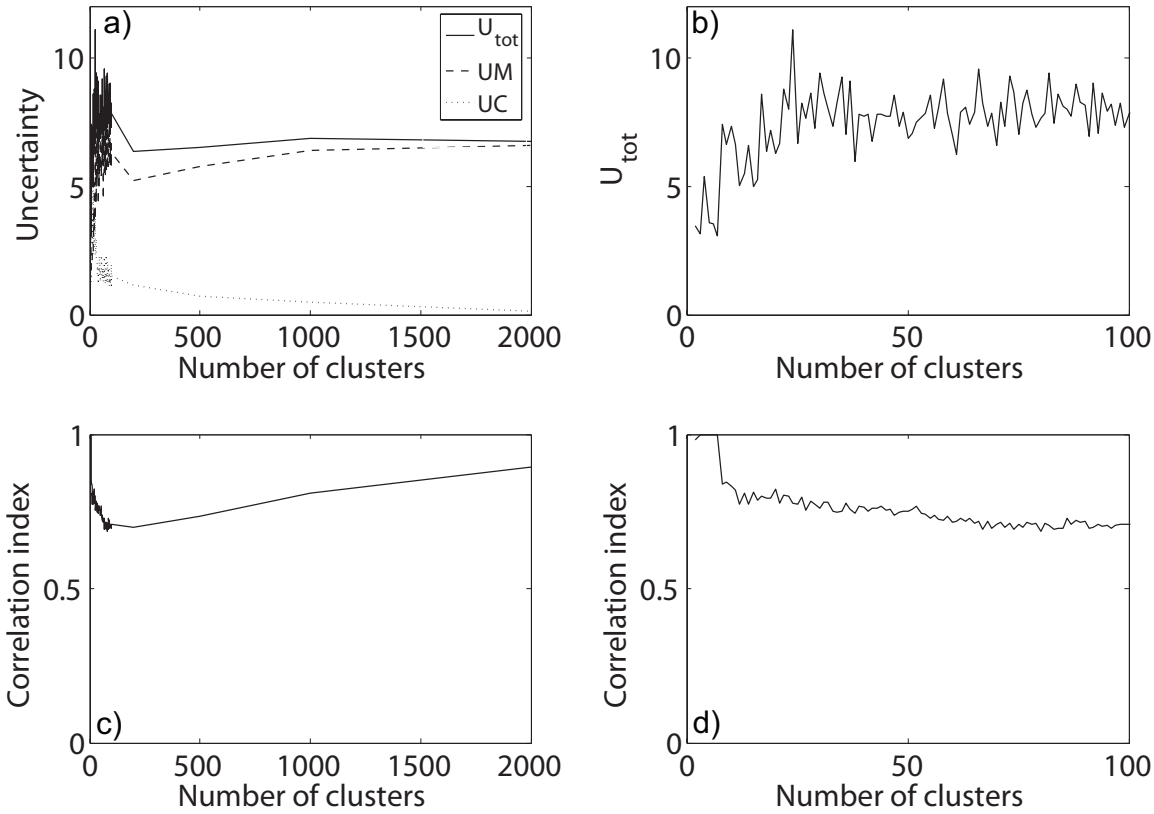

Figure 3.6: *a) Total relative error (U_{tot}), model uncertainty (UM) and the uncertainty of the climatic pattern (UC) for the CA solutions for different numbers of regions for the annual cycle of precipitation, b) detailed view of U_{tot}, c) correlation for different number of clusters for the annual cycle of precipitation and d) its detailed view.*

regional distinctions.

Whether the appropriate number of clusters is the same for JJA as for the whole annual cycle is unclear. As the analysis shows, for the correlation index the findings are similar to the ones in Figure 3.3 (compare with Fig. 3.8b). On the other hand, the results of U_{tot} is different (Fig. 3.8a) in that the function stays approximately constant for 25 to 30 clusters. Hence, in the case of a CA based on JJA temperatures a lower number of regions is favored, which in turn leads to more stable cluster solutions as well.

In the case of precipitation the two curves for U_{tot} and the correlation index look similar to the ones in Figure 3.6, although there are some differences. For JJA precipitation it is even clearer that fewer regions leads to more stable cluster solutions, and fewer regions are also favored by the function of U_{tot}. Therefore, about 20 to 23 regions is recommended in this case. Figure 3.4c and d show the suggested regions for temperature and precipitation based on JJA values.

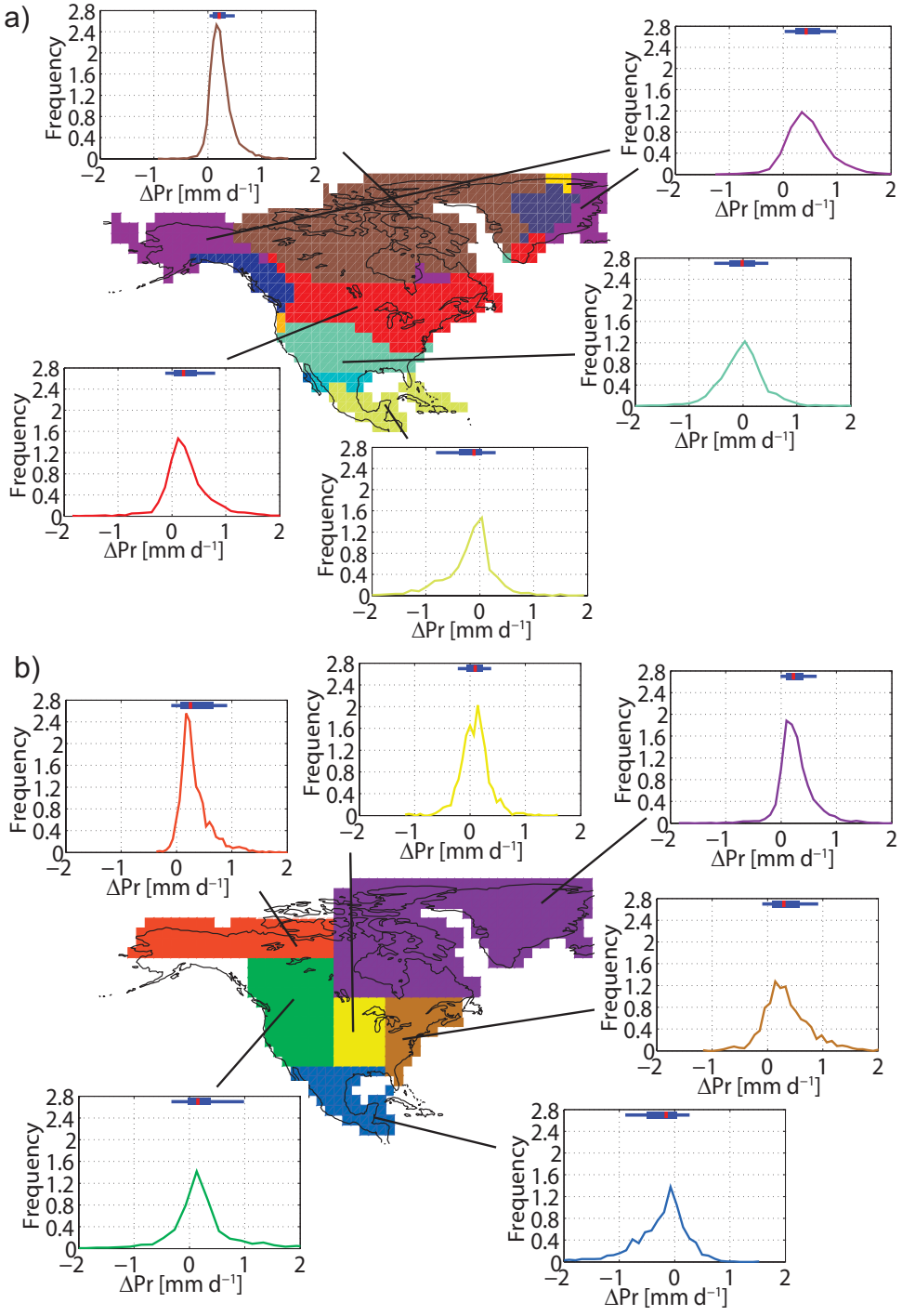

Figure 3.7: *a) CA solutions for 24 regions based on current mean and projected changes in the annual cycle of precipitation data (shown here is only North America). b) shows for the same area the old set of regions. For each region the distribution of the expected changes in precipitation for each grid cell in the region and across all the models is shown. The boxplot indicates the median (red), the 25 and 75 percent quantile (box) and the 10 and 90 percent quantile (blue line).*

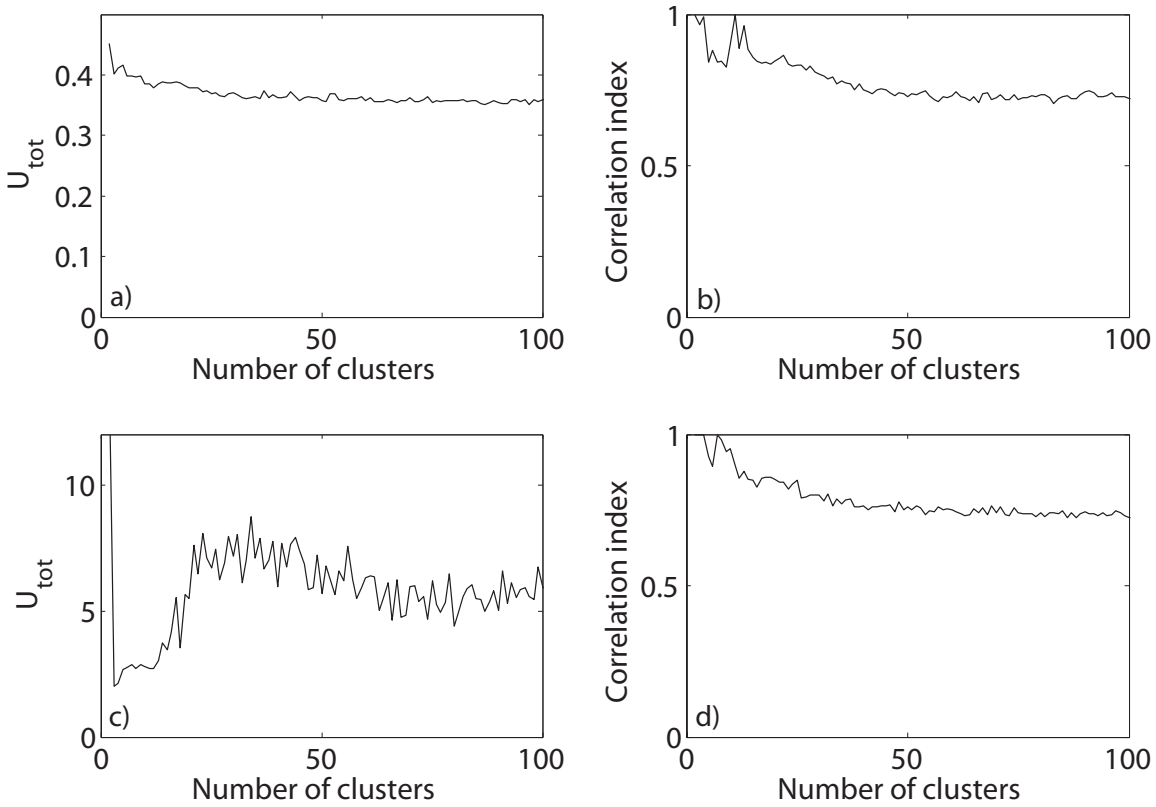

Figure 3.8: *Total uncertainty (U_{tot}) (a) and correlation index (b) of CA solutions for different numbers of regions based on current and projected changes in JJA temperature data and U_{tot} (c) and correlation index (d) for current and projected JJA precipitation data.*

3.3.3 Clustering temperature and precipitation

Various ecological risks are associated with the prospect of a changing climate. Novel temperature regimes as well as changes in precipitation lead to novel and disappearing climates by the end of the 21st century, which in turn may lead to novel species associations and other unexpected ecological responses (Williams et al., 2007). Therefore, in order to quantify the impact of climate change it may be best to look at changes in temperature and precipitation at the same time. By clustering current means of temperature and precipitation, as well as the projected changes in both of these variables, it is possible to identify regions where the current climate as well as both temperature and precipitation changes are similar. Similar patterns of current temperature and precipitation (but not trends) is the basis of the Köppen-Geiger climate classification, which represent the different vegetation groups, as plants are indicators for many climatic elements (Kottek et al., 2006).

Figure 3.9 shows that the cluster solution for 31 clusters (the number of Köppen-Geiger climate classifications) is very similar to the Köppen classification as given by Kottek et al. (2006). Note that a Köppen-Geiger climate classification can be derived based on observations, but here we use model data to calculate the classification. The advantage of the CA solution is that the projected changes are

already incorporated in the regional partitioning. Hence, the above defined regions are better suited to study climate change and climate change impacts.

Whether having 31 regions instead of 23 introduces more uncertainty again needs to be checked for temperature and precipitation. As before, the old set of regions serves as reference. The distributions are derived the same way as for Figure 3.5 and 3.7. Figure 3.10 shows that there is improvement in the temperature signal even for regions that are not only based on temperature data but on precipitation data as well. On average the distributions are narrower for the new regions. But again, as for precipitation, some of the regions shown are not limited to North America but for the analysis all the grid cells belonging to this region are used.

In case of precipitation the results in Figure 3.11 indicate some improvement as well. Over all, the distributions are narrower with one exception. The region to the very south shows a rather broad distribution. But on the other hand, for this region a clearer signal towards less precipitation can be found compared to matchable region in the old set of regions.

3.4 Conclusions

Climate change is one of the most serious problems that our society and economy is facing. In order to quantify the impact of climate change on a regional scale and to decide on adaptation and mitigation measures a quantitative picture of the magnitude of change of the different variables is necessary. So far, regional climate change results have often been presented on simple rectangular areas defined in a rather ad hoc way instead of being based on climatic features. A procedure is presented here which offers the opportunity to define regions in which certain variables of interest, e.g. the current climate, or the projected changes, have similar values. The number as well as the shape of the regions depends on the variable(s) and the time scale of interest. It is shown that by using a cluster analysis for the regional classification focused on one variable (e.g. temperature or precipitation) the spatial spread can be reduced significantly without introducing too much uncertainty in the model disagreement compared to the old set of regions used in previous studies (Tebaldi et al., 2004) and IPCC reports (Christensen et al., 2007). Furthermore, by using the uncertainty of the climate change pattern and the

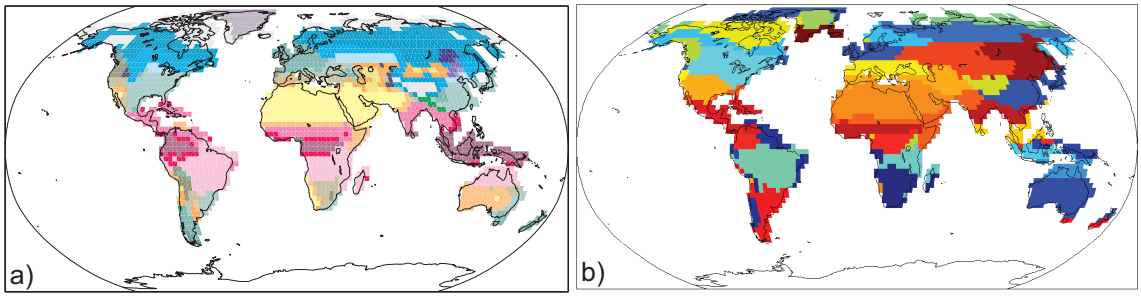

Figure 3.9: *a) Köppen-Geiger climate classification derived from multimodel mean data and b) CA solution for 31 regions based on the current mean and projected changes in the annual cycle of temperature and precipitation.*

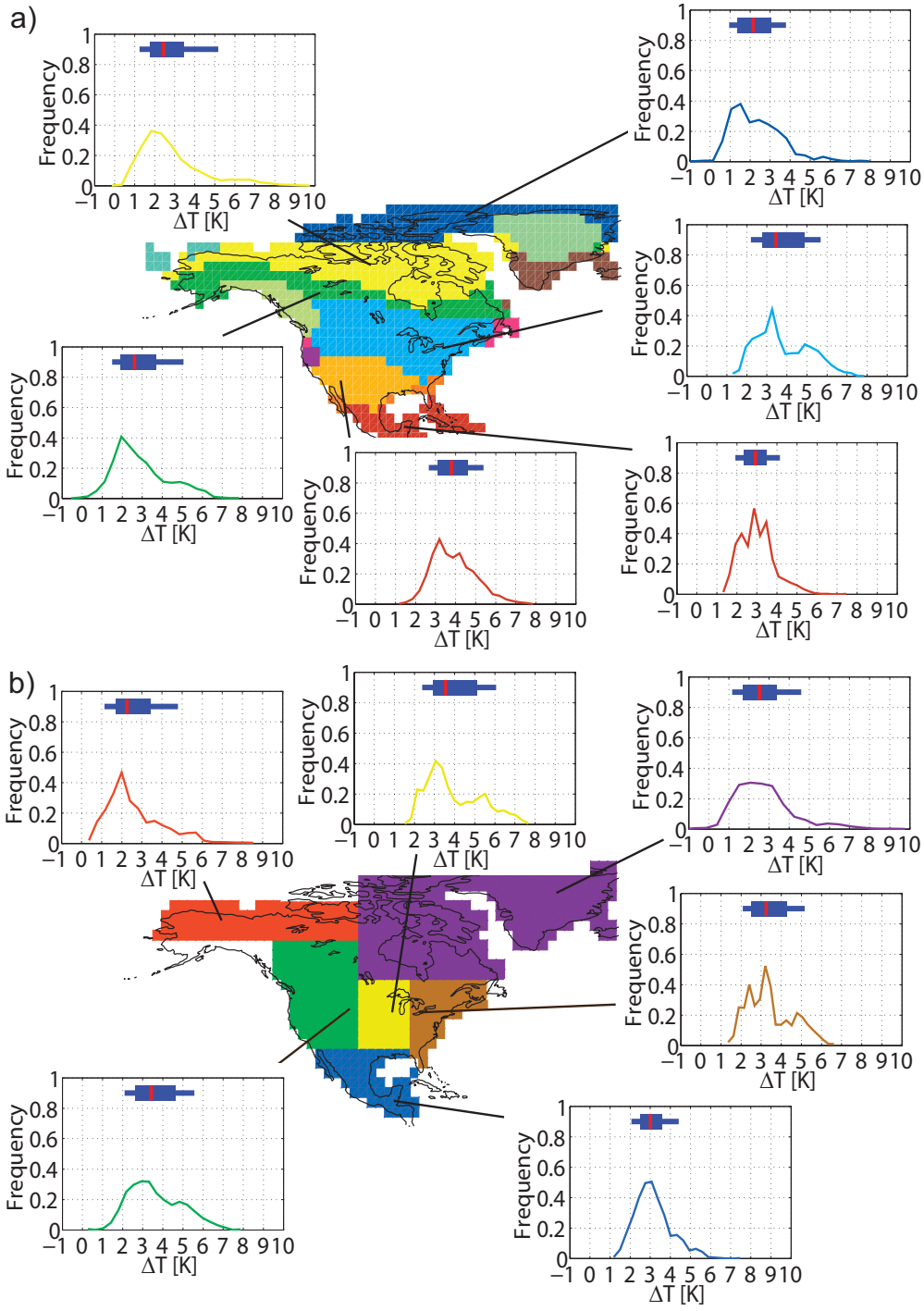

Figure 3.10: *a) CA solution for 31 regions based on the current and projected annual cycle of temperature and precipitation data (shown here is only North America). b) shows for the same area the old set of regions. For each region the distribution of the projected warming for each grid cell in the region and across all the models is shown. The boxplot indicates the median (red), the 25 and 75 percent quantile (box) and the 10 and 90 percent quantile (blue line).*

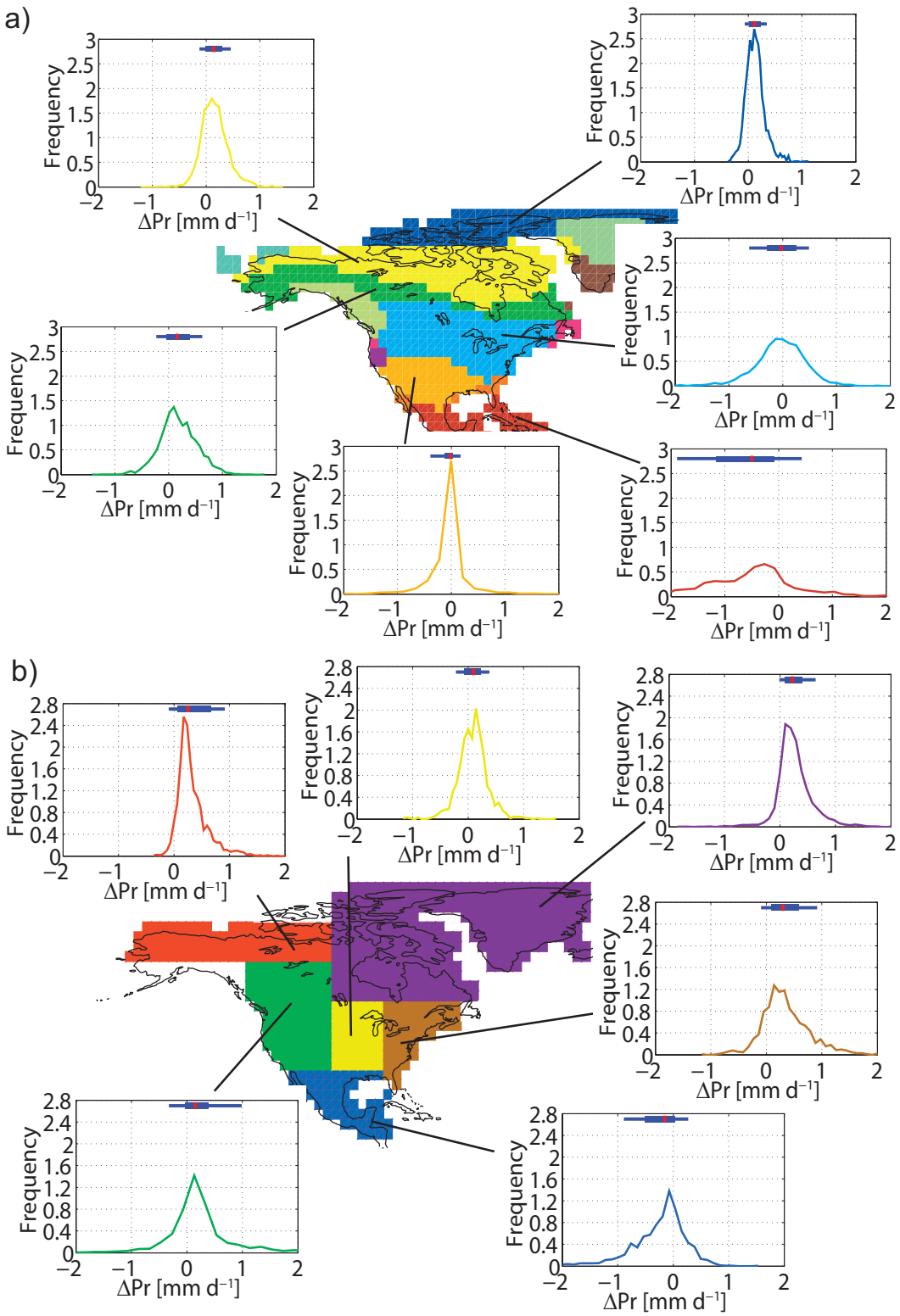

Figure 3.11: *Same as Figure 3.10 except that for each region the distribution of the projected changes in precipitation for each grid cell in the region and across all the models is shown.*

model disagreement in case of temperature we can conclude that the best information of the models can be obtained by increasing the number of regions compared to the old set of regions. Therefore, regions with climatic features of a smaller scale are found by clustering the data. On the other hand, due to large uncertainties, especially in the model agreement (Wang, 2005) in the precipitation data, we recommend to work with rather large regions. Although the number of regions is still larger for all the variables shown in this study than the number of regions used so far. This leads to regions encompassing climatic features of a rather small scale which in turn could introduce uncertainties due to model disagreement. But as could be shown in this study the total uncertainty, defined as spatial uncertainty and model disagreement, is on average still smaller than in the old set of regions.

One caveat with the presented algorithm is that there is the subjective component for the estimation of the optimal number of regions. There is small range concerning the number of regions which can be chosen from, the conclusions made here do not depend on the choices made. By introducing a lower and an upper limit of the number of regions we ensure a solution of high quality concerning the robustness of the cluster analysis solution as well as the total uncertainty including model disagreement and the local climate pattern. Furthermore, to derive a stable cluster analysis solution the multimodel mean had to be used with each model having an equal weight. This assumption of each model giving a plausible representation of reality is not necessarily true (Tebaldi and Knutti, 2007).

Cluster analysis also offers the possibility to combine different aspects of a climate such as temperature and precipitation, two characteristics which are important for impact studies because of their relevance in plant phenology and therefore in ecosystems. Comparing the Köppen classification with the regions defined by cluster analysis we find great similarities. Hence, these regions offer the opportunity to study climate change from an impacts perspective.

The proposed regions can be seen as a basis for discussions on the issue whether the old set of regions is still appropriate considering to the improvements that have been made in climate modeling, and whether it is justified to calculate regional climate change projections of different variables with the same set of regions if the pattern of different variables looks quite differently. Furthermore, it should be noted that the presented algorithm is not limited to the models and data used here. Instead of working with the CMIP3 models it is also possible to apply the same algorithm on regional model output or on data with a different resolution than T42.

Acknowledgments

We thank Christof Appenzeller, Jonas Bhend and Martin Jaggi for stimulating discussions. We also acknowledge the modeling groups, the Program for Climate Model Diagnosis and Intercomparison (PCMDI) and the WCRP's Working Group on Coupled Modelling (WGCM) for their roles in making available the WCRP CMIP3 multi-model dataset. Support of this dataset is provided by the Office of Science, U.S. Department of Energy.

Chapter 4

Substantial local warming unavoidable in low latitude countries

Substantial local warming unavoidable in low latitude countries

Irina Mahlstein[†], Reto Knutti[†] and Susan Solomon[‡]

[†]Institute for Atmospheric and Climate Science, ETH Zurich, Switzerland
[‡]NOAA Earth System Laboratory, Chemical Sciences Division, Boulder, CO, USA

(To be submitted)

Abstract

The observed warming of the Earth surface can be attributed to human influence with high confidence (Stott et al., 2000, IPCC, 2007). Successful attribution based on spatiotemporal patterns however does not imply significant changes at all locations; indeed only few studies have addressed the significance of local and regional signals relative to local variability (Giorgi, 2006, Baettig et al., 2007, Giorgi and Bi, 2009, Williams et al., 2007). Here we show that less than 1K global warming is sufficient for most locations areas over land for a significant temperature change to be identified with high confidence. Due to the small temperature variability in the low latitudes only a few tenths of a degree global warming already lead to significant changes. A local warming signal relevant for impacts has therefore emerged already in many developing countries, or will emerge in the next two decades irrespective of any plausible emission scenario. Most of the countries affected first by the warming emit small amounts of CO_2 and have contributed only marginally to the observed warming.

The Earth climate system has been warming over the past decades. The Intergovernmental Panel on Climate Change (IPCC) Working Group I Fourth Assessment Report states with very high confidence that human activity is responsible for most of these changes by emitting greenhouse gases into the atmosphere (IPCC, 2007). Attribution of surface warming is now possible on global and continental scales (Stott, 2003, Gillett et al., 2008), and improved observations allow attribution on climate variables other than surface temperature (Zhang et al., 2007, Santer et al., 2003, Gillett et al., 2003). Formal attribution of impacts is hampered by limited observations and confounding factors, most changes in biological systems (Rosenzweig et al., 2008) are consistent with a warming world. But while the world has undoubtedly warmed, some locations have not experienced significant changes so far, and few places have in fact seen clear shifts in precipitation or extreme events locally, even though those are projected from theory and models. The reason is that anthropogenic trends are superimposed on natural fluctuations on all timescales. This is analogous to real estate prices which on average have risen over the past twenty years, but not every persons house price or rent has increased. Higher prices usually appear earlier in densely populated areas at good locations. We intuitively understand this concept of an aggregated versus a local signal, yet the lack of warming over the past few years or the lack of a significant trend in some climate variables and locations is often misinterpreted to disprove climate change or to argue that local impacts are not severe. Here we approach the detection question from a local impacts point of view: at what time or in which scenario would we expect the local climate to be different from the preindustrial case with high confidence, taking into account spatial and temporal variations that may mask the trends?

The absolute warming observed so far is greatest in the high latitudes of the Northern Hemisphere (Serreze, 2010). Numerous studies point out the vulnerability of the ecosystems in high latitude regions to climate change due to the large absolute warming in these regions. According to climate model projections, future warming patterns will be similar to those observed. However, the regions showing the largest warming are also the regions featuring the highest interannual and interdecadal climate variability. The physical changes relative to the noise (defined here as the interdecadal variability) are therefore expected to be small. Thirteen atmosphere ocean general circulation models (AOGCM) are used to illustrate this assumption. As the region of interest is the low latitudes the models were chosen according to their ability to simulate tropical variability (see Methods). However, detection and attribution studies were shown to be insensitive to model weighting (Santer et al., 2009) and therefore the results are not changed significantly by the selection of models.

In order to detect local temperature changes the noise and trend is calculated separately for each grid cell. The noise in temperature is approximated by the interdecadal variability (see Methods), the signal (trend) is the difference between 1990-1999 and 1900-1999. The interdecadal variability of surface temperature (TAS) as illustrated in Figure 4.1a is highest in the Polar Regions, especially around the North Pole, and lowest in the Tropics. The signal of change is more pronounced over land than ocean and is particularly strong in the Northern high latitudes (Fig. 4.1b). Although the absolute trend is largest in the high latitudes, the signal to noise ratio (S/N) is rather low in this region due to the large interdecadal variability (Fig. 4.1c). The low latitudes with very low interdecadal variability but a detectable signal (Stott, 2003) therefore show the largest S/N. In summary the changes in TAS relative to its variability are greater in low than in high latitudes. Furthermore, this whole region shows

robust results across all models considered, with the only exception of the northwest coast of South America. The robustness of the results is shown in Figure 1d as model agreement (MA), defined as the mean change in temperature as calculated above averaged across all models, divided by the standard deviation across all models. Hence, a higher value means a better agreement. The low MA at the northwest coast of South America is probably due to the low topographical resolution of the Andes. In this case the high S/N should not be given too much weight. Note that the qualitative results are not sensitive to the time periods used in the 20th century. For example, the general patterns do not change using only data later than 1950 for the trend where data coverage and quality is much better locally.

In terms of impacts the signal to noise ratio is an important parameter. Changes in a climate with a large variability may have less severe impacts on ecosystems since species are adapted to large changes on short time scales. Species without the ability to adapt to environmental changes such as plants or ectotherms (Deutsch et al., 2008) are vulnerable to climate change. The smaller the global warming needed for the signal of change to emerge out of the natural variability, the more severe the impacts are expected to be. The amount of global warming for the signal of change to emerge from the noise can be estimated by comparing the TAS distribution functions of different time periods. Two samples of summer temperatures of two different time periods are significantly different when they do not originate from the same distribution (see Methods). Figure 4.2 depicts the global mean temperature increase for which 80% of the models indicate a significant change locally (see Methods). For the subsequent comparison to emissions the results are aggregated by countries. The results are similar to the S/N shown in Figure 1c. The low latitudes, namely Indonesia, the Middle East and large parts of Africa are already affected by a small increase in the global TAS. Figure 2 demonstrates

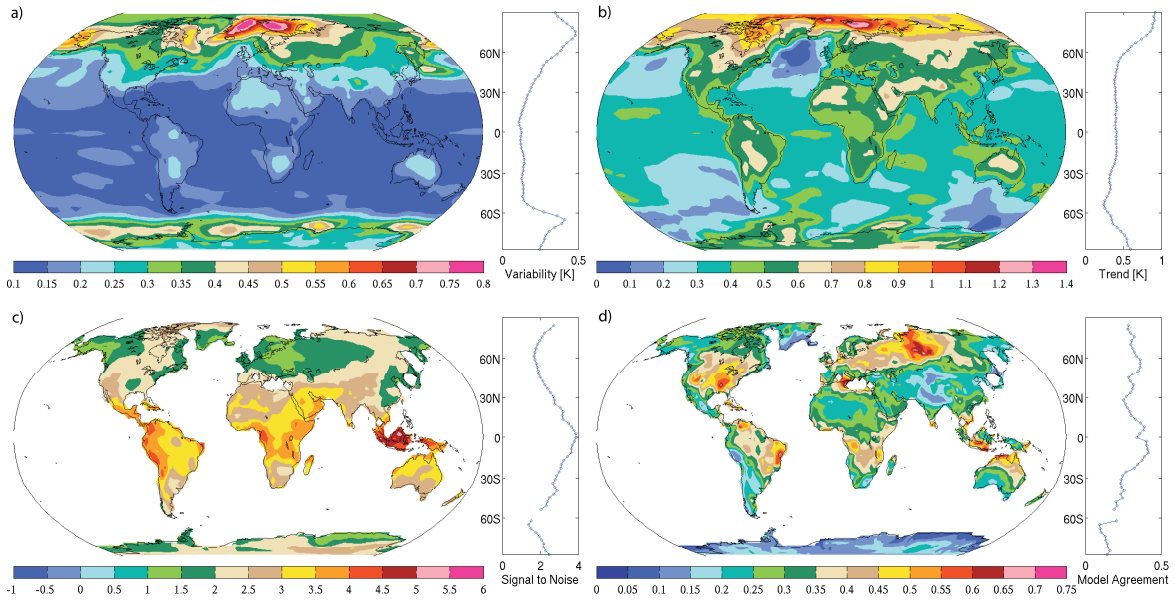

Figure 4.1: *a) Interdecadal variability (noise) of surface temperature (TAS), b) current signal of annual TAS calculated as the difference between 1990-2000 and 1900-2000, c) signal to noise ratio over land and d) model agreement over land. The blue line shows the latitudinal mean.*

that for most countries less than 1K warming is sufficient for significant local warming. These results demonstrate that many regions are already experiencing, or are committed to a significant local change in TAS. The commitment scenario (IPCC, 2007) projects a global warming of 1.2K, and zero carbon emissions today would result in a warming of 0.5 to 1K (depending on non-CO_2 emissions) (Solomon et al., 2009, Frölicher and Joos, 2009) but both are not economically plausible. All economically plausible scenarios predict a warming of near 2K or more, which would cause significant changes in all places. The reason why the results shown here are based on global temperature and not on a year of emergence is that the results are independent of an emission scenario.

The question whether a significant local change is actually measured is related, but complicated by the fact that observational records go only back to 1950. Therefore, when working with observations detectability is only achieved with a larger global warming than compared with model data starting at preindustrial conditions. The pattern of the results however is not sensitive to changes in the baseline time period or the transient climate response of the scenario, nor is the pattern significantly changed when annual means are used instead of summer means. The year when detection in an observational record since 1950 on a station level is possible is for most land parts later than 2015 as shown in Figure 4.3. However, for many parts in the world records do not reach very far into the past. In these cases, changes become visible even later than the proposed year in Figure 4.3. The same analysis shown here for temperature is also done for precipitation. However, only in a few land areas a signal is detected before 2100 even in the relatively high emission scenario A1B. The earliest locally significant signals appear after 2040. It is important to note that our findings do not contradict the detection study on precipitation by Zhang et al. (2007). Observed changes are significant when aggregated over space but not locally. Model projections indicate clear patterns of change in the water cycle if multiple models and scenario realizations are averaged (Knutti, 2010), and these changes are consistent with

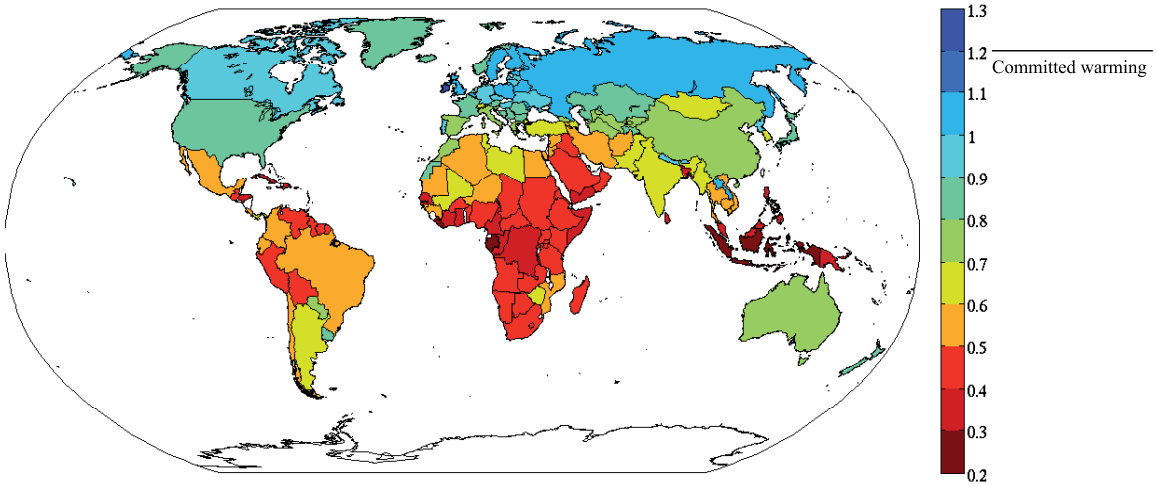

Figure 4.2: *Mean global temperature increase needed for a single location to country to undergo a significant change in surface temperature (TAS), aggregated on a country level. The black line denotes the committed warming if we all atmospheric constituents were fixed at year 2000 levels.*

theoretical arguments (Allen and Ingram, 2002). But because the variability is large, some locations may not experience any change, while others will see larger trends than projected. This is an obvious but often not appreciated result, and the argument of a missing observed local signal is often misused in the climate change debate.

The other striking result from our analysis is that most of the countries showing a significant change at a small global warming have low CO_2 emissions per capita
($http://www.iea.org/publications/free\_new\_Desc.asp?PUBS\_ID = 2143$). As shown in Figure 4.4 there is a negative correlation between the S/N and the CO_2 emission per capita. Countries affected most by the temperature increase are not the ones causing the increase. In contrast, some of the largest emitters in the past and present are among the least affected countries.

The results presented are remarkable for several reasons. First, we show that the low latitudes are most affected by temperature change relative to the local variability. The high latitudes will experience a large warming but at the same time their climate variability is also very large. The relative changes are important for ecosystems which have adapted to past climate variability. Furthermore, the local warming signal emerges from noise at global temperature increases that have already been observed or are unavoidable under any meaningful emission scenario. In contrast, local precipitation changes will not be significant in most places before about 2050 even with a perfect observing system, even though large scale changes are already detectable. Second, the local warming signal will emerge first from the noise for countries in low latitudes, even though their contributions to global greenhouse gas emissions are small. To estimate the risk of climate change, the local impacts, vulnerability and adaptive capacity need to be considered. Those are difficult to quantify in a single number, but they also tend to be unfavorable for developing countries in low latitudes. Note that relation between

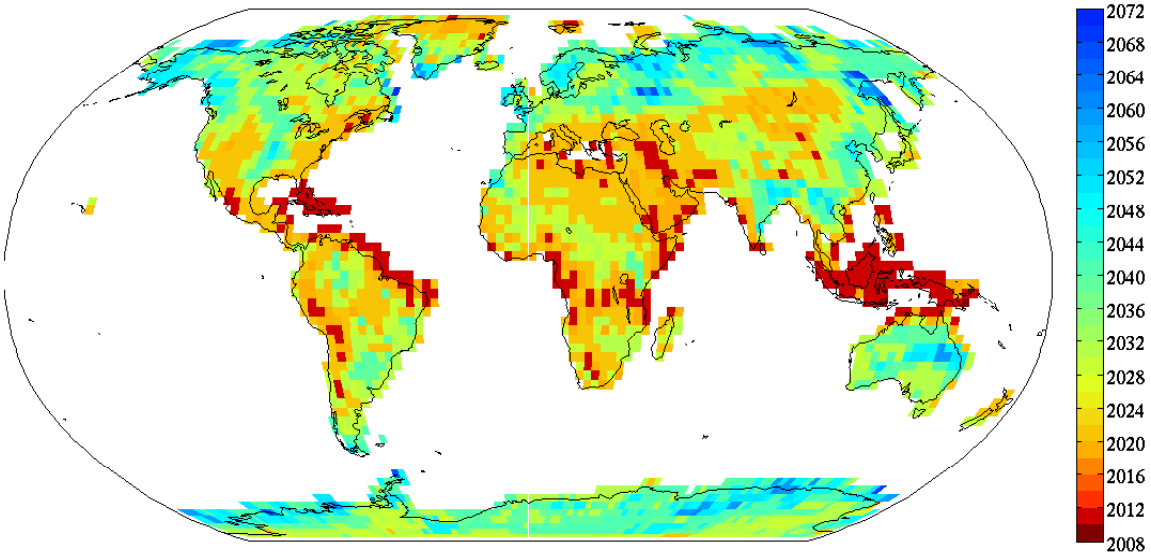

Figure 4.3: *Year of emergence on a grid scale level with 1950-1979 as a baseline for surface temperature.*

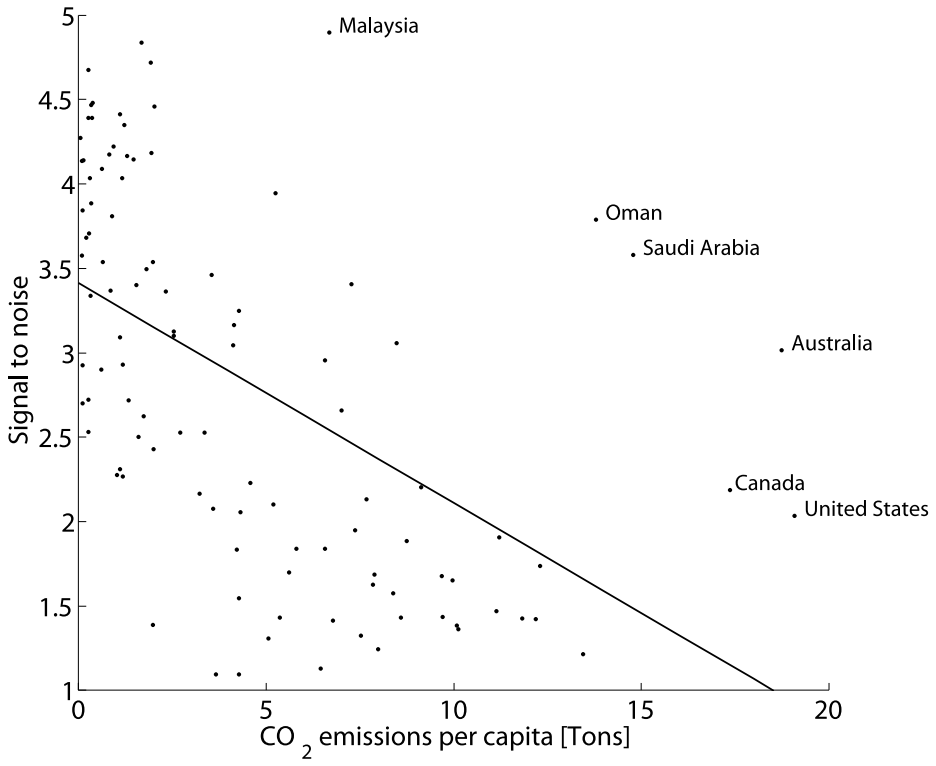

Figure 4.4: *Signal to noise ratio for each country versus CO_2 emissions per capita in year 2009. Only the outliers are labelled.*

emissions per capita and adaptive capacity for example are expected through financial assets. On the other hand, the fact that locally significant warming is tangible first in countries with low emissions has no obvious underlying economic or societal cause. But it is yet another issue that makes the climate negotiations challenging.

Methods

Variability test of the climate models

The AOGCM data is available from the World Climate Research Programme (WCRP) Coupled Model Intercomparison Project Phase 3 (CMIP3) (Meehl et al., 2007b). All data is regridded to a T42 grid. The variability of the sea surface temperatures (SST) is compared with NOAA/NASA (Advanced Very High Resolution Radiometer (AVHRR) Oceans Pathfinder SST data (Kilpatrick et al., 2001) over the time period 1989-2006. The models which pass two statistical for their ability to simulate the tropical variability are included in this study. The first test is described by Santer et al. (2008) and aims to estimate whether the interannual climate noise is realistically represented in the climate models. This test is. The second is the F-test which tests whether the natural variability of the models and the observations are similar or not. Of the models which passed both tests always the first run is used for the analysis. The models used are the following: BCCR-BCM2.0, CCCma CGCM3.1, CCCma CGCM3.1, CSIRO Mk3.0, GISS-AOM, GISS-EH, INMCM3.0, IPSL CM4, MIROC3.2(medres), MIUB-ECHO-

G, ECHAM5, UKMO HadCM3, UKMO HadGEM1.

Interdecadal variability
The interdecadal variability is estimated by detrending the time period 1900-1999. Then the standard deviation of the 10yr-means is calculated. The interdecadal variability is calculated individually for each model before averaging across models.

Significance test
Whether temperatures of two time periods are significantly different is tested on summer TAS means in a 30-years moving window at 10-years steps, starting with 1950-1979 as a baseline and ending in 2070-2099 for the SRES A1B model runs. Summer TAS is defined as the mean temperature of the three warmest consecutive months. This procedure is applied to each model and grid cell. The results are not significantly changed for different lengths of the moving window. The local warming is statistically detected when the two samples of the 30-years window are not drawn from the same distribution based on a Kolmogorov-Smirnov test with 95% significance. The last year of the moving window is taken as the year of emergence when the signal is detected in 80% of the models. This is done for each grid point and this year is then used to estimate the corresponding global temperature change based on the A1B simulation. Figure 4.2 simply averages the global temperature threshold across countries for comparison with Figure 4.4, but conclusions are similar without country aggregation.

Chapter 5

Small scale detectability of precipitation changes

Detection of human induced changes in precipitation on a global scale have only shortly been successful. By dividing the Earth into latitudinal bands Zhang et al. (2007) detected with the aid of the optimal finger printing method for some regions a drying or wetting over the past 100 years. However, if the same methods as used in Chapter 4 used for temperature are applied on the modeling results for precipitation it can be shown that detected changes on a grid cell level are still very sparse. Figure 5.1a shows the annual trend in precipitation computed in the same manner as for temperature and the same models as in Chapter 4 but using relative changes instead of absolute. The regions showing the strongest trend in drying are the regions which have the largest interdecadal variability, as well (compare with Fig. 5.1c). Figure 5.1b depicts the trends during dry season. Dry season is defined as the three dryest consecutive months in the year. The trend of the dry season is quite similar to Figure 5.1a, however trends are somewhat stronger for the dry season than for the annual mean. Model uncertainties are rather large in precipitation projections as shown in Figure 5.1d by the model agreement. The model agreement is the mean relative change across all models divided by the variability across all models. Hence, a high value means a good agreement.

Robust detection of changes in precipitation may be difficult for the following reasons: First, interedecadal variability is quite large in many regions. Especially the regions with an already dry climate and a strong drying trend feature a large variability. Second, the robustness of model projections is rather low. This is analyzed further below.

Analogous to Figure 4.3 and the method described in Chapter 4 the year when the signal emerges out of the noise is computed. The baseline time period is 1950-1979 and the end year of the 30-year window is taken in order to determine the year when the signal emerges out of the noise. Note that only regoins over land are considered. Figure 5.2 shows that in most regions over land a change in precipitation is not detectable before 2100 on a grid cell level (white areas). Shown are the results for three different assumptions: In Figure 5.2a the 90% quantile (very likely in IPCC terminology) of the models showing a result before 2100 and having the same signal in the trend of change (positive or negative) is used to compute the year of emergence. In Figure 5.2b the 80% quantile of the models

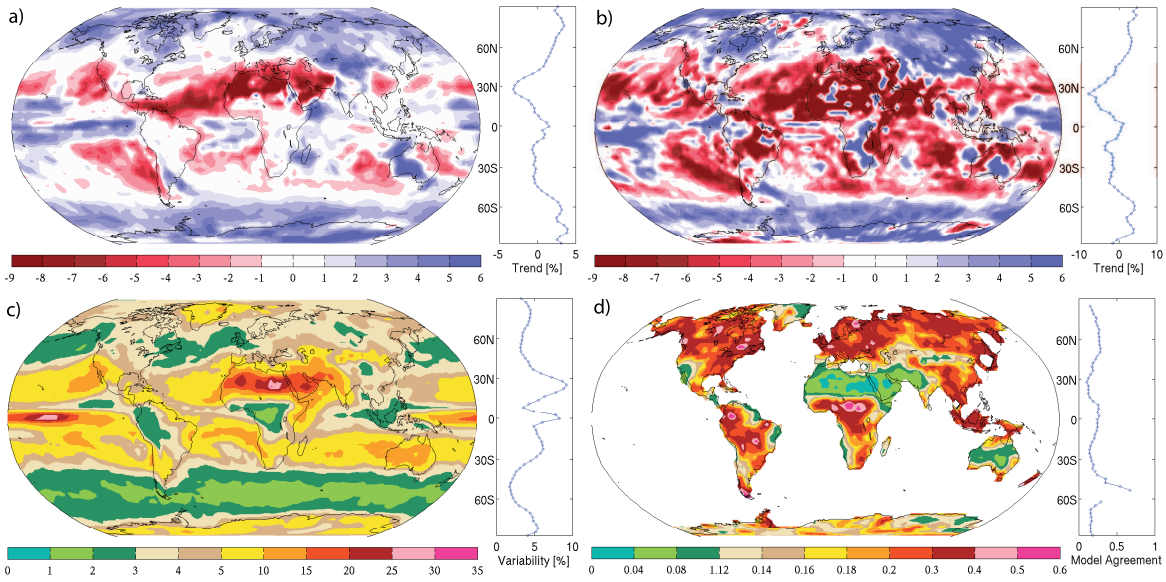

Figure 5.1: *a) Trend in annual precipitation estimated as the difference between 1990-1999 and 1900-1999, b) trend in precipitation during dry season estimated as the difference between 1990-1999 and 1900-1999, c) interdecadal variability and d) model agreement.*

showing a result and agreeing on the sign of trend is depicted. In Figure 5.2c the 66% quantile (likely in IPCC terminology) is used. No matter which assumption is used the white areas are very large and drying seems to be harder to detect than wettening. Interestingly, those areas which show the most severe drying do mostly not show up in the detection. One reason could be, as mentioned before, because of the poor model agreement. But one very possible reason could also be the large interdecadal variability in this area. This raises the question whether a severe drying in already dry areas is detectable at all.

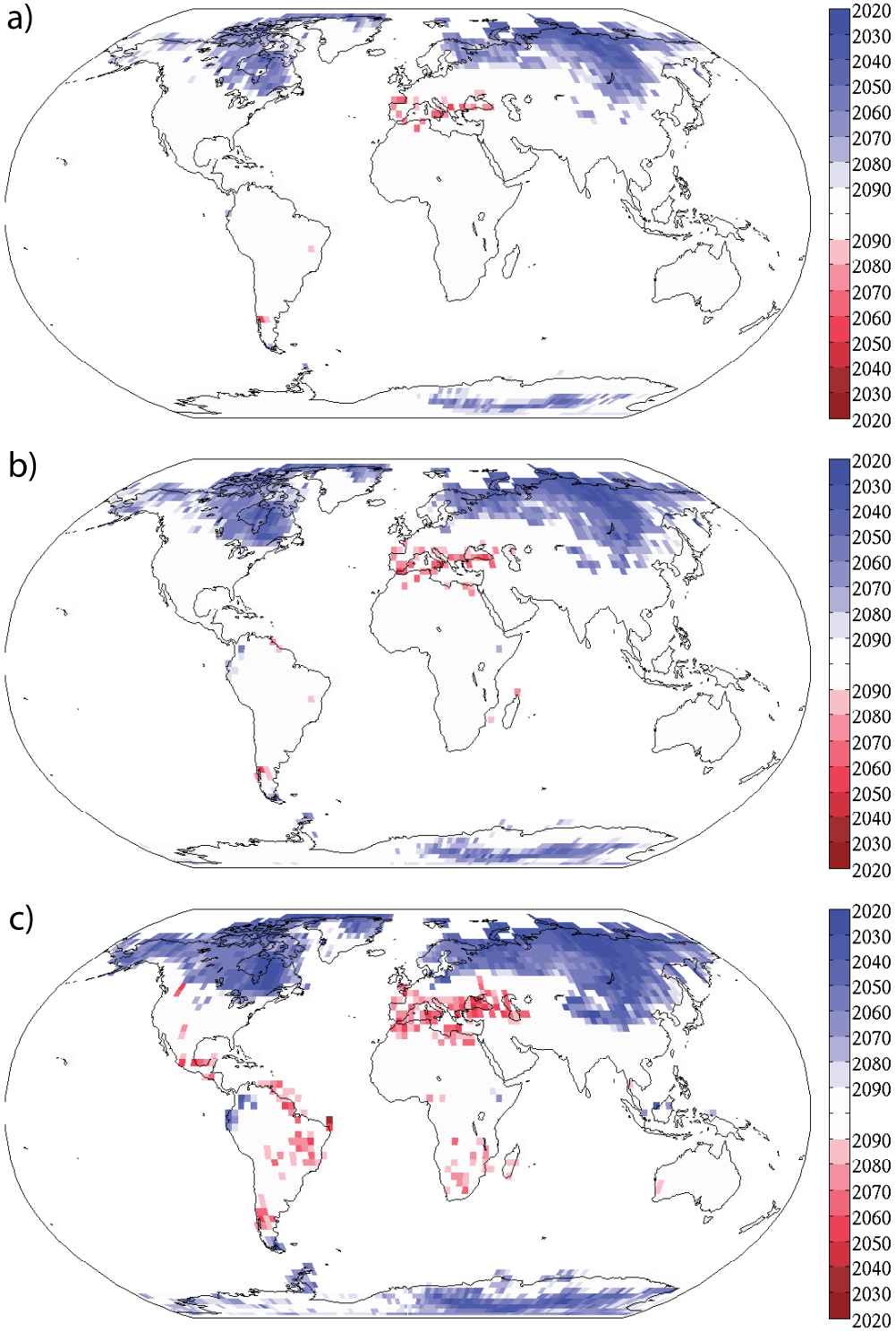

Figure 5.2: *Year when signal emerges of noise for precipitation over land. Blue colors indicate wettening, red colors indicate drying. a) using the 90% quantile (very likely), b) the 80% quantile and c) the 66% quantile (likely).*

Chapter 6

The unfavorable situation of developing countries in climate change

Temperatures are not warming equally across the globe. Landmasses are warming faster than oceans and the poles are more affected than other parts (Flato and Boer, 2001). However, studies focusing on the signal of change emerging of the natural climate variability, called the signal to noise ratio, find a different picture. The signal to noise ratio basically describes how far the changed climate is outside the natural variability of climate and therefore can not be explained by natural variability alone. When looking at the current signal to noise ratio, Chapter 4 shows that the greatest relative changes in temperature are found in the low latitudes where the changes are first detectable in time, as well. For precipitation detection on a small scale is problematic as described in Chapter 5.

For this study the year when the model emerges out of the noise is computed but no model weighting is applied. Therefore, up to 23 of the AOGCMS available from the World Climate Research Program (WCRP) Coupled Model Intercomparison Project Phase 3 (CMIP3) (Meehl et al., 2007a) are used. The year of emergence is computed in the same manner as in Chapter 4 and 5 for summer season in case of temperature and for dry season in case of precipitation using the time period 1950-1979 as a baseline. But in case of precipitation only 50% of the models need to show a year before 2100 and agree on the sign of the trend in order to increase detectability. The results are shown in Figure 6.1. Generally, in the high latitudes changes can be detected earliest. However, early detection is also possible for some countries in the lower latitudes.

As especially in case of temperature changes are earliest detectable in the low latitudes (compare with Chapter 4), but also for some low latitudes countries precipitation is early detectable, it is plausible that there are specific regions which are more affected by climate change than others. The countries located in the low latitudes are mostly developing countries. This suggests that developing countries are sooner and stronger affected by climate change, but it also implies that they are more vulnerable to climate change and have little capacity to adapt to the changes. To illustrate this hypothesis a climate change index is built consisting of four parameters: The first two parameters describe the year when the climate change signal is first detectable for the mean summer temperature and the mean driest three consecutive months in case of precipitation (see Chapter 4 for details). The third parameter describes the vulnerability of a country which is approximated by the percentage of people working

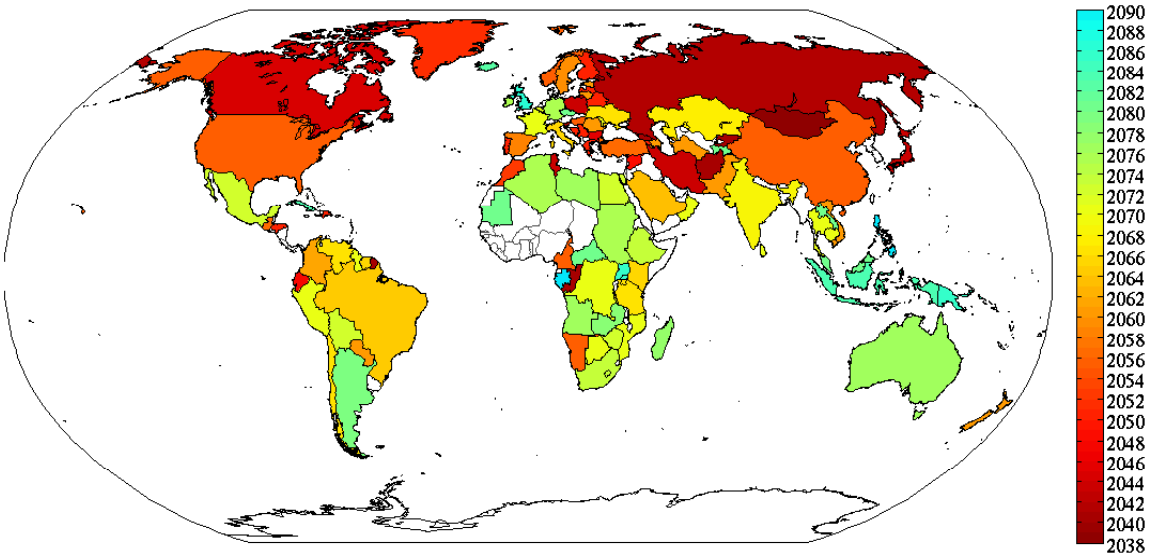

Figure 6.1: *Year of emergence for precipitation for the 50% quantile averaged over political countries.*

in the agricultural sector (AGRI) (FAO, 2009). Societies employing a large number of people in food production are more affected by climate change than service societies (Alexandratos, 2005). The number of people in the agricultural sector may be a very simple representative for the vulnerability. Brenkert and Malone (2005) mention the settlement/infrastructure, food, human population health and ecosystem sensitivity plus the water availability as factors contributing to sensitivity or vulnerability. However, at least two factors, food sensitivity and water availability are directly or indirectly included in the AGRI parameter. Yohe et al. (2006) define vulnerability as the ratio of exposure to adaptive capacity. Their exposure is approximated by the mean annual change in temperature. This definition is critical for several reasons: First, approximating the exposure with atmospheric parameters can be misleading. Second, they use only temperature for the approximation. Precipitation is not included. Third, the vulnerability is dependent on adaptive capacity. These are two different parameters which should not be mixed.

The fourth parameter used in this study is the Human Development Index (HDI) (ul Haq, 1995, UNDP, 2009) which describes the adaptive capacity. The HDI is a composite statistic and combines three dimesions which are life expectancy at birth, knowledge and education as measured by the adult literacy rate (with two-thirds weighting) and the combined primary, secondary, and tertiary gross enrollment ratio (with one-third weighting) and the standard of living as measured by the natural logarithm of gross domestic product per capita at purchasing power parity. The ability to react to changes in the environment are at least to a large part determined by the know-how and the wealth of a country. The HDI combines this information in one number. The only parameter which is not included in the HDI as an approximation for adaptive capacity compared to Brenkert and Malone (2005) is environmental coping and environmental adaptive capacity. This however is different for every species and therefore very difficult to obtain on a country level.

To combine the four different parameters each was classified individually in ten linear classes beginning at the minimum and ending at the maximum of each scale. The lowest class is unfavorable and is given 1 point, the highest is favorable and is given 10 points. For the two climatic parameters it means that the sooner (later) climate change is detectable the more unfavorable (favorable) it is for a country. For the HDI the lower (higher) and for AGRI the higher (lower) the value is the more unfavorable (favorable) it is. Averaging across all parameters yields a number which comprises the information how unfavorable or favorable the situation of climate change is for a country. These results are shown in Figure 6.2. The African continent is clearly affected in the most negative way. Large parts of South Asia are also in an unfavorable condition. Overall, the developing countries are in a worse position than the highly developed countries.

This climate change index provides an indication where the most affected regions are. However, the spread of the different parameters within one country can be very large as shown in Figure 6.3. Only in a few countries the changes in temperature and precipitation are both very unfavorable or very favorable.

Nevertheless, there is clear indication that some regions in the world are more affected than others. The most problematic regions are the poor countries which do not emit large amounts of CO_2. This is not surprising since the gross domestic product (GDP) is correlated with the HDI as the GDP is part of the HDI. Consequential the GDP and HDI are also correlated with the CO_2 as low income countries do not have the financial asset which could lead to high CO_2 emissions. Figure 6.4 illustrates that the countries in the more unfavorable situation emit less CO_2 than the countries in a more favorable situation.

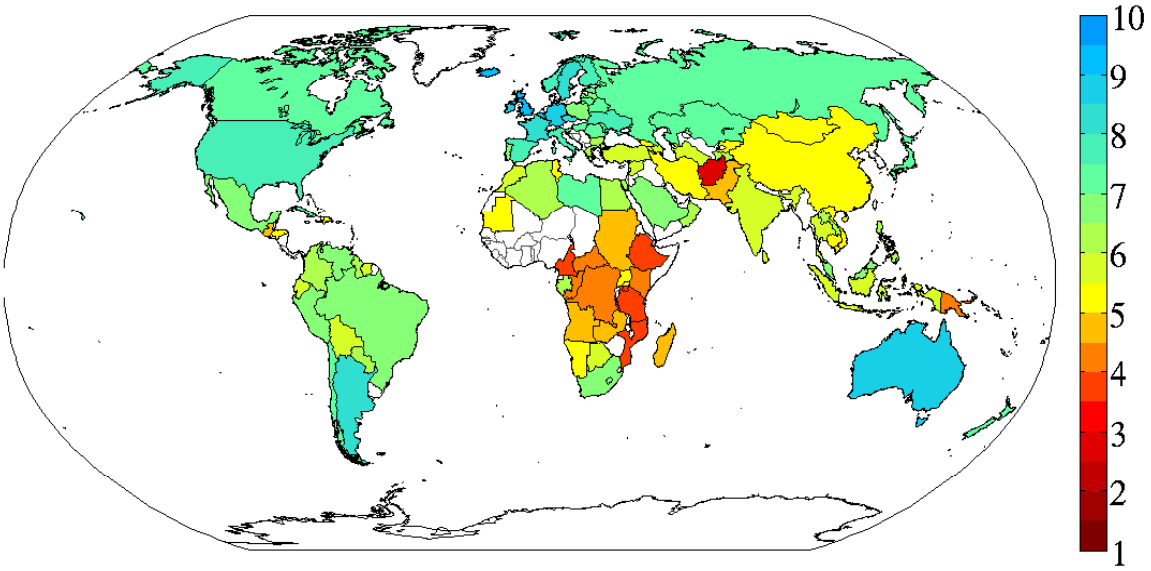

Figure 6.2: *Climate change index. A low number indicates unfavorable conditions whereas a higher number indicates more favorable conditions.*

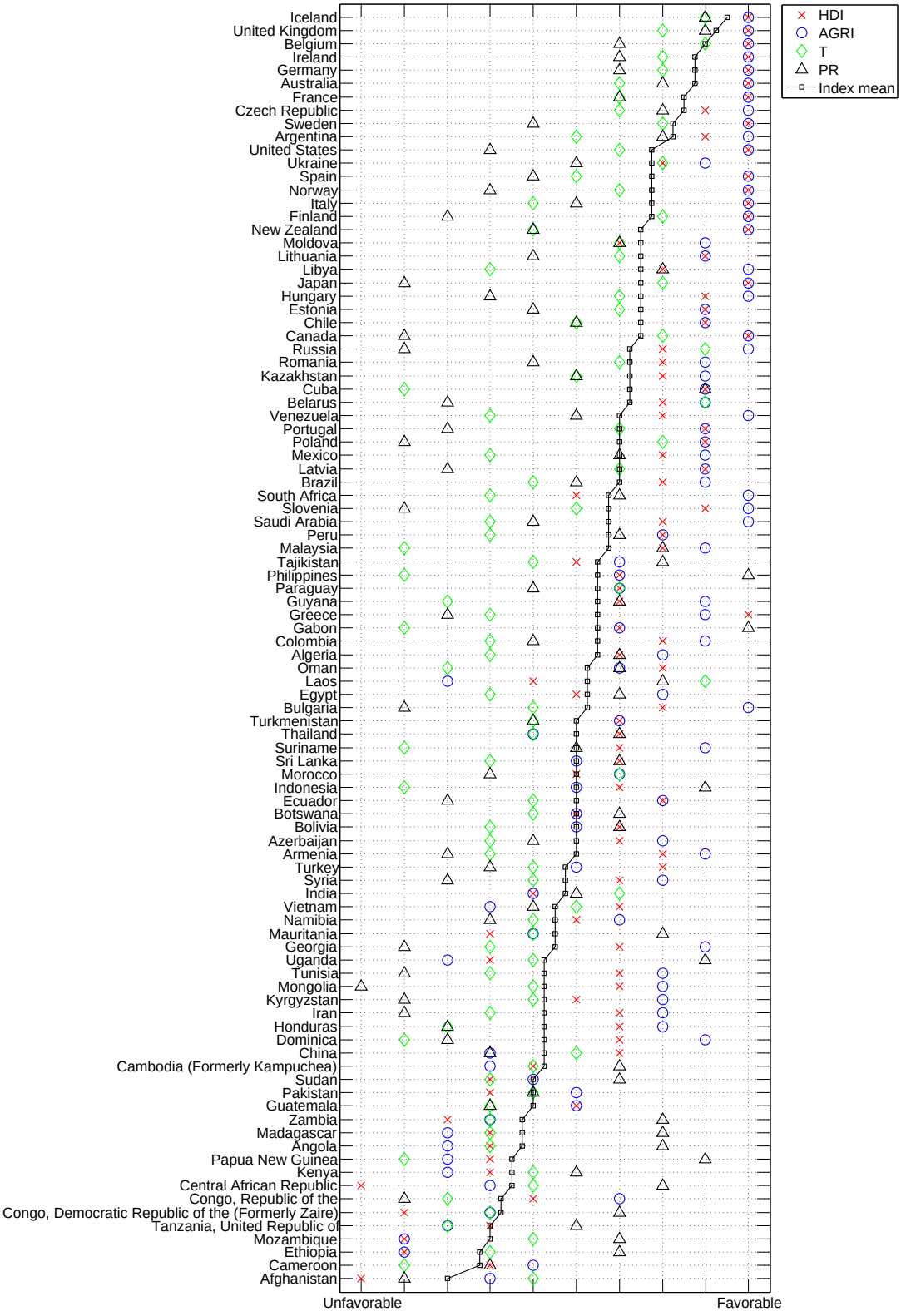

Figure 6.3: *Parametric overview of the climate change index for each country.*

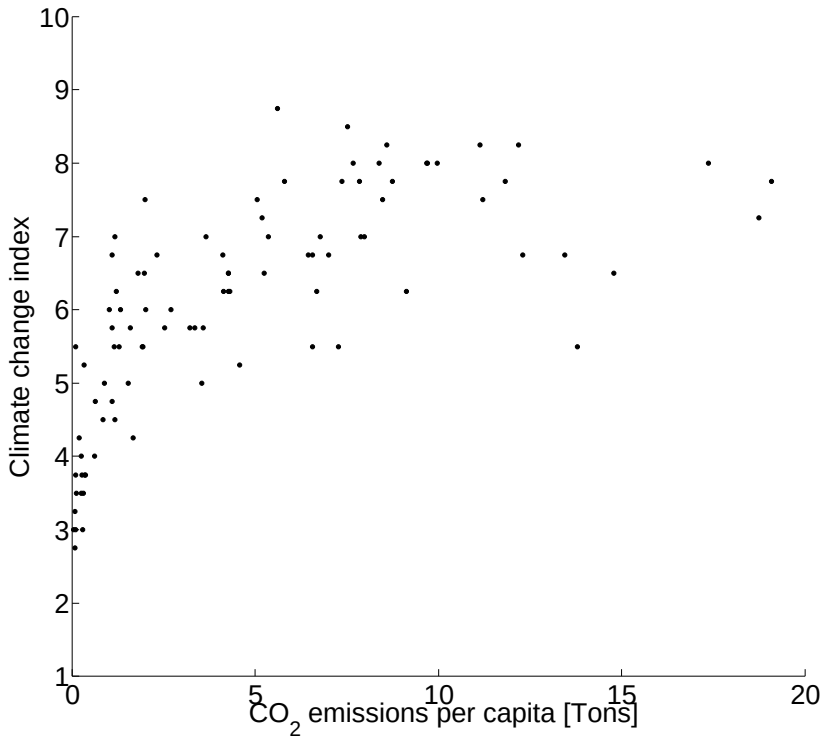

Figure 6.4: *Scatterplot of the climate change index and the CO_2 emissions per capita.*

One critical point of this analysis may be that it is questionable whether for an ecosystem or a society the absolute or the relative changes (signal to noise) are more relevant. And it is also not clear whether changes in temperature or precipitation are more severe. Some species react more sensitive to changes in temperature and some more to changes in precipitation. In case of precipitation the matter is even more complex since it can get dryer or wetter whereas in case of temperature it only gets warmer. Is more rain positive or negative? What is the threshold at which a strong increase in precipitation has more negative consequences than positive? These are questions which need to be addressed by the impact community since every ecosystem and society reacts differently and is sensitive to different aspects of climate change. We admit that our analysis is very simple in these terms since our assumption is that every change results in negative impacts, which is not true in all cases. Yet the aim of this study is to answer the questions where climate change is most prominent and whether the countries concerned are vulnerable and whether they have the ability to adapt to these changes, if the changes should be negative.

Under the here made assumptions the answer to this question is clear. The countries affected most by climate change are the ones being least able to defend it because most of them have a low adaptive capacity. Furthermore, these countries are in general not responsible for the changes observed because even though one can argue that components of the climate change index are subjectively chosen the countries with the highest signal to noise ratio are the ones emitting the least CO_2 (compare with Chapter 4). This raises the question whether the polluter can afford not to take action to reduce its

greenhouse gas emissions or whether he should face their responsibility. This is a moral question which can not be answered by science alone.

Chapter 7

Conclusions and Outlook

7.1 Conclusions

This thesis has focused on exploring new ways to reduce uncertainty in long term climate projections and to generate climate change results based on model results which are as robust as possible. Three of the five presented studies focus on regional aggregation or a specific region and two novel approaches are described which lead to a reduction in uncertainty. The last two chapters are based on the results in Chapter 4 and highlight detectability of local precipitation changes and the social aspects of climate change. The following overall conclusions can be drawn:

- **Physical key processes:** Physical processes exist which have a large influence on today's climate of a region and are furthermore important for the magnitude of future climate changes. These processes can be identified as demonstrated in Chapter 2 in case of the northward ocean heat transport. The various implementations of this process in the AOGCMs results in different realizations of the sea ice extent depending on the amount of heat transported to the Arctic. Sea ice influences the climate by its albedo feedback and by the amount of solar energy which can be stored in the oceans. The sea ice albedo feedback is strong enough to have an effect on the global climate. In summary, processes exist which are crucial in the climate system and therefore can be used to constrain the climate models.

- **Eliminating 'bad' models:** In Chapter 2 models which do not meet basic performance criteria, in this case the five models which show a strong temperature bias towards too cold temperatures and have sea ice which has a too large extent and is too thick, are excluded. Thereupon the uncertainty of the lower bound of Arctic warming can be reduced by about 1.5K.

- **Reducing uncertainty using a regional climate classification:** Averaging climate change results over spatial areas can reduce uncertainty since models agree better on a larger scale (Räisänen, 2007). However, if the area is too large different climate regimes are averaged and the signal of change is blurred. By choosing the optimal size of a region which is depending on the region and climate parameter of interest, the model uncertainty is reduced.

- **Less than 1 K warming is needed for most locations to undergo a significant change in temperature:** We show that the warming to which we are already committed is enough for a

large part of the world to undergo a significant change in local surface temperature. In the low latitudes only a few tenth degrees warming are enough for a significant change. Furthermore, these countries are the ones with the lowest CO_2 emissions.

- **Detectability of precipitation changes on a local scale:** Detectability of changes in precipitation on a local scale can not be expected before 2020. But even if for some areas changes can be detected, for most areas local changes are not apparent before 2100. The precipitation increase in the high latitudes is easiest to detect whereas drying in areas of low precipitation is difficult to detect.

- **Developing countries and climate change:** Looking at climate change from a country's perspective is important for policy makers to be able to make decisions based on the political agenda of each country. There are parts of the world which will experience and need to address changes caused by climate change sooner than others. However, not every country has the same ability to adapt because know-how and investments are needed. The countries where climate change is most prominent relative to the natural range of variability are more vulnerable to climate change and have a lower adaptive capability.

Overall, the thesis demonstrates two approaches how uncertainties in climate projections can be reduced. Evaluating climate models using present day data does not necessarily result in a better convergence of the projections. Therefore, novel approaches are needed to make best use of the model data available today.

Furthermore, local detectability of temperature and precipitation changes are explored. It is shown that for temperature only a few tenth degrees warming are needed for a significant change to emerge, whereas changes in precipitation are only visible in some areas before 2100. The low latitudes are most affected by the changes caused by climate change.

7.2 Outlook

The aim of climate modeling should be that the model converges to the real world. As the model resolution is getting higher and process understanding is improving, climate projections will get more accurate. However, some processes are too small to be simulated by climate models. Therefore, uncertainties in climate projections will always exist. To wait until the models are perfect is not a wise strategy since there will never be a perfect model. Furthermore, we simply do not have the time to wait for the perfect model to come. The only possibility is to work with the data available today.

In my understanding there are three main points which need to be addressed in the next years:

1. **Metrics to evaluate the skill of climate models:** Evaluating climate models is by far not a simple task. In case of temperature novel approaches have been found as illustrated in Chapter 2. However, precipitation may be more limitting for a number of ecosystems. In large parts of the Earth the models do not even agree on the sign of change in precipitation.
   Nevertheless, climate models are getting better at simulating today's climate and the resolution

increases for every generation of models. More processes are included in the simulations, the complexity of the models is increasing. Evaluation of climate models on a regional scale is still very challenging because accurate observational data is needed with a long time record. For most parameters such datasets simply do not exist and if they do exist then measurements are only local and do not cover a whole region. Even if enough observational data is acquired to evaluate the models using the past, this does not necessarily mean that the uncertainties in the projections decrease. Therefore, better metrics to evaluate climate model projections are needed.

A problem arising in the next year will be that the number of AOGCM versions and the amount of climate data to process is strongly increasing. Metrics to routinely evaluate models are therefore needed. The aim of climate modeling is to generate projections of the climate on longer time scales. As the amount of data is increasing it gets more challenging to produce climate change predictions which can be used by end users. Hence, methods to check for a model's quality, to decide whether models should be included in an analysis need to be developed in order to reduce the amount of data which need to be processed by other science communities or end users.

However, methods to evaluate models need to be chosen carefully. In many cases end users are interested in specific regions and climate parameters. A 'broad brush' analysis where a large number of climate parameters are evaluated on a global scale does not necessarily lead to the information needed. Evaluating smaller scale regions for one or more parameters may be a more appropriate approach.

2. **Process understanding:** An other reason for uncertainties are lacks in process understanding. Small scale processes which are not well understood such as land-atmosphere interactions can lead to large local differences in the climate models. Observations can help to improve process understanding. Many observed climate parameters already show a signal of change. Using observations the processes at work for climate change can be better understood. A better understanding of processes leads to a more accurate implementation of theses processes in the models. Especially processes which involve the coupling between land-atmosphere, land use change and the carbon cycle are getting more and more important.

3. **Procedures to reduce uncertainties:** Even if models are evaluated on a routine and 'bad' models are excluded from the analysis and even if processes are understood to the very last detail there will be uncertainties in climate predictions. The predictions are computed by models and therefore by definition they will never (re)produce the real world. It is always a simplified representation of what we observe. Hence, methods to reduce uncertainties will always be needed.

   Based on model evaluation regions which show the largest uncertainties are easily detected. The reason for a large uncertainty in a region may be based on a specific process (see Chapter 2). But regions might exist where numerous processes lead to uncertainties. In these cases statistical methods such as neural networks or Baysian statistics can help to reduce uncertainty.

Bibliography

Ainsworth, E. A. L. and J. M. McGrath, 2010: Direct effects of rising atmospheric carbon dioxide and ozone on crop yields. Springer, 109–130 pp.

Alexandratos, N., 2005: Countries with rapid population growth and resource constraints: Issues of food, agriculture, and development. *Population And Development Review*, **31 (2)**, 237–258.

Allen, M. R. and W. J. Ingram, 2002: Constraints on future changes in climate and the hydrologic cycle. *Nature*, **419 (6903)**, 224–232.

Arzel, O., T. Fichefet, and H. Goosse, 2006: Sea ice evolution over the 20th and 21st centuries as simulated by current AOGCMs. *Ocean Modelling*, **12 (3-4)**, 401–415, doi:10.1016/j.ocemod.2005.08.002.

Bacon, S., 1997: Circulation and fluxes in the north Atlantic between Greenland and Ireland. *Journal Of Physical Oceanography*, **27 (7)**, 1420–1435.

Baettig, M. B., M. Wild, and D. M. Imboden, 2007: A climate change index: Where climate change may be most prominent in the 21st century. *Geophysical Research Letters*, **34**, doi:10.1029/2006GL028159.

Boé, J., A. Hall, and X. Qu, 2009a: Current GCMs' unrealistic negative feedback in the Arctic. *Journal Of Climate*, **22 (17)**, 4682–4695, doi:DOI:10.1175/2009JCLI2885.1.

Boé, J., A. Hall, and X. Qu, 2009b: Deep ocean heat uptake as a major source of spread in transient climate change simulations. *Geophysical Research Letters*, **36**, L22 701, doi:10.1029/2009GL040845.

Boé, J. L., A. Hall, and X. Qu, 2009c: September sea-ice cover in the Arctic ocean projected to vanish by 2100. *Nature Geoscience*, **2 (5)**, 341–343, doi:10.1038/NGEO467.

Bonfils, C., N. de Noblet-Ducoudre, J. Guiot, and P. Bartlein, 2004: Some mechanisms of mid-holocene climate change in Europe, inferred from comparing PMIP models to data. *Climate Dynamics*, **23 (1)**, 79–98, doi:10.1007/s00382-004-0425-x.

Brenkert, A. and E. Malone, 2005: Modeling vulnerability and resilience to climate change: A case study of India and Indian states. *Climatic Change*, **72 (1)**, 57–102.

Brewer, S., S. Alleaume, J. Guiot, and A. Nicault, 2007a: Historical droughts in Mediterranean regions during the last 500 years: a data/model approach. *Climate Of The Past*, **3 (2)**, 355–366.

Brewer, S., J. Guiot, and F. Torre, 2007b: Mid-holocene climate change in Europe: a data-model comparison. *Climate Of The Past*, **3 (3)**, 499–512.

Bromwich, D. H., R. L. Fogt, K. I. Hodges, and J. E. Walsh, 2007: A tropospheric assessment of the ERA-40, NCEP, and JRA-25 global reanalyses in the polar regions. *J. Geophys. Res.*, **112 (D10)**, D10 111.

Byrne, R. H., S. Mecking, R. A. Feely, and X. W. Liu, 2010: Direct observations of basin-wide acidification of the North Pacific Ocean. *Geophysical Research Letters*, **37**, L02 601.

Cazenave, A. and W. Llovel, 2010: Contemporary sea level rise. *Annual Review Of Marine Science*, **2**, 145–173.

Chapman, W. L. and J. E. Walsh, 2007: Simulations of Arctic temperature and pressure by global coupled models. *Journal Of Climate*, **20 (4)**, 609–632, doi:10.1175/JCLI4026.1.

Christensen, J. H., et al., 2007: Regional climate projections. *Climate Change 2007: The Physical Science Basis. Contribution of Working Group I to the Fourth Assessment Report of the Intergovernmental Panel on Climate Change, edited by S. Solomon, et al.*, 847–845, cambridge University Press, Cambridge.

Collins, M., B. B. B. Booth, G. Harris, J. M. Murphy, D. M. H. Sexton, and M. J. Webb, 2006: Towards quantifying uncertainty in transient climate change. *Climate Dynamics*, **27**, 127–147.

Deser, C., R. Tomas, M. Alexander, and D. Lawrence, 2010: The seasonal atmospheric response to projected arctic sea ice loss in the late twenty-first century. *Journal Of Climate*, **23 (2)**, 333–351.

Deutsch, C. A., J. J. Tewksbury, R. B. Huey, K. S. Sheldon, C. K. Ghalambor, D. C. Haak, and P. R. Martin, 2008: Impacts of climate warming on terrestrial ectotherms across latitude. *Proceedings Of The National Academy Of Sciences Of The United States Of America*, **105 (18)**, 6668–6672.

Eyring, V., et al., 2007: Multimodel projections of stratospheric ozone in the 21st century. *Journal of Geophysical Research*, **112 (D16)**, D16 303.

FAO, 2009: Summary of world food and agriculutural statistics 2009. http://www.fao.org/economic/ess/en/.

Fischer, E. M., S. I. Seneviratne, D. Luthi, and C. Schar, 2007: Contribution of land-atmosphere coupling to recent European summer heat waves. *Geophysical Research Letters*, **34 (6)**, L06 707.

Flato, G. M. and G. J. Boer, 2001: Warming asymmetry in climate change simulations. *Geophysical Research Letters*, **28 (1)**, 195–198.

Frölicher, T. and F. Joos, 2009: Reversible and irreversible impacts of greenhouse gas emissions in multi-century projections with the NCAR global coupled carbon cycle-climate model. *Climate Dynamics*.

Furrer, R., R. Knutti, S. R. Sain, D. W. Nychka, and G. A. Meehl, 2007a: Spatial patterns of probabilistic temperature change projections from a multivariate Bayesian analysis. *Geophysical Research Letters*, **34**, doi:10.1029/2006GL027754.

Ganachaud, A. and C. Wunsch, 2000: Improved estimates of global ocean circulation, heat transport and mixing from hydrographic data. *Nature*, **408 (6811)**, 453–457.

Gillett, N. P., D. A. Stone, P. A. Stott, T. Nozawa, A. Y. Karpechko, G. C. Hegerl, M. F. Wehner, and P. D. Jones, 2008: Attribution of polar warming to human influence. *Nature Geoscience*, **1 (11)**, 750–754, doi:10.1038/ngeo338.

Gillett, N. P., F. W. Zwiers, A. J. Weaver, and P. A. Stott, 2003: Detection of human influence on sea-level pressure. *Nature*, **422 (6929)**, 292–294.

Giorgi, F., 2006: Climate change hot-spots. *Geophysical Research Letters*, **33**, L08 707, doi:08710.01029/02006GL025734.

Giorgi, F. and X. Bi, 2005: Updated regional precipitation and temperature changes for the 21st century from ensembles of recent AOGCM simulations. *Geophysical Research Letters*, **32**, L21 715, doi:10.1029/2005GL024288.

Giorgi, F. and X. Bi, 2009: Time of emergence (TOE) of GHG-forced precipitation change hot-spots. *Geophysical Research Letters*, **36**, L06 709, doi:10.1029/2009GL037593.

Giorgi, F. and R. Francisco, 2000: Uncertainties in the prediction of regional climate change. *Global Change and Protected Areas*, 127–139, edited.

Giorgi, F. and L. O. Mearns, 2002: Calculation of average, uncertainty range and reliability of regional climate changes from AOGCM simulations via the reliability ensemble averaging (REA) method. *Journal of Climate*, **15**, 1141–1158.

Giorgi, F. and L. O. Mearns, 2003: Probability of regional climate change based on the Reliability Ensemble Averaging (REA) method. *Geophys. Res. Lett.*, **30**, 1629, doi:10.1029/2003GL017130.

Giorgi, F., et al., 2001: Regional climate information - evaluation and projections. *Climate Change 2001: The Scientific Basis. Contribution of Working Group I to the Third Assessment Report of the Intergovernmental Panel on Climate Change, edited by J. T. Houghton, et al.*, 583–638, cambridge University Press, Cambridge.

Gleckler, P. J., K. E. Taylor, and C. Doutriaux, 2008: Performance metrics for climate models. *Journal of Geophysical Research-Part D-Atmospheres*, **113 (D6)**, D06 104–1–20.

Hall, A., 2004: The role of surface albedo feedback in climate. *Journal Of Climate*, **17 (7)**, 1550–1568, doi:10.1175/1520-0442(2004)017.

Hall, A. and X. Qu, 2006: Using the current seasonal cycle to constrain snow albedo feedback in future climate change. *Geophysical Research Letters*, **33**, L03 502, doi:10.1029/2005GL025127.

Harris, G., D. M. H. Sexton, B. B. B. Booth, M. Collins, J. M. Murphy, and M. J. Webb, 2006: Frequency distributions of transient regional climate change from perturbed physics ensembles of general circulation model simulations. *Climate Dynamics*, **27**, 357–375.

Hawkins, E. and R. Sutton, 2009: The potential to narrow uncertainty in regional climate predictions. *Bulletin of the American Meteorological Society*, **90 (8)**, 1095–1107, doi:10.1175/2009BAMS2607.1.

Heathwaite, A. L., 2010: Multiple stressors on water availability at global to catchment scales: understanding human impact on nutrient cycles to protect water quality and water availability in the long term. *Freshwater Biology*, **55**, 241–257.

Holland, M., M. Serreze, and J. Stroeve, 2010: The sea ice mass budget of the Arctic and its future change as simulated by coupled climate models. *Climate Dynamics*, **34 (2)**, 185–200, doi:10.1007/s00382-008-0493-4.

Holland, M. M. and C. M. Bitz, 2003: Polar amplification of climate change in coupled models. *Climate Dynamics*, **21 (3-4)**, 221–232, doi:10.1007/s00382-003-0332-6.

Holland, M. M., C. M. Bitz, and B. Tremblay, 2006: Future abrupt reductions in the summer Arctic sea ice. *Geophysical Research Letters*, **33 (23)**, L23 503.

IPCC, 2007: Climate change 2007: The physical science basis. Contribution of working group I to the Fourth Assessment Report of the Intergovernmental Panel on Climate Change [Solomon, S., D. Qin, M. Manning, Z. Chen, M. Marquis, K.B. Averyt, M. Tignor and H.L. Miller (eds)]. *Cambridge University Press, Cambridge, United Kingdom and New York, NY, USA*, 996pp.

Jain, A. K., M. N. Murty, and P. J. Flynn, 1999: Data clustering: A review. *ACM Computing Surveys*, **31 (3)**, 264–323.

John, R., J. Q. Chen, N. Lu, and B. Wilske, 2009: Land cover/land use change in semi-arid Inner Mongolia: 1992-2004. *Environmental Research Letters*, **4 (4)**, 045 010.

Jones, P. D. and A. Moberg, 2003: Hemispheric and large-scale surface air temperature variations: An extensive revision and an update to 2001. *Journal Of Climate*, **16 (2)**, 206–223.

Joos, F., I. C. Prentice, S. Sitch, R. Meyer, G. Hooss, G. K. Plattner, S. Gerber, and K. Hasselmann, 2001: Global warming feedbacks on terrestrial carbon uptake under the Intergovernmental Panel on Climate Change (IPCC) emission scenarios. *Global Biogeochemical Cycles*, **15 (4)**, 891–907.

Jungclaus, J. H., et al., 2006: Ocean circulation and tropical variability in the coupled model ECHAM5/MPI-OM. *Journal Of Climate*, **19 (16)**, 3952–3972, doi:10.1029/2004GL019858.

Kaufmann, L. and P. Rousseeuw, 1990: *Finding groups in data: An introduction to cluster analysis*. John Wiley and Sons, New York, pp. 342.

Kilpatrick, K. A., G. P. Podesta, and R. Evans, 2001: Overview of the NOAA/NASA advanced very high resolution radiometer Pathfinder algorithm for sea surface temperature and associated matchup database. *Journal Of Geophysical Research-Oceans*, **106 (C5)**, 9179–9197.

Knutti, R., 2010: The end of model democracy? *Climatic Change*, doi:10.1007/s10584-010-9800-2.

Knutti, R., R. Furrer, C. Tebaldi, J. Cermak, and G. A. Meehl, 2010: Challenges in combining projections from multiple climate models. *Journal Of Climate*, **23 (10)**, 2739–2758.

Knutti, R. and G. C. Hegerl, 2008: The equilibrium sensitivity of the earth's temperature to radiation changes. *Nature Geoscience*, **1 (11)**, 735–743.

Knutti, R., G. A. Meehl, M. R. Allen, and D. A. Stainforth, 2006: Constraining climate sensitivity from the seasonal cycle in surface temperature. *Journal Of Climate*, **19 (17)**, 4224–4233.

Knutti, R., T. F. Stocker, F. Joos, and G. K. Plattner, 2003: Probabilistic climate change projections using neural networks. *Climate Dynamics*, **21 (3-4)**, 257–272.

Knutti, R., et al., 2008: A review of uncertainties in global temperature projections over the twenty-first century. *Journal Of Climate*, **21 (11)**, 2651–2663.

Koenigk, T., U. Mikolajewicz, J. H. Jungclaus, and A. Kroll, 2009: Sea ice in the Barents Sea: seasonal to interannual variability and climate feedbacks in a global coupled model. *Climate Dynamics*, **32 (7-8)**, 1119–1138, doi:10.1007/s00382-008-0450-2.

Kottek, M., J. Grieser, C. Beck, B. Rudolf, and F. Rubel, 2006: World map of the Köppen-Geiger climate classification updated. *Meteorologische Zeitschrift*, **15 (3)**, 259–263, doi:10.1127/0941-2948/2006/0130.

Manabe, S. and R. J. Stouffer, 1980: Sensitivity of a global climate model to an increase of CO_2 concentration in the atmosphere. *Journal Of Geophysical Research-Oceans and Atmospheres*, **85 (NC10)**, 5529–5554.

Meehl, G. A., W. D. Collins, B. A. Boville, J. T. Kiehl, T. M. L. Wigley, and J. M. Arblaster, 2000: Response of the NCAR climate system model to increased CO_2 and the role of physical processes. *Journal Of Climate*, **13 (11)**, 1879–1898.

Meehl, G. A., C. Covey, T. Delworth, M. Latif, B. McAvaney, J. F. B. Mitchell, R. J. Stouffer, and K. E. Taylor, 2007a: The WCRP CMIP3 multimodel dataset - a new era in climate change research. *Bulletin Of The American Meteorological Society*, **88**, 1383–1394, doi:10.1175/BAMS-88-9-1383.

Meehl, G. A., C. Covey, B. McAvaney, M. Latif, and R. J. Stouffer, 2005: Overview of the coupled model intercomparison project. *Bulletin Of The American Meteorological Society*, **86**, 89–93.

Meehl, G. A., et al., 2007b: Global climate projections. *Climate Change 2007: The Physical Science Basis. Contribution of Working Group I to the Fourth Assessment Report of the Intergovernmental Panel on Climate Change, edited by S. Solomon, et al.*, 747–845, cambridge University Press, Cambridge.

Murphy, J. M., D. M. H. Sexton, D. N. Barnett, G. S. Jones, M. J. Webb, M. Collins, and D. A. Stainforth, 2004: Quantification of modelling uncertainties in a large ensemble of climate change simulations. *Nature*, **429**, 768–772.

Omann, I. i., A. Stocker, and J. Jaeger, 2009: Climate change as a threat to biodiversity: An application of the DPSIR approach. *Ecological Economics*, **69 (1)**, 24–31.

Philipp, A., P. M. Della-Marta, J. Jacobeit, D. R. Fereday, P. D. Jones, A. Moberg, and H. Wanner, 2007: Long-term variability of daily north Atlantic-European pressure patterns since 1850 classified by simulated annealing clustering. *Journal Of Climate*, **20 (16)**, 4065–4095, doi: 10.1175/JCLI4175.1.

Piani, C., D. J. Frame, D. A. Stainforth, and M. R. Allen, 2005: Constraints on climate change from a multithousand member ensemble of simulations. *Geophysical Research Letters*, **32**, L23 825.

Räisänen, J., 2001: CO_2-induced climate change in CMIP2 experiments: Quantification of agreement and role of internal variability. *Journal Of Climate*, **14 (9)**, 2088–2104.

Räisänen, J., 2007: How reliable are climate models? *Tellus Series A-Dynamic Meteorology And Oceanography*, **59 (1)**, 2–29, doi:10.1111/j.1600-0870.2006.00211.x.

Räisänen, J. and T. N. Palmer, 2001: A probability and decision model analysis of a multimodel ensemble of climate change simulations. *Journal of Climate*, **14**, 3212–3226.

Rayner, N. A., D. E. Parker, E. B. Horton, C. K. Folland, L. V. Alexander, D. P. Rowell, E. C. Kent, and A. Kaplan, 2003: Global analyses of sea surface temperature, sea ice, and night marine air temperature since the late nineteenth century. *Journal of Geophysical Research*, **108 (D14)**, ACL2–1–29, doi:10.1029/2002JD002670.

Reichler, T. and J. Kim, 2008: How well do coupled models simulate today's climate? *Bulletin Of The American Meteorological Society*, **89 (3)**, 303–311.

Robock, A., 1985: An updated climate feedback diagram. *Bulletin Of The American Meteorological Society*, **66 (7)**, 786–787.

Rosenzweig, C., et al., 2008: Attributing physical and biological impacts to anthropogenic climate change. *Nature*, **453 (7193)**, 353–U20.

Santer, B. D., et al., 2003: Contributions of anthropogenic and natural forcing to recent tropopause height changes. *Science*, **301 (5632)**, 479–483.

Santer, B. D., et al., 2008: Consistency of modelled and observed temperature trends in the tropical troposphere. *International Journal Of Climatology*, **28 (13)**, 1703–1722, doi:10.1002/joc.1756.

Santer, B. D., et al., 2009: Incorporating model quality information in climate change detection and attribution studies. *Proceedings Of The National Academy Of Sciences Of The United States Of America*, **106 (35)**, 14 778–14 783.

Serreze, M. C., 2010: Understanding recent climate change. *Conservation Biology*, **24 (1)**, 10–17.

Serreze, M. C., A. P. Barrett, A. G. Slater, M. Steele, J. Zhang, and K. E. Trenberth, 2007: The large-scale energy budget of the Arctic. *Journal of Geophysical Research-Part D-Atmospheres*, **112**, 1–17, doi:10.1029/2006JD008230.

Serreze, M. C. and J. A. Francis, 2006: The Arctic amplification debate. *Climatic Change*, **76 (3-4)**, 241–264, doi:10.1007/s10584-005-9017-y.

Smith, D. M., S. Cusack, A. W. Colman, C. K. Folland, G. R. Harris, and J. M. Murphy, 2007: Improved surface temperature prediction for the coming decade from a global climate model. *Science*, **317 (5839)**, 796–799.

Solomon, S., G. K. Plattner, R. Knutti, and P. Friedlingstein, 2009: Irreversible climate change due to carbon dioxide emissions. *Proceedings Of The National Academy Of Sciences Of The United States Of America*, **106 (6)**, 1704–1709.

Stainforth, D. A., et al., 2005: Uncertainty in predictions of the climate response to rising levels of greenhouse gases. *Nature*, **433**, 403–406.

Stern, N., 2007: *The Economics of Climate Change: The Stern Review*. Cambridge University Press.

Stott, P. A., 2003: Attribution of regional-scale temperature changes to anthropogenic and natural causes. *Geophysical Research Letters*, **30 (15)**, CLM2–1–4.

Stott, P. A., S. F. B. Tett, G. S. Jones, M. R. Allen, J. F. B. Mitchell, and G. J. Jenkins, 2000: External control of 20th century temperature by natural and anthropogenic forcings. *Science*, **290 (5499)**, 2133–2137, doi:10.1126/science.290.5499.2133.

Stroeve, J., M. M. Holland, W. Meier, T. Scambos, and M. Serreze, 2007: Arctic sea ice decline: faster than forecast. *Geophysical Research Letters*, **34 (9)**, 1–5.

Tebaldi, C. and R. Knutti, 2007: The use of the multi-model ensemble in probabilistic climate projections. *Philosophical Transactions of the Royal Society A*, **365**, 2053–2075, doi:10.1098/rsta.2007.2076.

Tebaldi, C. and D. B. Lobell, 2008: Towards probabilistic projections of climate change impacts on global crop yields. *Geophysical Research Letters*, **35 (8)**, doi:10.1029/2008GL033423.

Tebaldi, C., L. O. Mearns, D. Nychka, and R. L. Smith, 2004: Regional probabilities of precipitation change: A Bayesian analysis of multimodel simulations. *Geophysical Research Letters*, **31**, L24 213, doi:10.1029/2004GL021276.

Tebaldi, C. and B. Sanso, 2009: Joint projections of temperature and precipitation change from multiple climate models: a hierarchical Bayesian approach. *Journal Of The Royal Statistical Society Series A-Statistics In Society*, **172**, 83–106.

Tebaldi, C., R. W. Smith, D. Nychka, and L. O. Mearns, 2005: Quantifying uncertainty in projections of regional climate change: A Bayesian approach to the analysis of multi-model ensembles. *Journal of Climate*, **18**, 1524–1540.

Trenberth, K. E. and J. M. Caron, 2001: Estimates of meridional atmosphere and ocean heat transports. *Journal Of Climate*, **14 (16)**, 3433–3443.

ul Haq, M., 1995: *Reflections on Human Development*. New York: Oxford University Press.

UNDP, 2009: Human development report 2009. http://hdr.undp.org/en/reports/global/hdr2009/.

Uppala, S. M., et al., 2005: The ERA-40 re-analysis. *Quarterly Journal Of The Royal Meteorological Society*, **131 (612)**, 2961–3012.

van Oldenborgh, G. J., S. Y. Philips, and M. Collins, 2005: El Niño in a changing climate: a multi-model study. *Ocean Science*, **1**, 81–95.

Walsh, J. E., W. L. Chapman, V. Romanovsky, J. H. Christensen, and M. Stendel, 2008: Global climate model performance over Alaska and Greenland. *Journal Of Climate*, **21 (23)**, 6156–6174.

Wang, G. L., 2005: Agricultural drought in a future climate: results from 15 global climate models participating in the IPCC 4th assessment. *Climate Dynamics*, **25 (7-8)**, 739–753, doi: 10.1007/s00382-005-0057-9.

Wang, M. and J. E. Overland, 2009: A sea ice free summer Arctic within 30 years? *Geophysical Research Letters*, **36**, doi:10.1029/2009GL037820.

Wilks, D. S., 1998: *Statistical Methods in the Atmospheric Sciences*. Elsevier, New York, pp. 419.

Williams, J. W., S. T. Jackson, and J. E. Kutzbach, 2007: Projected distributions of novel and disappearing climates by 2100 AD. *Proceedings Of The National Academy Of Sciences Of The United States Of America*, **104**, 5738–5742, doi:10.1073/pnas.0606292104.

Winton, M., 2006: Amplified Arctic climate change: What does surface albedo feedback have to do with it? *Geophysical Research Letters*, **33 (3)**, L03 701, doi:10.1029/2005GL025244.

Yohe, G., E. Malone, A. Brenkert, M. Schlesinger, H. Meij, X. Xing, and D. Lee, 2006: A synthetic assessment of the global distribution of vulnerability to climate change from the IPCC perspective that reflects exposure and adaptive capacity. *Palisades, New York: CIESIN (Center for International Earth Science Information Network), Columbia University*.

Zhang, X. B., F. W. Zwiers, G. C. Hegerl, F. H. Lambert, N. P. Gillett, S. Solomon, P. A. Stott, and T. Nozawa, 2007: Detection of human influence on twentieth-century precipitation trends. *Nature*, **448 (7152)**, 461–U4, doi:10.1038/nature06025.

Zhang, X. D., 2010: Sensitivity of Arctic summer sea ice coverage to global warming forcing: towards reducing uncertainty in Arctic climate change projections. *Tellus Series A-Dynamic Meteorology And Oceanography*, **62 (3)**, 220–227.

Zhang, X. D. and J. E. Walsh, 2006: Toward a seasonally ice-covered Arctic ocean: Scenarios from the IPCC AR4 model simulations. *Journal Of Climate*, **19 (9)**, 1730–1747.

Acknowledgments

Many people contributed in their own way to the success of this thesis. Some offered me advice, some offered me guidance, and some others offered me their encouragement or even their friendship. I would like to express my special thanks to some of these people:

⋆ First and special thanks belong to my doctoral supervisor Reto Knutti for his support, his guidance and for his open door during the last three years. He has truly been a wonderful advisor with a never ending pot of ideas and enthusiasm. His professional expertise helped me when I got lost in details or produced shower curtains for weeks. I appreciated the stimulating discussions on many scientific and not so scientific topics. I am also greateful to him for letting me travel and present my work at great conferences and workshops. In many ways I got more support for my work than usually offered, and for that I wish to express my gratitude. And I am also very thankful for his understanding for my constant desire to run around in the mountains.
⋆ I would like to thank Christof Appenzeller and Susan Solomon for their collaboration and their ideas which contributed to the publications presented here.
⋆ A special thank goes to Urs Beyerle for his endless support and his very efficient way to solve IT problems. A dreadful scream from my office was most of the time enough for Urs to address my problems.
⋆ Great thanks also go to our postdocs Jan Cermak, Jan Sedlacek and Erich Fischer. Erich offered me a lot of advice already in the beginning of my PhD and therefore I did not mind at all his return to our institute.
⋆ I would like to thank my office mates David Masson and Markus Huber for their distraction when needed - or even when not needed. And I also thank Nathalie Schaller, Heidi Mittelbach and Andreas Lustenberger for their encouragement.
⋆ Thanks go to Arrhenius and our diva Firebolt which (at least most of the time) never let me down. For all other cases I had Urs to help me out.
⋆ Friends are essential in life. I want to thank them for laughing with me and cheering me up. I want to thank Barbara Ineichen for just always being there and Judith Schlapbach for running around in the mountains with me.
⋆ A warm and deep thank goes to my family for their never ending support and belief in my skills. To my mom for cooking a delicious dinner in times when needed and to my dad for repairing my notebook zillion times after I ruined it again.
⋆ My deepest and warmest thanks go to Tobias for his love, support and patience and for keeping the work at bay when needed.

Curriculum Vitae

Irina Mahlstein, Agnesstrasse 49, 8004 Zurich, Switzerland
born on 4 July 1979 in Sursee (LU)
citizen of Schenkon (LU) and Luzern (LU)

EDUCATION AND PROFESSIONAL TRAINING

Jul 2007	-	present	Ph.D. student in the group of Prof. R. Knutti, Institute for Atmospheric and Climate Science, ETH Zurich, Switzerland
Jul 2009			Visit at the National Center for Atmospheric Research (NCAR) and NOAA Earth System Research Laboratory (ESRL), Boulder (CO), USA
Oct 2006	-	Apr 2007	NatCat Analyist, Converium, Zurich, Switzerland
Mar 2006	-	Sep 2006	Diploma thesis under the guidance of Prof. H. Davies and Dr. Olivia Martius in the Dynamics group, Institute for Atmospheric and Climate Science, ETH Zurich, Switzerland
Nov 2004	-	Mar 2005	Internship at WSL Institute for Snow and Avalanche Research (SLF), Davos, Switzerland
Oct 2001	-	Sep 2006	Studies in Environmental Science majoring in atmospheric physics at ETH Zurich, Switzerland
Aug 1997	-	Jun 1998	Exchange year at Senior High School, Broken Arrow (OK), USA
Aug 1992	-	Jun 2000	Highschool education at Kantonsschule Sursee, Switzerland, Graduation: Matura type C (Mathematics and Science)

AWARDS

Best High School Graduation for Matura type C

PUBLICATIONS

Mahlstein, I. and R. Knutti, 2010. Ocean heat transport as a cause for model uncertainty in projected Arctic warming. Accepted in Journal of Climate.

Huber, M. B., R. Knutti, I. Mahlstein, M. Wild and J. Fasullo, 2010. Constraints on climate sensitivity from radiation patterns in climate models. Accepted in Journal of Climate.

Mahlstein, I. and R. Knutti, 2009, Regional climate change patterns identified by cluster analysis, Climate Dynamics, 35, 587-600, doi: 10.1007/s00382-009-0654-0

ORAL PRESENTATIONS

Mahlstein, I. and R. Knutti, 2010, Ocean heat transport as a cause for model uncertainty in projected Arctic warming. International Meetings of Statistical Climatology, Edinburgh, United Kingdom, July 2010.

Mahlstein, I. and R. Knutti, 2010, Ocean heat transport as a cause for model uncertainty in projected Arctic warming. Internation Polar Year, Oslo, Norway, June 2010.

Mahlstein, I. and R. Knutti, 2009, Regional climate change patterns identified by cluster analysis. MOCA: IAMAS IAPSO IACS 2009 Joint Assembly, Montreal, Canada, August 2008.

POSTER PRESENTATIONS

11th Swiss Global Change Day, Bern, Switzerland, April 2010
7th NCCR Climate Summer School, Monte Verità, September 2008
EGU General Assembly, Vienna, Austria, April 2008
9th Swiss Global Change Day, Bern, Switzerland, April 2008

“When I was a child, everything went well. The animals ate well, the people ate well, and everything went well. But in our day, theres a big change. A really big change. It is because water has slowed down, there is no more water, water has changed, water does not come as it did before. Now the water is very, very, very low.”